MINISTRY OF SUPPLY

AERONAUTICAL RESEARCH COUNCIL
REPORTS AND MEMORANDA

Experiments with Slotted and Perforated Walls in a Two-dimensional High-speed Tunnel

By

D. W. HOLDER, Ph.D., R. J. NORTH and A. CHINNECK, B.Sc.,

of the Aerodynamics Division, N.P.L.

LONDON : HER MAJESTY'S STATIONERY OFFICE

1956

PRICE 17s 0d NET

Experiments with Slotted and Perforated Walls in a Two-dimensional High-speed Tunnel

By

D. W. Holder, Ph.D., R. J. North and A. Chinneck, B.Sc.,

of the Aerodynamics Division, N.P.L.

Summary.—Preliminary tests have been made with a $7\frac{1}{2}$-in. $\times$ 3-in. two-dimensional induced-flow tunnel fitted with slotted or with perforated walls, and with a closed tunnel and an open jet of the same size. The experiments include observations of the pressures in the empty tunnel, and of the pressure distribution and flow pattern round a 2-in. chord aerofoil at angles of incidence of 0 deg and 2 deg. The reliability of the measurements on the aerofoil at high subsonic speeds is estimated by comparison with measurements in the 20-in. $\times$ 8-in. Tunnel on an aerofoil of the same section and chord.

By suitable design the Mach number in the empty tunnel can be varied continuously between zero and about $1 \cdot 2$, and reasonably uniform distributions can be obtained at all Mach numbers within this range. When the aerofoil is present, choking can be avoided, and it is found that in all cases the major interference effect at zero incidence arises from blockage. The slot area ratio (about $0 \cdot 04$) needed to minimize blockage is smaller than originally expected, and walls with larger slot area give blockage effects similar to those observed in the open jet. This agrees with the predictions of calculations which were completed after the experiments had been made. Although the blockage could be made small at Mach numbers up to about $0 \cdot 9$, it tended to the value for an open jet at higher subsonic speeds.

When the model is at incidence, the lift coefficients in the slotted tunnels lie between those measured in the closed and open tunnels, but the lifts measured in the walls which give minimum blockage are in reasonable agreement with those obtained in the 20-in. $\times$ 8-in. Tunnel where the blockage is thought to be negligible. With these walls it was, however, only just possible to reach supersonic speeds, so that it seems that in two dimensions the design requirements which must be satisfied to give minimum interference at subsonic speeds are incompatible with those giving uniform supersonic flows at the highest possible Mach numbers. It seems from recent American work that this is not the case in a tunnel designed for three-dimensional testing.

It is difficult to estimate the reliability of the present tunnels at transonic speeds because the flow round a two-dimensional aerofoil is insensitive to changes of Mach number near unity, and because reliable transonic data are not available for comparison. Also, little information has been obtained on the interference in a slotted tunnel when running at supersonic speeds.

The tests were made in two dimensions because a tunnel suitable for three-dimensional work was not available, and it seems that the design of a satisfactory two-dimensional slotted tunnel[†] is more difficult than the design of a three-dimensional one. The utility of transonic tests on two-dimensional aerofoils is, however, doubtful, and the main object of the present work was to provide information and experience which would be useful in the design of a three-dimensional slotted working-section when a suitable tunnel became available.

---

1. *Introduction.*—The idea of using a working-section with partly open and partly closed boundaries to reduce the effects of wall interference is of long standing and is, for example, discussed in Refs. 1 to 3 which were written between 1936 and 1941. The authors of these papers considered low speeds and were, therefore, more interested in the interference associated with the lift than with the blockage of the model. In about 1940, however, Sir Geoffrey Taylor suggested that the blockage might be reduced and choking delayed in a high-speed tunnel by the use of slotted walls, and an investigation of the method was placed on the programme of work in the High Speed Laboratory at the National Physical Laboratory. In view of the pressure of other work, and because it was thought that the method would take a long time to develop, the investigation was given a low priority and the use of solid adjustable walls shaped[4] to approximate to streamlines of an unlimited flow was preferred.

When it was learned, however, that Wright and Ward had succeeded[5] not only in avoiding choking and reducing blockage, but also in obtaining reasonably uniform supersonic flows at adjustable Mach number without altering the wall shape, it was decided that preliminary experiments with slotted walls should be started at the N.P.L., and the present experiments were made.

It was clear from the work of Wright and Ward and from that reported during the course of the present investigation by Bates[6] and by Nelson and Bloetscher[7] that a number of separate problems were involved in using slotted walls in a high-speed tunnel. Firstly there was the problem of the interference associated with the lift and blockage of the model at low subsonic speeds, secondly there were a number of problems associated with interference and choking at high subsonic and transonic speeds, and thirdly there were the problems of designing a tunnel to give uniform supersonic flow and of the interference effects at supersonic speeds. In addition, there was the important practical question of measuring and, if possible, reducing the relatively large pressure ratio needed to drive a tunnel fitted with slotted walls. It seemed doubtful whether a single tunnel could be built to give the optimum arrangement from all these different aspects, or whether a single series of tests could be devised to investigate them all. It was decided, therefore, to examine the problems of interference at subsonic and transonic speeds and of obtaining a uniform velocity distribution at supersonic speeds. The questions of interference in a slotted supersonic tunnel (*i.e.*, of wave reflection from a slotted wall), and of power economy have been investigated only indirectly.

It seemed that the question of interference at high subsonic speeds could be approached most easily by comparing tests on a body in a slotted tunnel with tests on a similar body in a larger tunnel of conventional design in which the interference was smaller and more fully understood. With the facilities which were available at the N.P.L., the only method of obtaining a direct comparison at transonic speeds would have been to test similar models of different scale in the slotted tunnel. This would have required the construction of several (pressure plotting) models of very small size, and would have involved uncertainties as to the magnitude of the effects of departures from exact geometrical similarity and of changes in Reynolds number. It was, therefore, decided to make tests instead on a single model in a conventional tunnel at high subsonic and low supersonic speeds, and to estimate by interpolation the reliability of the transonic data obtained on a similar model in the slotted tunnel.

The only available tunnels which were large enough to make tests on models were of narrow cross-section, and designed for two-dimensional tests. The experiments were, therefore, made in two dimensions using solid side walls and slotted walls at the top and bottom of the working-section only. The main object of the experiment was not, however, to develop a transonic tunnel technique for two-dimensional models, but to obtain information and experience which could be applied to three-dimensional testing when a suitable tunnel became available.

The tunnel used in the tests was of the induction type, and any difficulties peculiar to the use of slotted walls in this sort of tunnel had, therefore, to be investigated also.

2

In spite of the limitations of the theory, it was thought that it would be of value to calculate the ratio of closed to open boundary for zero interference in the manner described for a three-dimensional tunnel by Wright and Ward. The computations were made by the Mathematics Division, N.P.L., but the results did not become available until the present tests were nearly complete. The theoretical work is discussed briefly in section 14 of the present paper, and is described in detail by Tomlinson[8].

Since at the beginning of the work the authors had no guide from the theory as to the slot arrangement which was likely to give the best results, it was decided to test first a wide range of wall designs. These tests (together with the subsequently completed theory) suggested that a much smaller slot area was required than was originally conjectured and further walls were made and tested. In this report, however, the experiments are not always described in chronological sequence.

The tests reported by Wright and Ward with slotted walls showed that when the tunnel was running at supersonic speeds the pressure varied sinuously along the axis. In an attempt to avoid this it was decided that the present experiments should include observations with perforated as well as slotted walls.

2. *General Arrangement of the Slotted Tunnel.*—The experiments with slotted and perforated walls were made in the 9-in. × 3-in. induced-flow tunnel[9]. The working-section is formed between side panels spanning the 9-in. dimension, and carrying glass windows for flow visualization, and 3-in. wide metal channels at the top and bottom which carry the solid liners used during normal running. The slotted walls also were made up as liners as shown in Fig. 1 so that they could be interchanged or replaced by conventional solid liners for subsonic or supersonic running. Each liner consisted of two solid wooden blocks A and B between which the slotted or perforated plate was stretched. The plates were previously bent to shape on a wooden former, and were secured by screws fitting into threads tapped into metal plates attached to the wooden blocks. The upstream ends of the blocks A faired into the 16 : 1 contraction of the tunnel, and the down-stream ends of the blocks B were connected to the injector used to drive the tunnel.

Further details of the apparatus are given in the appropriate sections below.

3. *The Effect of an Expansion Downstream of the Working-Section.*—It was thought that the amount by which the tunnel expanded downstream of the working-section before the slots came to an end would have an important effect on the highest Mach number which could be reached. Preliminary tests to determine the most suitable expansion ratio were made using the apparatus shown in Fig. 2. The wooden blocks A were designed so that the tunnel was 6·56-in. high at the beginning of the slots which were formed between $\frac{1}{8}$-in. thick brass strips attached to the blocks A, and to the blocks B downstream. Each slot was 0·061-in. wide, and there were gaps of half this amount between the side walls of the tunnel and the adjacent strips. The ratio of the open area to the total area on each 3-in. side of the tunnel was 0·143. The chambers beneath the slotted walls were approximately 3-in. high at the beginning of the slots, and the working-section expanded by 0·008 in. per inch on each slotted wall to allow for the growth of the boundary layer. The side walls of the tunnel were parallel.

At 20-in. downstream of the beginning of the slots the slotted walls began to diverge at a total angle of about 18 deg, and finally blended into the tunnel circuit just ahead of the injector. Three downstream blocks B, B′ and B″ were made so that the amount by which the tunnel expanded before the exits from beneath the walls were closed could be varied. The pressure distributions measured along the centre-lines of the middle strip of each slotted wall are plotted in Fig. 3 for the three different amounts of downstream expansion. The maximum Mach number which could be reached is set out against the expansion ratio (*i.e.*, the ratio of the cross-sectional area of the tunnel at the end of the slots to that at the beginning of the slots) in Table 1.

3

TABLE 1

*Effect of an Expansion Downstream of the Working-Section
on the Maximum Mach Number*

Expansion ratio $\frac{h'}{h}$ (Fig. 3)	Maximum Mach number
1·05 (Block B Fig. 2)	0·89
1·14 (Block B′ Fig. 2)	1·20
1·39 (Block B″ Fig. 2)	1·26

4. *Tuft and Schlieren Observations in the Empty Tunnel.*—In order to obtain a physical picture of the means by which supersonic flow was produced in the working-section, the tunnel with the largest amount of downstream expansion (*see* above) was run up to top speed, and the flow was observed with a schlieren apparatus and by placing cotton streamers about 1-in. long in the chamber beneath one slotted wall. The flow which was revealed by these techniques is sketched in Fig. 4.

The Mach number reaches unity across the throat, and the flow expands into the slots through a Prandtl-Meyer expansion centered where they begin. The boundaries of the jets passing through the slots soon became diffuse because of mixing, and could no longer be observed with the schlieren apparatus. The flow which has passed into the chamber beneath the wall at the upstream end escapes through the slots into the downstream expanding part of the tunnel separating from the slotted walls as it does so. The supersonic flow in the expanding part of the tunnel breaks down in a shock-wave a little ahead of the ends of the slots, and a small amount of reversed flow takes place through the slots; this probably arises because there is a region of relatively high static-pressure behind the shock. There is a large eddy in the chamber beneath the slotted wall, the flow being reversed in a region extending from about $1\frac{1}{2}$ in. (*i.e.*, about half the chamber height) below the wall to the bottom of the chamber.

The conditions in the working-section seem to resemble those in a free jet emerging from a sonic orifice when the static pressure at the orifice exceeds that surrounding the jet. The flow from the throat expands through the slots until the static pressure in the jet becomes equal to that in the chamber beneath the slots. By this means the Mach number in the jet can be varied by varying the pressure in the surrounding chamber. It was not possible to see from the schlieren observations whether the jet boundary contracted again after expanding as it would if the jet were free, or whether the expansions at the corners of the throat were reflected as compression waves. The pressure distributions discussed below suggest, however, that when the slot area is large the disturbances in the tunnel resemble those in a jet.

5. *Attempts to Reduce the Static Pressure Beneath the Slotted Walls by Modifications to the Downstream Expansion.*—Attempts were made to reduce the static pressure in the chambers beneath the slotted walls (and thus raise the maximum Mach number in the tunnel) by modifying the expansion of the tunnel at the downstream end of the working-section. It seemed that the static pressure below the walls could be reduced by reducing the pressure in the tunnel at the slot exits. In an attempt to do this the slots were blocked from the beginning of the expanding part of the tunnel to a point close to the end of the expansion (*see* Fig. 5) in the hope that the supersonic flow in the working-section would expand to a lower pressure before it was joined by the stream from beneath the walls. The top Mach numbers which could be reached in the working-section are set out in Table 2 against the ratio of the area of the tunnel at the end of the blocked slots to that at the beginning of the slotted wall.

TABLE 2

Effect on the Maximum Mach Number of Partially Blocking the Slots in the Expansion

Area ratio	Maximum Mach number
1·39 (slots blocked to end of expansion)	0·89
1·33	0·94
1·22	1·05
1·15	1·13

This table shows that the top Mach number is in fact reduced by blocking the slots, and the explanation was sought by making schlieren observations. These showed that the stream in the expanding part of the tunnel did expand to a lower pressure when the slots were partially blocked, but that the break-down shock wave was then bifurcated with the front limb located at the end of the blocked region. Because of the pressure rise in this shock it is thought that the static pressure at the exit from the slots was higher than when they were not blocked, and the working-section Mach number was thus reduced.

Further investigations of the effect of the downstream conditions on the top speed in the working-section were made by testing the arrangements shown in Fig. 6. The slotted walls used (wall B of Table 3) were those designed for the main series of tests and are described below. In the first modification to the original design (Fig. 6a) the walls were arranged as shown in Fig. 6b so that the flow from beneath them could pass directly into the tunnel without going through the wall. The other modifications shown in Figs. 6c and 6d were similar except that the length of the wall or the fairing at exit was altered. The top-speed wall-pressure distributions are shown in Fig. 6 and indicate that the maximum Mach numbers obtained with the modified wall were lower than for the original design shown in Fig. 6a. The corresponding inducing-air pressure ratios are also shown in Fig. 6 and show that the power requirements are smallest with the original design.

It is interesting to note that the maximum Mach numbers reached in the present tests are of the same order as those obtained in the American[5] and Royal Aircraft Establishment experiments in which a downstream expansion was used to give a low static pressure. If some means other than a downstream expansion is used to reduce the static pressure in the chamber beneath the walls relative to that at the throat, much higher speeds can be obtained (*see* for example Ref. 6), but the velocity distribution deteriorates rapidly with rising speed as it would do in a free jet.

It is possible that the Mach number could be raised by designing the slot exit so that the air leaves in a direction inclined away from the tunnel axis instead of parallel to it as in Fig. 5. In this way the shock wave springing from the slot exit may be avoided. Further tests are required to investigate this arrangement.

6. *Modifications to the Tunnel for the Main Tests.*—It seemed from the tests described above that it was unnecessary to use a downstream expansion as large as 39 per cent (*see* Table 1), or a chamber beneath the slotted walls as deep as 2·9 in. The remainder of the tests were, therefore, made with the arrangement shown in Fig. 7, in which the expansion ratio downstream of the working-section is 1·25. The working-section was 7·5-in. × 3-in. that is, a ⅜-scale model of the 20-in. × 8 in. Tunnel in which the comparative tests on the aerofoil were made (*see* section 10). The slotted walls were again made from ⅛-in. thick brass sheet and props P (Fig. 7) were introduced at the point where the tunnel began to expand in order to eliminate a small amount of distortion under aerodynamic loading which had been observed during the preliminary experiments described above. Tests were made to ensure that these props had no effect on the

5

top speed of the tunnel or on the pressure distribution in the working-section. Tie bars Q (Fig. 7) were also introduced to connect the wooden blocks A and B in order to facilitate the removal and replacement of the wall.

The perforated walls were made of $\frac{1}{16}$-in. thick steel sheet and the patterns chosen were standard products of Messrs. G. A. Harvey Ltd., Greenwich.

7. *Details of the Slots and Perforations.*—The shapes of the slots and perforations used are sketched in Fig. 8 and details are set out in Table 3. In all cases the openings were of constant cross-section through the walls, and the corners at the two surfaces sharp.

After the original walls had been tested it was thought that an improvement could be produced by cutting additional slots in the expanding part of the walls with small slot areas. The walls shown in Fig. 9 were accordingly built and tested.

TABLE 3

Details of the Slotted and Perforated Walls

(a) *Longitudinal Slots*

Wall	Width of each slot (in.)	Number of slots	Ratio of width to depth of slot	Ratio of open to total area
A	0·067	15	0·54	0·333
B	0·067	9	0·54	0·200
C	0·061	7	0·49	0·143
D	0·038	9	0·30	0·111
E	0·010	12	0·08	0·040
F	0·060	2	0·48	0·040
G	0·060	1	0·48	0·020
H	0·060	2 additional slots in expansion (Fig. 9)	0·48	0·040
I	0·060	1 additional slots in expansion (Fig. 9)	0·48	0·020

(b) *Perforations*

Wall	Dimensions of perforations (in.)	Number of perforations per sq in.	Ratio of width to depth of perforations	Ratio of open to total area
J	2·0 × 0·1		2·0	0·262
K	0·454 × 0·059		1·2	0·232
L	0·343 × 0·030		0·6	0·171
M	0·104 diam.	20	2·1	0·170
N	0·069 diam.	8	1·4	0·030

8. *Pressure Distributions in the Empty Tunnel.*—The pressures measured along the centre-line of the solid strip on or nearest to the centre-line of the slotted wall are plotted in Figs. 10 to 18 against the distance from the beginning of the slots. The variation of static pressure along the axes of some of the slotted tunnels are shown in Figs. 19 to 24. The measurements were made

6

with a $\frac{1}{4}$-in. diameter tube extending right through the working-section from upstream of the contraction to downstream of the injector. In all cases the tube was traversed and the manometer observed continuously so that it is known that they are no sharp pressure changes* between the points shown. The variation of pressure along the axes of the tunnels with perforated walls are shown in Figs. 25 to 29. No wall-pressure distributions are shown for the perforated walls as measurements were made close to the beginning of the walls only. Cross-traverses in the slotted tunnels are shown in Fig. 30.

The observations show that the distributions both along and across all of the working-sections are reasonably uniform at Mach numbers up to quite close to unity.

When the tunnel is running at a supersonic speed, the pressure along the axis falls from a value corresponding to the speed of sound near the beginning of the slots or perforations in a manner which is similar to that for a free jet discharging from a sonic orifice into still air at a static pressure lower than that at the orifice. This is illustrated by Fig. 19 where the measured pressures for wall A are compared with those calculated for a free jet. It is seen that the calculations are in agreement not only with the measured pressure fall but also with the subsequent pressure rise. Further downstream the pressures on the axis continue to rise and fall in a manner similar to that in a free jet. Additional evidence that the flow is similar to that in a free jet is provided by the fact that the pressure fluctuations at the wall are much smaller than those on the axis.

The maximum speed which could be obtained appears to be almost independent of the slot area, and of the perforation area and shape for area ratios greater than about $0 \cdot 1$. For the $0 \cdot 04$ area ratio slots, supersonic flow could only just be obtained in the working-section, and supersonic running was impossible with the $0 \cdot 02$ area ratio slots and the $0 \cdot 03$ area ratio perforations.

When the area ratio of the slots or perforations is small and the tunnel is running near top speed, the pressure falls rapidly at the beginning of the expansion downstream of the working-section. This pressure drop is particularly large for the very small area ratios where quite high Mach numbers (up to about $1 \cdot 4$) are reached in the expansion. It was thought that the top speeds of the tunnels with small area ratios might be increased by placing additional slots in the expansion and walls H and I were built. It was found that the top speed was in fact raised by this modification as shown in Figs. 15 and 17 or 16 and 18. The rise of Mach number in the expansion was also reduced and this is discussed in section 16 in connection with the power requirements of the tunnel.

Some of the walls gave reasonably uniform supersonic flow in the working-section. For example, walls D and M when working at $M = 1 \cdot 1$ gave axial static pressures which were constant to within ± 1 per cent over a length of one tunnel height, and to within $\pm \frac{1}{2}$ per cent. over a length of half the tunnel height. The traverses shown in Fig. 30 suggest that there are no sharp changes of static pressure across the working-section (*i.e.*, along lines at right-angles to the slots).

9. *Wall Pressures when an RAE 104 Aerofoil is Present.*—The 2-in. chord RAE 104 aerofoil[10] shown in Fig. 31a was rigged in the tunnel midway between the slotted walls, and the wall pressures were measured over a range of tunnel speed. The results for an incidence α of 0 deg are plotted in Figs. 32 to 40 and those for α = 2 deg in Figs. 41 to 49.

At α = 0 deg. the effect of the aerofoil on the wall pressures is small for the larger slot areas, but increases as the slot area is reduced. The wall pressure begins to rise ahead of the model and then falls to a minimum nearly opposite or a little downstream of the trailing edge. The position of this minimum moves downstream as the tunnel speed is raised, and schlieren

---

* Other than those masked by the softening effect of the boundary layer on the exploring tube.

observations suggested that at the higher speeds it corresponded with the point where the shock wave from the model struck the wall. Further downstream the effect of the model on the wall pressures becomes confused with that of the expansion, but an indication of the wall pressures downstream is given by Fig. 50 where the model was placed 4 in. upstream of its usual position.

In most cases the pressure upstream of the model settles down to a roughly level value p_0 before the beginning of the slots is reached, and this value* has been used to determine the free-stream Mach number.

When the model is at incidence, the pressures on the two walls differ as shown in Figs. 41 to 49 because of the lift on the aerofoil, and a mean has been taken in determining the tunnel speed.

10. *Observations on the RAE 104 Aerofoil.*—(i) *Measurements in the 9-in. × 3-in. Tunnel.*— The pressures at the surface of the aerofoil were measured at the ten 0·01-in. diameter static-pressure holes shown in Fig. 31a. Two of the holes were in the same position along the chord, one in the upper and the other in the lower surface. The model was set to zero aerodynamic incidence by adjusting the incidence until the pressures at these two holes were equal. To obtain additional values of the pressure when the model was at incidence, tests were made at equal positive and negative angles.

The method of plotting the results is illustrated by Fig. 51. The measured local pressure p (expressed in non-dimensional form by dividing by the total head H_0 of the undisturbed stream) is plotted against the free-stream pressure coefficient p_0/H_0 measured at the wall far upstream of the model (*see* section 9). A separate figure is given for each point along the aerofoil chord, and each curve is for a different wall arrangement; the curves are staggered vertically to avoid confusion. The results for $\alpha = 0$ deg are reproduced in Figs. 52 to 60; values for $\alpha = 2$ deg are included in the original paper which may be obtained on application to the Aeronautical Research Council Secretariat.

In addition to those in the slotted and perforated walls, tests were made in a closed tunnel and in a two-dimensional open jet of the same size as the slotted tunnel. The closed tunnel was formed by filling in the space between the blocks A and B in Fig. 1 with a solid wooden block, and the open jet was made by removing the slotted wall so that the jet emerged from the orifice formed by blocks A into the chamber between the top and bottom channels of the working section. At some speeds the conditions in the open jet (as judged by the pressure readings) appeared to be unsteady. The results of the tests in the closed and open tunnels are included in Figs. 52 to 60.

Tests were also made at supersonic speeds by fitting the tunnel with conventional solid nozzle-shaped liners. The Mach numbers used (1·42, 1·60 and 1·79) were sufficiently high for the model to be free from tunnel interference. The results are shown in Figs. 52 to 60 where they are joined by broken lines to the curves obtained in the slotted and perforated tunnels.

(ii) *Measurements in the 20-in. × 8-in. Tunnel.*—To provide data for comparison with those obtained in the slotted and perforated tunnels, an aerofoil of the same chord and section as that described above but of 8-in. span was made for the 20-in. × 8-in. tunnel. This aerofoil is shown in Fig. 31b.

Tests were made up to the highest Mach number obtainable using the adjustable walls of the tunnel to minimise tunnel interference in the manner described in Ref. 4. The results of these measurements are included in Figs. 52 to 60 and the method of plotting is illustrated by Fig. 51; in cases where confusion might occur owing to the presence of too many curves on one graph some results have been superimposed in red on the main figures.

---

* When the tunnel is running at a supersonic speed the pressure falls at the beginning of the walls because of the expansion leading to the supersonic flow. The tunnel speed has then been measured in the region of level pressure downstream of this initial fall.

In the absence of more reliable results, it is assumed that the measurements made in the 20-in. × 8-in. Tunnel are free from interference, and they are used here to assess the interference effects encountered in the tests in the slotted and perforated tunnels.

(iii) *Schlieren Photography.*—A Toepler schlieren photograph of the flow round the model was taken for each case examined. The exposures were of the order of one microsecond. Examples showing typical, or particularly interesting features are reproduced in Figs. 61 to 66; the other photographs are available at the N.P.L.

11. *Comparison Between the Measurements in the 9-in. × 3-in. and the 20-in. × 8-in. Tunnels.*— (i) *Results at Zero Incidence.*—Examination of Figs. 52 to 60 shows that a major difference between the results for most of the slotted and perforated tunnels and those for the 20-in. × 8-in. Tunnel is that the free-stream pressure coefficients for a given local pressure on the aerofoil are higher in the 20-in. × 8-in. Tunnel. In other words, there is a negative blockage effect in the slotted tunnels which results in the measured free-stream Mach number being too high. This may be seen most clearly in Figs. 59 and 60, which show the pressures measured over the rear of the model. Here the sharp fall of pressure which takes place as the shock wave moves back occurs more gradually as the free-stream Mach number is raised in the slotted tunnels than in the 20-in. × 8-in. Tunnel. Comparison of the photographs for the 20-in. × 8-in. Tunnel (Fig 61) with typical photographs (Fig. 64) show that the changes of flow pattern which occur as the Mach number is raised are similar in the two tunnels, but again suggest that the Mach numbers measured in the slotted tunnels are too high. In fact the observations in the slotted and perforated tunnels seem to be in better agreement with the measurements in the open jet than with those made in the 20-in. × 8-in. Tunnel. This is illustrated more clearly in the diagrams discussed below.

In order to see more clearly whether the major part of the discrepancy was due to blockage (*i.e.*, to a change of free-stream Mach number only) the observations shown in Figs. 52 to 60 ($\alpha = 0$ deg) have been replotted in a different way in Fig. 67. Here the free-stream pressure coefficient p_0/H_0 in the slotted tunnel has been plotted against the value (' True ' p_0/H_0) in the 20-in. × 8-in. Tunnel which gives the same local pressure coefficient at a particular point on the surface of the aerofoil. If the discrepancy arises solely from blockage, the points for all of the pressure holes in the aerofoil should lie on a single curve which gives the correction to be applied to the free-stream pressure coefficient. In Fig. 68a which shows results for wall H and is discussed in detail below, the scatter is typical of that for the other slotted and perforated walls. The maximum departures from the mean curve shown are seen to occur at the higher Mach numbers and are then about ± 2 per cent on p_0/H_0 (*i.e.*, ± 0·015 on M at $M = 0·85$). Although part of this scatter may arise from experimental errors*, it may occur also because the model is too large for the tunnel so that there is a distortion as well as a blockage effect. Comparison between Figs. 68a and 68b shows that the scatter is no worse in the slotted tunnel than in the 7½-in. × 3-in. closed tunnel.

Nevertheless in the absence of a better procedure it seems reasonable to draw mean blockage curves of the type shown in Fig. 68 and these curves for walls A to G, J to N and for the open and closed tunnels are compared in Fig. 67. It appears from this diagram that the blockage curves for these slotted and perforated walls are in fair agreement with that for the open jet. An exception occurs for slotted wall F which gives a smaller blockage correction at the lower speeds but begins to approach the curve for the open jet as the free-stream pressure coefficient p_0/H_0 is reduced below about 0·63. Also, the results obtained with perforated wall N behave in an anomalous way over the whole range of Mach number covered.

When the region of supersonic flow round the model had extended to the wall, the schlieren photographs revealed shock waves springing from the extremities of the apertures in the perforated walls. Examples are shown in the photographs reproduced in Fig. 65.

---

* These are particularly likely to arise in an experiment of this kind where the tunnel had to be dismantled and reassembled many times during the course of the work. The fact that the scatter does not increase greatly as the Mach number is raised suggests that part of it arises from experimental errors.

The free-stream pressure coefficient at which wall F begins to give an appreciable blockage correction in Fig. 67 is roughly that at which sonic conditions are first reached in the rapid pressure drop (*see* Fig. 37) at the beginning of the expansion downstream of the working-section. Additional slots were, therefore, cut in the walls of the expansion to give wall H as described in section 7 and shown in Fig. 9. The pressure distributions obtained on the model aerofoil in this modified tunnel are compared in Fig. 69 with those measured in the 20-in. × 8-in. Tunnel, and the blockage curves are shown in Figs. 67 and 68a. It is seen that the blockage at high Mach number is reduced, but remains negative. In an attempt to reduce this negative blockage correction further, the slots adjacent to the side walls of the tunnel were blocked so that wall I shown in Fig. 9 was produced. The blockage curve for this wall is shown in Fig. 67 where it is seen that the blockage correction is larger than for wall H and is positive over the range of Mach number covered.

Of the walls used, therefore, wall H with three slots giving an area ratio of 0·04 appears to give the smallest blockage correction over the range (0·6 to 0·926) of free-stream Mach numbers for which a comparison with the results for the 20-in. × 8-in. tunnel can be made. Although it also enables tests to be made at slightly supersonic speeds, the top speed reached is not as high, and the velocity distribution less uniform than for some of the other walls.

(ii) *Results at 2 deg Incidence.*—The lift coefficients* obtained by integrating the pressure distributions shown for $\alpha = 2$ deg (*see* for example Fig. 70) are plotted in Fig. 71 against free-stream pressure coefficient. The lift coefficients and free-stream pressure coefficients have been corrected for blockage by using the mean blockage curves† for $\alpha = 0$ deg plotted in Fig. 67. Discrepancies in Fig. 71 between the curves for the slotted and perforated tunnels and that for the 20-in. × 8-in. Tunnel are thus due mainly to wall interference associated with the lift on the aerofoil.

Fig. 71 shows that the lift coefficients in the open jet are, as expected, lower than those in the $7\frac{1}{2}$-in. × 3-in. and the 20-in. × 8-in. Tunnel, and that the values obtained in the slotted tunnels lie in general between the curves for the open jet and the 20-in. × 8-in. results. The results do not change systematically as the slot area is changed and this may arise because the number of slots was not kept constant. The values for wall H are seen in Fig. 71c to be in reasonable agreement with those for the 20-in. × 8-in. Tunnel, and Fig. 71d suggests that if they were extrapolated to a higher Mach number they would agree reasonably well with values measured in a conventional supersonic tunnel.

12. *Blockage and Lift Corrections in the Closed and Open Jets.*—(i) $\alpha = 0$ *deg.*—The pressures measured on the surface of the RAE 104 aerofoil in the $7\frac{1}{2}$-in. × 3-in. closed and open jets are included in Figs. 52 to 60, and the mean experimental blockage curves determined in the manner described in section 11 are reproduced in Fig. 72a. This diagram includes curves for the blockage calculated from the usual formula

$$\frac{\Delta M}{M} = (1 + \tfrac{1}{5}M^2)\varepsilon$$

where ε is the sum of the solid blockage factor ε_s and the wake blockage factor ε_w (taken to be zero in the open jet). These factors are given by

$$\varepsilon_s = \frac{\pi}{6}\frac{A}{h^2}\left(1 + 1\cdot2\,\frac{t}{c}\right)\frac{1}{\beta^3} \text{ for the closed jet,}$$

$$\varepsilon_s = -\frac{\pi}{12}\frac{A}{h^2}\left(1 + 1\cdot2\,\frac{t}{c}\right)\frac{1}{\beta^3} \text{ for the open jet,}$$

---

* The number of pressure holes in the aerofoil was insufficient to enable the lift coefficient to be obtained very accurately, and appreciably different values could be obtained by drawing different (but equally plausible) curves through the measured points. Errors arising in this way are, however, unlikely to be large enough to invalidate the conclusions drawn from the work described in this section.

† It seems reasonable to use these curves at $\alpha = 2$ deg because the drag coefficient (and hence the wake blockage) does not change very much with incidence between 0 deg and 2 deg, and because the solid blockage is to a fair approximation independent of incidence.

and

$$\varepsilon_w = \frac{1}{4} \frac{c}{h} C_D \frac{1}{\beta^2}$$

where A is the cross-sectional area, t the thickness and c the chord of the aerofoil, and h is the tunnel height. As usual $\beta = \sqrt{(1 - M^2)}$. The profile-drag coefficients C_D used in determining the wake blockage were measured by the wake-traverse method.

It is seen from Fig. 72a that the calculated blockage curves are in reasonable agreement with the experimental ones at low Mach number but that calculation underestimates the blockage at high Mach number.

It was thought that it would be of interest to compare the form of the pressure distributions measured in the $7\frac{1}{2}$-in. × 3-in. closed jet at and beyond choking with those measured in the 20-in. × 8-in. Tunnel and in the open jet. The chordwise pressure distributions for the $7\frac{1}{2}$-in. × 3-in. closed jet at the onset* of choking and for fully developed† choked flow are shown in Fig. 73 where the pressure distributions measured in the 20-in. × 8-in. Tunnel and in the $7\frac{1}{2}$-in. × 3-in. open jet for the same pressure close to the trailing edge of the aerofoil are included for comparison. It is seen that the distributions are in fair agreement over the whole surface, and this suggests that even far beyond choking the major interference effect in a closed tunnel still arises from blockage.

(ii) $\alpha = 2$ *deg.*—The lift coefficients obtained from the tests in the $7\frac{1}{2}$-in. × 3-in. closed and open jets have been corrected for blockage by using the experimental blockage curves reproduced in Fig. 72a and are plotted in Fig. 72b against the corrected free-stream pressure coefficient. The corrections for the interference associated from the lift of the aerofoil have been calculated from the formulae‡

$$\frac{\Delta C_L}{C_L} = - \frac{\pi^2}{24\beta^2} \left(\frac{c}{h}\right)^2 \text{ for the closed tunnel}$$

and

$$\frac{\Delta C_L}{C_L} = \frac{\pi^2}{12\beta^2} \left(\frac{c}{h}\right)^2 + \frac{\pi}{2\beta} \frac{c}{h} \text{ for the open jet,}$$

and values corrected for the lift effect are included in Fig. 72b. It is seen that the lift coefficients obtained in the $7\frac{1}{2}$-in. × 3-in. closed tunnel are in good agreement with those measured in the 20-in. × 8-in. Tunnel but that there is a considerable discrepancy in the case of the open jet.

Pressure distributions measured at $\alpha = 2$ deg in the $7\frac{1}{2}$-in. × 3-in. closed tunnel at and beyond choking are compared§ in Fig. 74 with the distributions measured in the 20-in. × 8-in. Tunnel. The agreement again suggests that the major interference effect in a closed tunnel arises from blockage even well beyond choking.

13. *Observations on a 6 per cent Thick Double Wedge.*—Pressure measurements and schlieren observations were made on a 6 per cent thick symmetrical double wedge held at zero incidence in the tunnel fitted with walls C. Photographs showing the development of the flow as the Mach number is raised are reproduced in Fig. 75. The measured distance between the apex of the bow wave and the leading edge is plotted in Fig. 76 against free-stream Mach number, and the distribution of pressure over the surface of the model is shown in Fig. 77.

---

* This occurs at an uncorrected free-stream Mach number of 0·802 which is lower than the value (0·825) calculated on one-dimensional theory.

† *i.e.*, the condition reached when further increase of pressure ratio across the ends of the working-section produces no further change in the flow at the model.

‡ In these formulae it is assumed that the slope of the lift curve is $2\pi/\beta$ since insufficient measurements were made to enable the experimental slope to be found.

§ This comparison is not strictly permissible because of the presence of an interference effect associated with the lift of the model in the $7\frac{1}{2}$-in. × 3-in. closed tunnel. It is seen in Fig. 72b, however, that this effect is small.

At a sufficiently high Mach number the speed of sound is reached just ahead of the shoulder, and the sonic point then remains there with further increase of Mach number up to the maximum value (1·13) reached. An expansion to a supersonic speed occurs round the shoulder and is followed by a shock wave which moves downstream as the Mach number is raised and reaches the tail at a free-stream Mach number just below unity. The pressure over the rear of the aerofoil ahead of the shock wave is substantially independent of free-stream Mach number. This would be expected because with the sonic point at the shoulder on the front face of the model the pressure over the rear face is to a first approximation a function of the angle turned through at the shoulder only.

In Fig. 75 there is evidence that the bow wave is reflected at the slotted wall; at $M = 1·132$ the reflected compression can be seen running towards the model and passing into the expansion springing from the shoulder. The pressure change in this reflected wave is not detectable in the surface pressure-distributions, but it should be noted that there were no pressure holes in the region where the wave appears to strike the surface.

The measured positions of the detached bow wave are seen in Fig. 76 to lie on a smooth curve drawn through the point where theory predicts wave attachment to the nose, but measurements* made by Drougge[11] on an 8 per cent thick biconvex section suggest a much more gradual approach of the bow wave to the nose as the Mach number is raised. If it is assumed that the curves for the two different sections should have the same form, it seems that the Mach numbers measured in the tunnel and quoted in Figs. 75 to 77 are again higher than the true free-stream values.

14. *Comparison with Theory.*—The calculated values of the interference velocity on the tunnel axis at the position of the model for two-dimensional[8] and three-dimensional[5] slotted tunnels are plotted in Fig. 78 against the ratio of the open to total area.

In spite of its limitations, the theory is seen to predict results which are of the same order as those found in the present experiments on two-dimensional tunnels. In particular, the calculations confirm that most of the walls tested would be expected to give blockage effects which are similar to those for an open jet. The value of the area ratio† for zero blockage estimated‡ from the calculations also appears to be of the same order as that suggested by the experimental results.

15. *An Explanation of the Anomalous Choking Speeds Previously Reported for the 20-in. × 8-in. Tunnel.*—Beavan has reported[12] that the choking speeds measured in the 20-in. × 8-in. Tunnel are higher and not, as would be expected, lower than those calculated on the assumption that choking occurs when the speed of sound is reached uniformly across the section of minimum area between the model and the walls. He attributed this anomaly to the possibility of non-uniform flow across the tunnel, but in view of the present results, which show that a small slot may have a large effect on choking, the explanation may lie in the existence of two narrow slots§ in each of the 8-in. wide adjustable walls. These slots together with the gaps at the sides of the wall have an area ratio of 0·008.

16. *Power Requirements.*—The distance between the end of the slotted section and the injector unit was insufficient to enable the mean total head to be measured, and hence the pressure ratio needed to drive the tunnel to be estimated. An indication of the relative power requirements with the wall arrangements used was, however, obtained by measuring the total head of the

---

* Using an inclined wedge to vary the Mach number at the model.

† The number of slots used in the experiments on wall H was smaller than that assumed in the calculations. Since the ratio of open to total area for zero blockage increases as the number of slots is reduced, the value to be compared with the experiments is somewhat greater than that suggested by Fig. 78. Also the ratio of the height to width of tunnel assumed in the calculations (2 : 1) differed from that (2½ : 1) used in the experiments.

‡ It is clear from Fig. 78 that the calculated points do not permit this to be done accurately.

§ The slots were included partly because it was not possible to obtain a sufficiently wide strip of spring steel to cover the whole width of the tunnel, and partly to balance the pressure across each adjustable wall.

inducing air needed to drive the tunnel. Values of this pressure are plotted in Figs. 79, 80 and 81 against free-stream pressure coefficient. These diagrams show that the presence of an expansion between the working-section and the injector requires a rise of inducing air pressure even when the working-section is closed, and that the power requirements are further increased by the use of an open or a slotted or perforated section. The additional power is needed to overcome the losses in the slotted section, and because the flow at entry to the injector and diffuser of the tunnel is disturbed. The losses ahead of the injector arise from friction at the slotted or perforated walls, from eddying motion in the chamber beneath the walls, and from shock waves and flow separation in the expansion downstream of the working-section. At the higher free-stream Mach numbers the rate at which the inducing air pressure curves rise is greatest for the walls in which the highest Mach number is reached ahead of the breakdown shock wave in the expansion. This is illustrated by the curves for walls F and N in Figs. 79a and 79b and by Fig. 80 which shows the effect of cutting additional slots in the expansion. Figs. 15 to 18 show that the Mach number in the expansion is reduced by cutting additional slots in wall G (to produce wall I) and in wall F (to produce wall H), and Fig. 80 shows that the power requirements at high speeds are reduced by these modifications although the requirements at low speeds are slightly increased.

Comparison between Figs. 79a and 81 shows that the presence of a model aerofoil in the tunnel has only a small effect on the inducing air pressure.

17. *Notes on the Flow Round a Two-dimensional Aerofoil Moving at Transonic Speeds.*—Although tunnel interference has not been entirely eliminated, there is little doubt that the present tests indicate correctly the general nature of the changes which occur in the flow round a two-dimensional aerofoil as the free-stream Mach number is raised through unity. When the Mach number is raised from a low value, large changes of pressure distribution begin to occur soon after the speed of sound is first reached at the surface, and go on while the shock waves continue to move downstream towards the trailing edge. At some free-stream Mach number (depending on the section of the aerofoil and its incidence) below unity, however, the shock waves have moved back to the trailing edge. Further increase of Mach number then decreases the angle between the shock waves and the aerofoil chord (*see* for example, Figs. 61 to 66) although there is only a small change in the local Mach numbers over the aerofoil. The major changes thus occur when the shocks are moving back along the chord. This is illustrated by the fact that the slopes of the curves in Figs. 52 to 60 become small for free-stream Mach numbers between roughly 0·9 and 1·2 (p_0/H_0 from 0·59 to 0·41). Apart from the appearance of a bow shock wave, the flow pattern round, and the pressure distribution on the aerofoil are similar at Mach numbers just below and just above unity. This is illustrated by Fig. 82 which shows results obtained in the open-jet tunnel used in some of the present tests.

Because it is insensitive to changes of free-stream Mach number close to unity, the pressure distribution on a two-dimensional aerofoil is an unsatisfactory criterion for assessing the accuracy of a technique for transonic testing. For this reason, and because of the absence of data for comparison, it is difficult to estimate the reliability of the tunnels used in the present work at free-stream Mach numbers very close to unity. According to the elementary theory of the effects of sweep, it should be possible to design a swept-back wing so that it is much more sensitive to changes of Mach number around unity.

18. *Note on the Near-normal Shock Wave Visible in Some of the Photographs Behind the Trailing Edge of the Aerofoil.*—Some of the photographs (for example, Fig. 64, $M = 1·06*$) show that when the shock waves have reached the trailing edge, there is a near-normal shock running between them. A shock of this type was observed in all of the tests in the $7\frac{1}{2}$-in. $\times$ 3-in. tunnel, and in the 20-in. $\times$ 8-in. Tunnel. The development of the near-normal shock as the free-stream Mach number is raised is not revealed by the photographs reproduced here because the intervals of Mach number were too large, but visual observations on the RAE 104 aerofoil in the 20-in. $\times$ 8-in. Tunnel showed the following phenomena.

---

* It should be remembered that there is a considerable negative blockage correction for the walls used when this photograph was taken. The flow is actually subsonic.

When the free-stream Mach number was raised, a (subsonic) value was reached at which the shock waves were at the trailing edge. With further increase of Mach number, the angle between the shock waves and the direction of the undisturbed stream became more acute, and a small near-normal shock occurred a little behind the trailing edge. This near-normal shock then moved downstream as the Mach number was raised.

Although the explanation* for the presence of this near-normal shock wave is only partially understood, it can be argued that it might occur in some cases at subsonic free-stream speeds behind an aerofoil in free air. The local speed ahead of the shock waves depends on the free-stream Mach number and on the shape and incidence of the aerofoil, and when the shocks are at the trailing edge the flow deflection through the shock wave depends† on the trailing-edge angle and the incidence. At a subsonic free-stream speed the local supersonic speed near the surface just ahead of the trailing edge may be sufficiently high for the flow to remain supersonic in a small region behind the tail shock waves. A further shock or shock system may then be required to give subsonic flow far downstream of the aerofoil, and its position depends on the variation of Mach number along the wake and on the free-stream Mach number (which must be reached at infinity downstream). When the free-stream Mach number exceeds unity the requirement of subsonic flow far downstream must still be satisfied in a wind tunnel and the second shock wave (which is now well downstream of the aerofoil) then becomes the break-down shock wave in the tunnel.

In a conventional supersonic tunnel the free-stream Mach number and the position of the break-down shock can be controlled independently, the former by altering the nozzle shape, and the latter by adjusting the pressure ratio across the ends of the nozzle. This is not necessarily the case in a slotted tunnel of the type used in the present work, however, because the strength and position of the tunnel shock and the free-stream Mach number would seem from the observations described in section 4 to be interdependent. Nevertheless, the limited number of tests described show that the tunnel shock can be located so far downstream that it does not interfere with the flow past the model.

19. *Conclusions.*—(*a*) *Empty Tunnel.*—(i) By using a suitable wall design, the Mach number in the empty tunnel can be varied between zero and about $1 \cdot 2$ by adjusting the pressure ratio across the ends of the working-section.

(ii) The maximum supersonic speed depends on the amount by which the tunnel expands downstream of the working-section before the slots or perforations are closed. With no expansion supersonic running is not possible, and little increase in maximum Mach number is obtained by expanding more than about 25 per cent on area. Further work is needed before the mechanism by which the supersonic flow is established can be fully understood.

(iii) The maximum supersonic speed which can be reached is almost independent of the area ratio of the slots or perforations provided this exceeds about $0 \cdot 1$. Supersonic flow could not be obtained with an area ratio of $0 \cdot 04$ unless additional slots were cut in the expansion.

(iv) The pressure changes along the tunnels with large area ratio slots running at supersonic speeds resemble those in a free jet.

(v) At subsonic speeds the flow appears to be reasonably uniform in all of the slotted and perforated tunnels, but at supersonic speeds the uniformity depends on the wall design. The best results were obtained with slots of area ratio $0 \cdot 11$ (wall D)‡ or perforations having an area ratio of $0 \cdot 17$ (wall M), and the static pressure on the axis was then constant to within about $\pm \frac{1}{2}$ per cent over a length of half the tunnel height.

---

* For a more detailed explanation reference may be made to the following paper by D. W. Holder: Note on the flow near the tail of a two-dimensional aerofoil moving at a free-stream Mach number close to unity. C.P.188. June, 1954.

† In the absence of thickening or separation of the boundary layer.

‡ Details of the walls are given in Table 3 in section 7.

14

(vi) At all speeds the conditions in the slotted tunnels were reasonably uniform across the tunnel (i.e., at right-angles to the slots).

(b) *Results with an Aerofoil in the Tunnel*.—These results are unsatisfactory partly because tests on a two-dimensional aerofoil are an insensitive means of assessing the reliability of a technique for transonic testing, and partly because reliable transonic data could not be obtained for comparison with the results obtained in the slotted and perforated tunnels. The results obtained in the 20-in. × 8-in. Tunnel may not be completely reliable at the highest speeds, and there may be differences between the 20-in. × 8-in. and the slotted tunnels other than those arising from wall interference. In this connection the effects of free-stream turbulence, side wall interference, and small geometrical differences between the two aerofoils should be considered. Also, the number of pressure holes in the aerofoils was not sufficient to enable the lift coefficient to be evaluated accurately.

In spite of these difficulties, however, it is thought that the following conclusions may be drawn from this part of the work :

(i) When an aerofoil is present, the wall pressures become uniform (the value being used to determine the tunnel speed) at a distance upstream which increases as the slot area is reduced. For an area ratio of 0·04 (wall H) the required wall length ahead of the model is about two tunnel heights. When the tunnel is running at a supersonic speed the pressure falls near the beginning of the wall because of the expansion leading to the supersonic flow, and the tunnel speed should be measured a little downstream. For a model at incidence the pressures on the two slotted walls differ because of the lift, and a mean has to be used in estimating the tunnel speed. It should be possible to avoid this by measuring the tunnel speed on the centre-line of one of the side walls.

(ii) Choking near the model can be avoided by using slotted or perforated walls.

(iii) The changes of flow pattern round the model which occur as the Mach number is raised are qualitatively similar for all the walls, and most of the major differences between the results obtained with the different walls can be accounted for by differences of blockage. All walls with area ratios of about 0·1 or more gave blockage corrections similar to those for an open jet. The flow in the slotted tunnels appeared, however, to be steadier than in the open jet.

The minimum blockage effect was obtained with wall H which had an area ratio of 0·04 in the working-section and 0·2 in the expansion. With this wall the blockage was small up to about $M = 0·9$, but tended towards the value for an open jet at higher speeds. Supersonic flow could only just be obtained with this wall. The conclusion that a very small slot area is needed to minimize blockage in a two-dimensional tunnel is in qualitative agreement with the predictions of theory. Detailed comparison between experiment and theory is, however, impossible because the number of slots differed in the two cases, and because of the limited number of calculations which have been made.

(iv) The blockage effect appears to vary over the chord of the aerofoil, but the relative contributions of flow-distortion effects and experimental errors to this scatter are difficult to estimate. The scatter appears to be no worse in the slotted tunnels than in a closed tunnel of the same size, and does not increase greatly as the Mach number is raised.

(v) When the supersonic flow near the model extends to the perforated walls shock waves running from the edges of the perforations could be observed.

(vi) The lift coefficients at α = 2 deg obtained from measurements in the slotted tunnels lie between those measured in an open jet and in a closed tunnel, but the values for a slot area ratio of 0·04 (wall H) are in reasonable agreement with those measured in the 20-in. × 8-in. Tunnel, and if extrapolated, would agree quite well with measurements made in a supersonic tunnel.

15

(c) *Interference at Supersonic Speeds*.—The results give little information on the behaviour of compression or expansion waves when they strike a slotted or perforated wall. In some cases the bow wave ahead of the aerofoil appears to be reflected at the wall and to strike the model, but no pressure disturbance could be detected at the surface. This may be because there were insufficient pressure holes, or because the bow wave (unlike the shock on the surface or at the trailing edge of the aerofoil) is too weak to produce an appreciable disturbance on reflection.

(d) *Power*.—The power requirements are considerably greater for slotted or perforated walls than for a closed jet. With high speeds in the working-section the additional power seems to be greatest for walls in which the flow expands to a high Mach number ahead of the break-down shock in the expansion. For small slot areas this Mach number and hence the power can be reduced by cutting additional slots in the expansion.

(e) *Other Conclusions*.—(i) The results show clearly the qualitative changes of flow which take place as the free-stream Mach number ahead of a two-dimensional aerofoil is raised through unity. As expected, it is found that rapid changes occur only while the shock waves are moving back on the surface of the aerofoil, and are complete at a free-stream Mach number below unity when the shocks have reached the trailing edge.

(ii) In the present work the usual corrections underestimate the blockage in a closed tunnel and in an open jet at high Mach number, and the lift effect in an open jet.

(iii) Comparisons between the measurements in a $7\frac{1}{2}$-in. $\times$ 3-in. closed tunnel and in the 20-in. $\times$ 8-in. Tunnel suggest that blockage, (*i.e.*, a change of free-stream Mach number only), continues to be the major interference effect at, and well beyond, choking.

Acknowledgement.—Miss N. A. Bumstead helped throughout the experimental work and was responsible for the major part of the reduction of the observations.

REFERENCES

No.	Author	Title, etc.
1	K. Kondo	Boundary interference of partially closed wind tunnels. Rep. Aero. Res. Inst. Tokyo No. 137. 1936.
2	E. Pistolesi	Sull' interferenca di una galleria aerodinamica a contorno misto. *Commentationes della Pontificia Academia*, Vol. IV, No. 9. 1940.
3	J. Grinzel, F. Riegels and F. Vandrey	Korrekturfaktoren für Windkanäle mit teilweise offener und teilweise geschlossener Mebstrecke. A.V.A. LA 101. 1941.
4	C. N. H. Lock and J. A. Beavan	Wall interference at compressibility speeds using the flexible walls of the 20-in. $\times$ 8-in. High-speed Tunnel. R. & M. 2005. September, 1944.
5	R. H. Wright and V. G. Ward	NACA transonic wind-tunnel test sections. N.A.C.A. Research Memo. L8J06. October, 1948. A.R.C. 12,076.
6	G. P. Bates	Preliminary investigation of 3-inch slotted transonic wind-tunnel sections. N.A.C.A. Research Memo. L9D18. September, 1949. A.R.C. 12,681.
7	W. J. Nelson and F. Bloetscher	Preliminary investigation of a variable Mach number two-dimensional supersonic tunnel of fixed geometry. N.A.C.A. Research Memo. L9D29a. June, 1949. A.R.C. 12,682.
8	R. C. Tomlinson	The theoretical interference velocity on the axis of a two-dimensional wind tunnel with slotted walls. C.P. 181. August, 1950.
9	D. W. Holder and R. J. North	The 9-in. $\times$ 3-in. N.P.L. Induced-flow High-speed Wind Tunnel. R. & M. 2781. June, 1949.
10	R. C. Pankhurst and H. B. Squire	Calculated pressure distributions for the RAE 100-104 aerofoil sections. C.P. 80. March, 1950.
11	G. Drougge	A method for the continuous variation of the Mach number in a supersonic wind tunnel and some experimental results obtained at low supersonic speeds. F.F.A. Report No. 29. 1949.
12	J. A. Beavan	Limiting Mach number for aerofoil tests in the 20-in. by 8-in. Rectangular High-speed Tunnel. A.R.C. 8720. May, 1945. (Unpublished.)
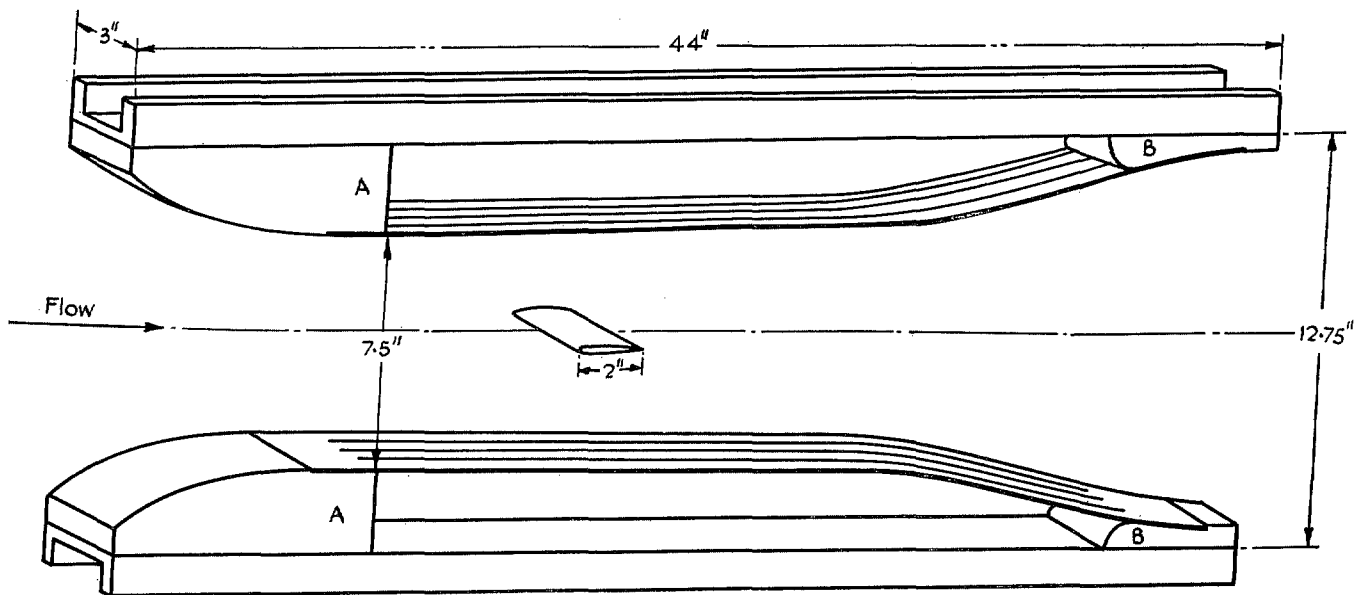
FIG. 1. General arrangement of the slotted tunnel with the 10 per cent thick RAE 104 aerofoil in position (side walls removed).
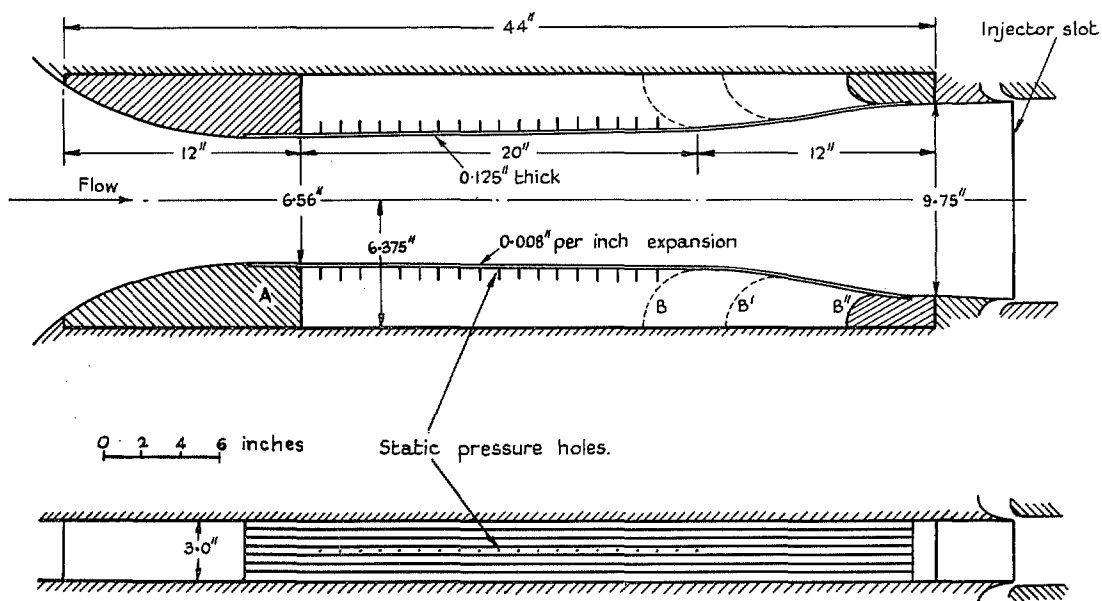
FIG. 2. Details of the walls used in the preliminary tests.

17
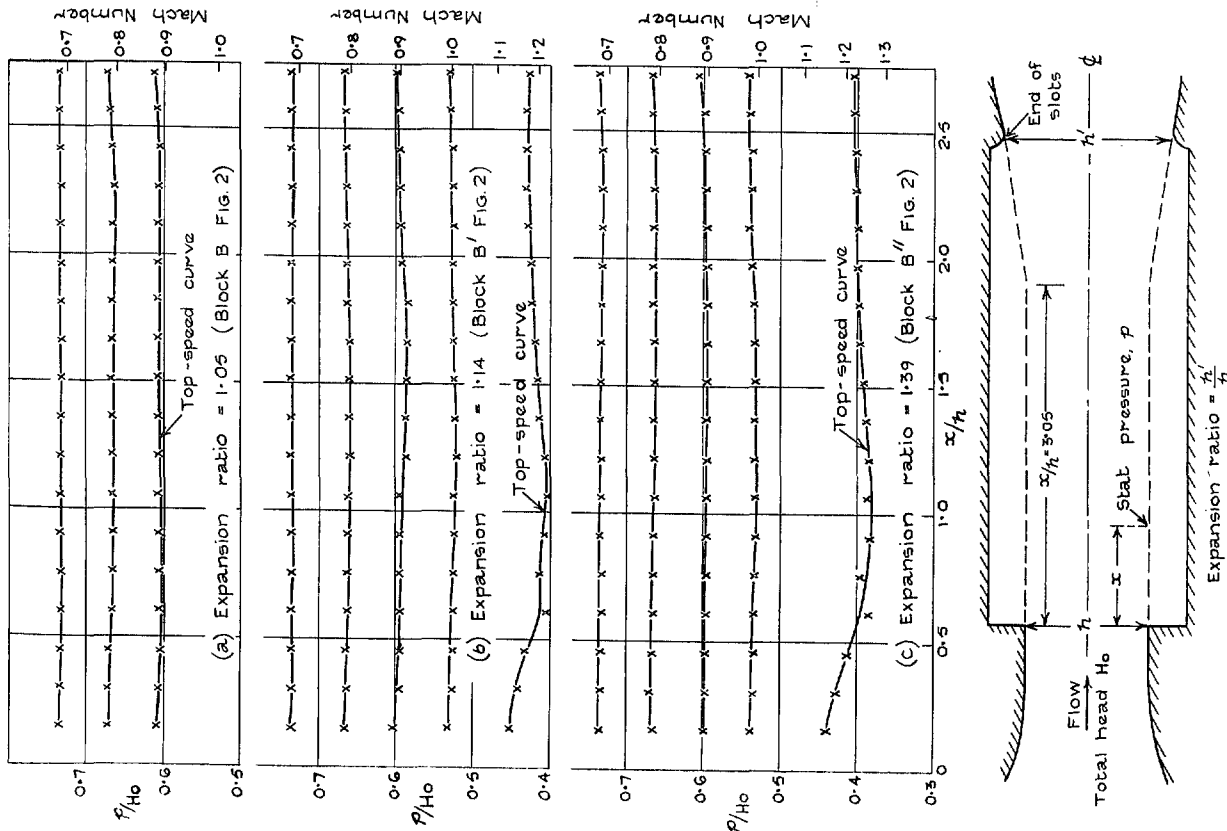
FIG. 3. Effect of an expansion downstream of the working-section on the Mach number at the working-section.
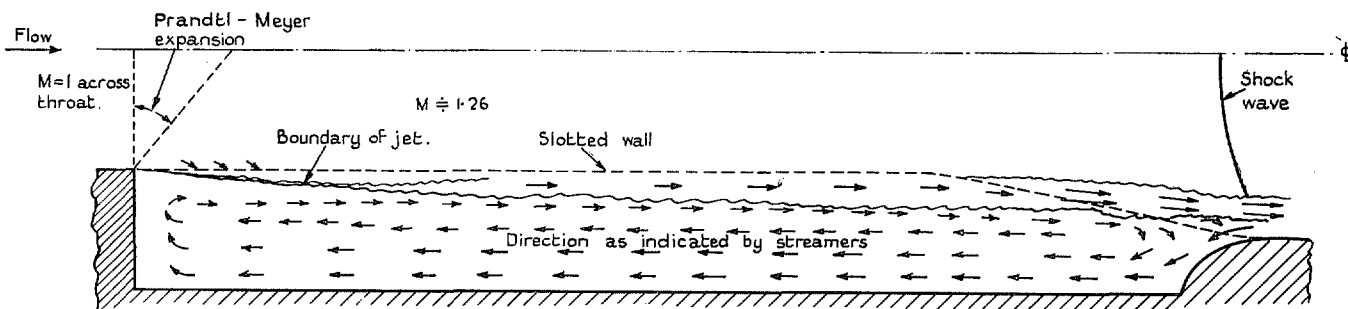
FIG. 4. Sketch of flow pattern in the tunnel when running at a supersonic speed.
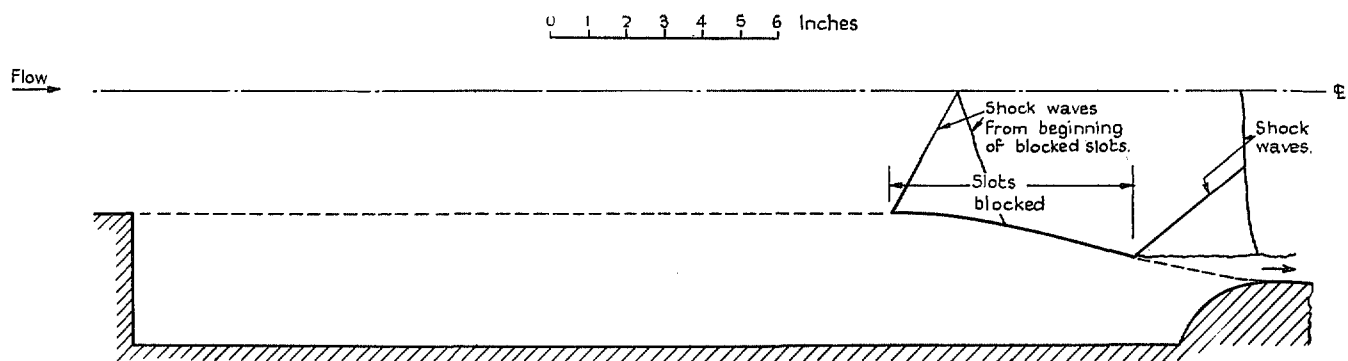
FIG. 5. Arrangement for tests with partially blocked slots in the expanding part of the tunnel.
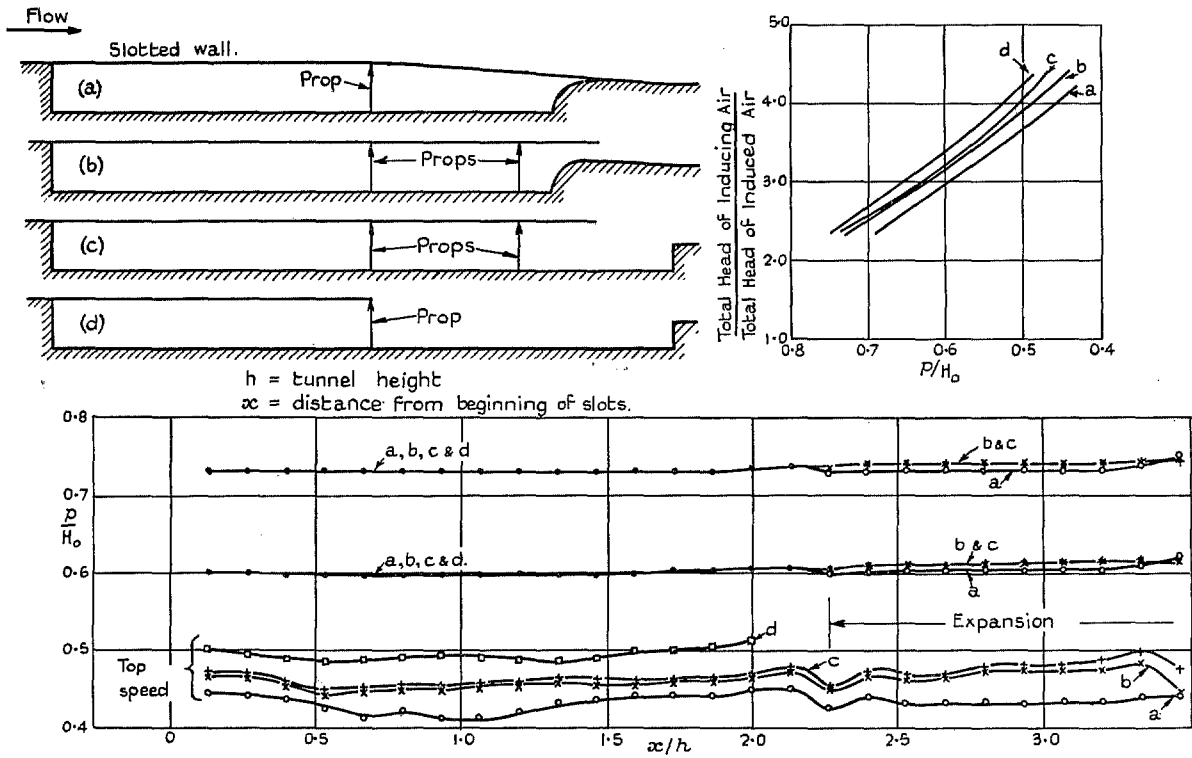
FIG. 6. Effects of changing the conditions at the rear of slotted wall B.
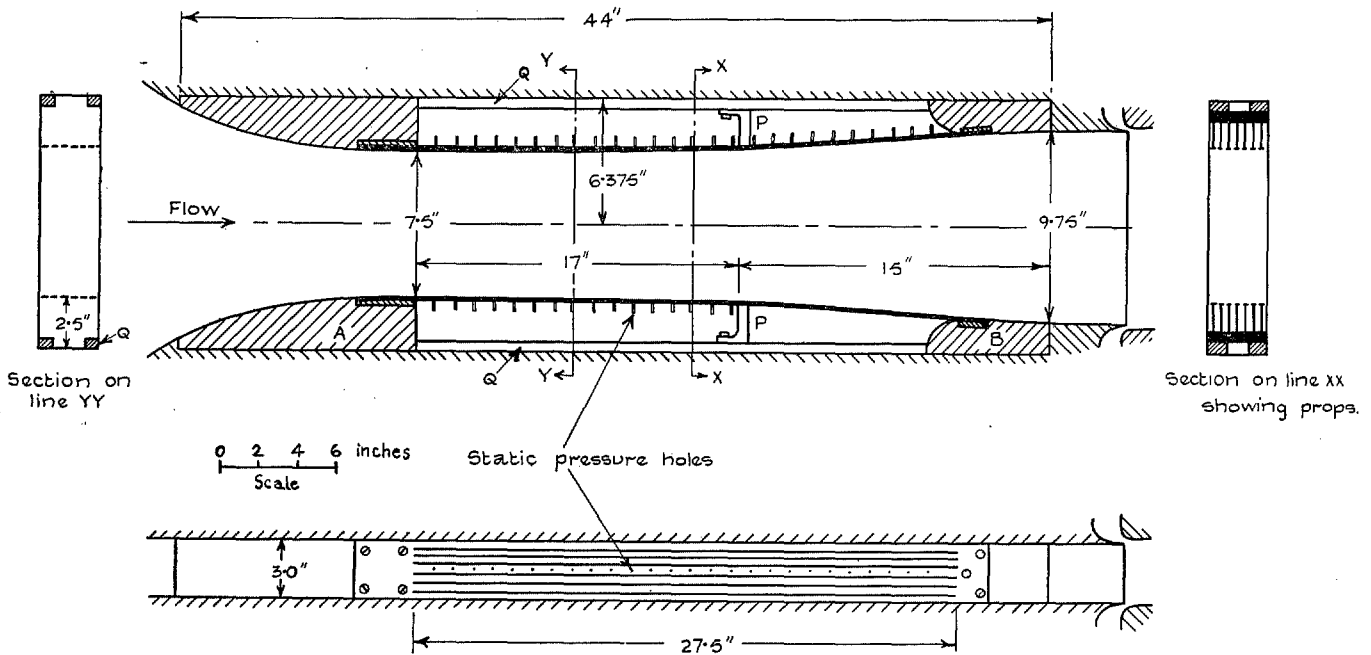
FIG. 7. Details of the walls used in the final tests.

19
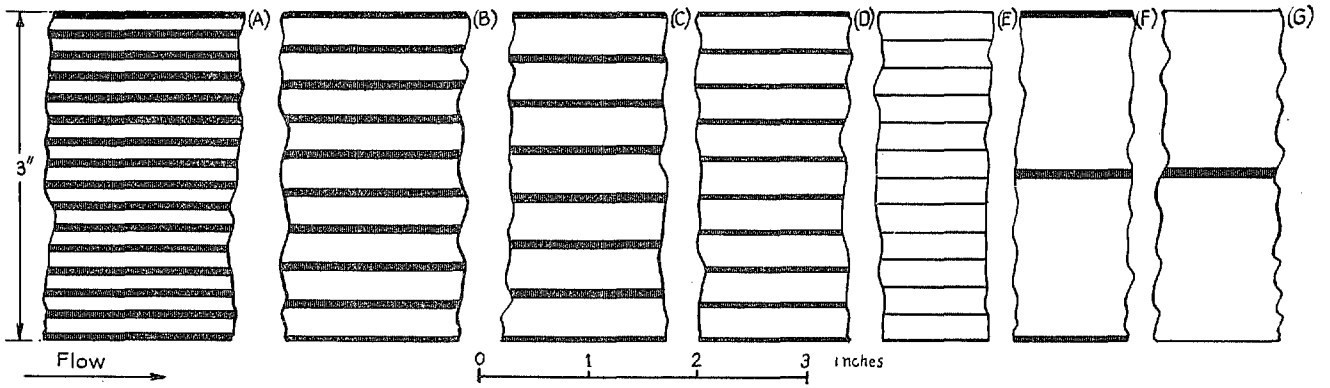
FIG. 8a.   Plan view of slots tested.   For walls H and I *see* Fig. 9.
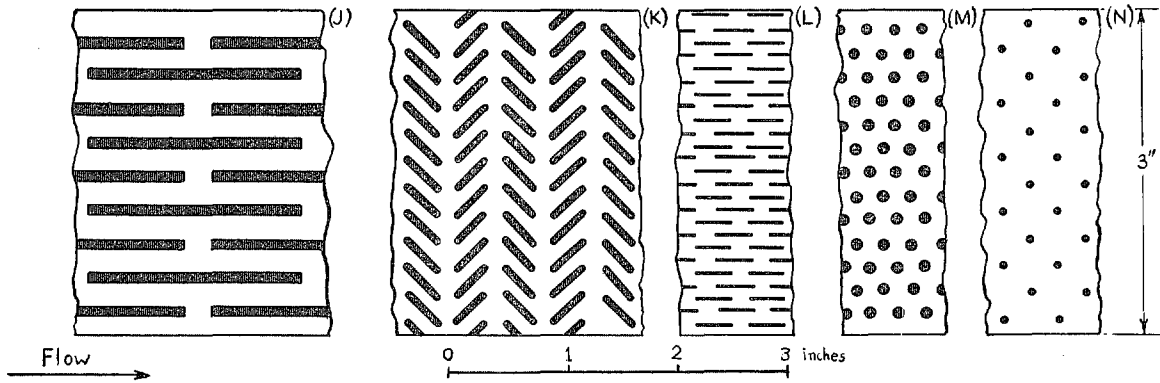
FIG. 8b.   Shapes of perforations tested.
Note: Slots and perforations are shown black.
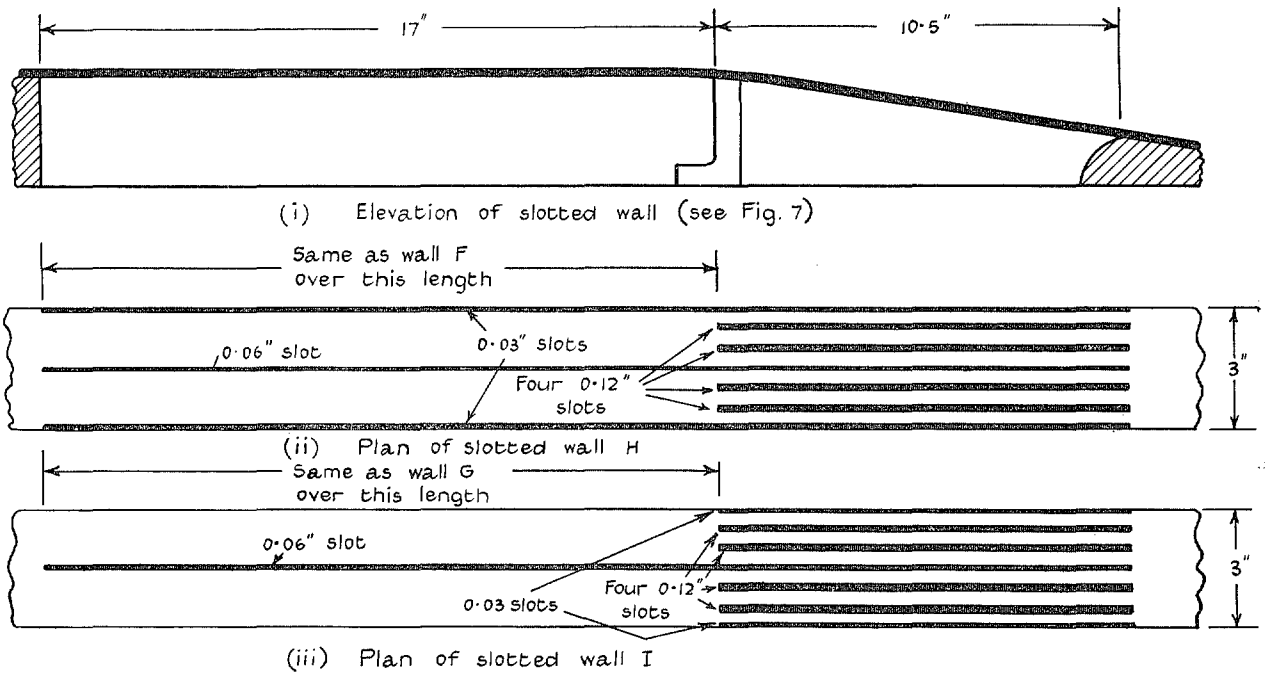
FIG. 9.   Details of the walls with additional slots in the expansion.

20
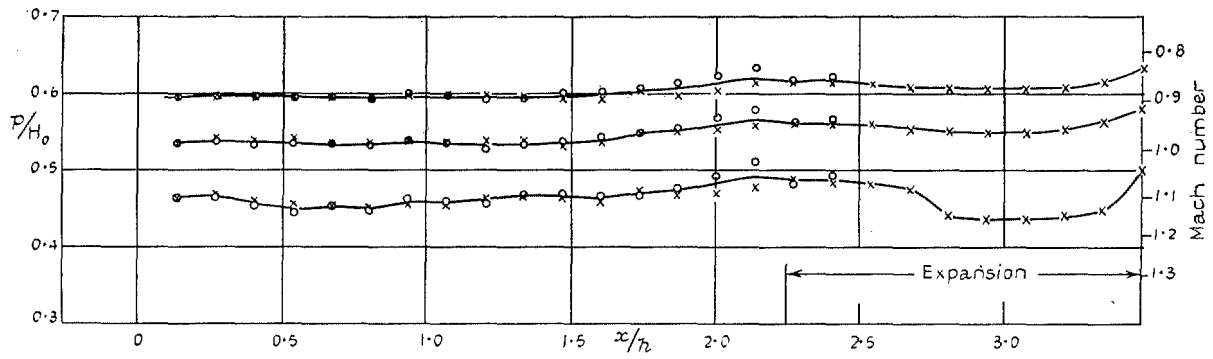
FIG. 10.   Pressure distribution along slotted wall A.   Area ratio = 0·333.
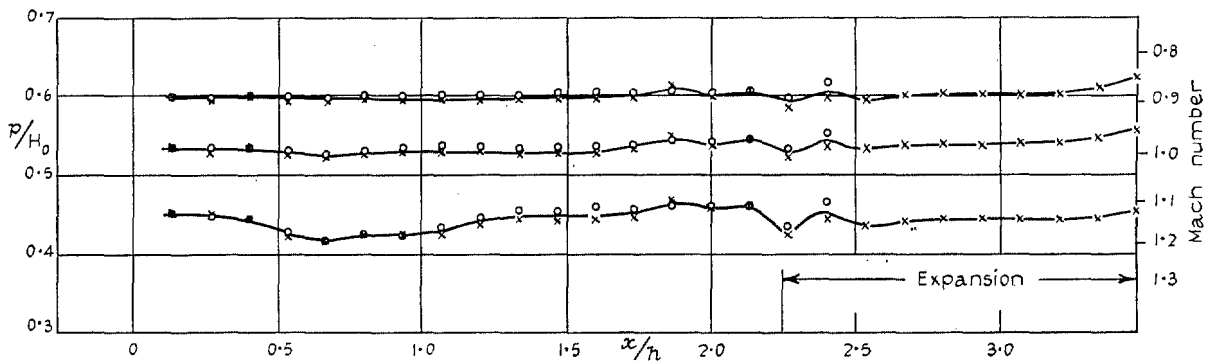
FIG. 11.   Pressure distribution along slotted wall B.   Area ratio = 0·200.
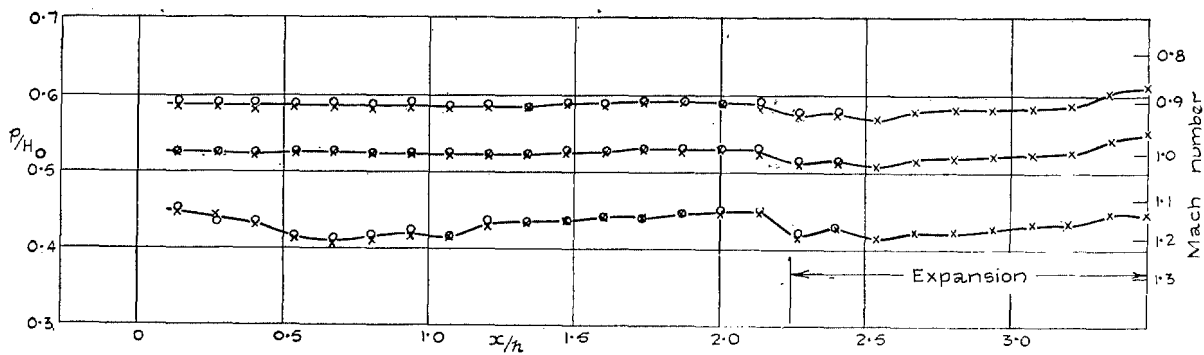
FIG. 12.   Pressure distributions along slotted wall C.   Area ratio = 0·143.
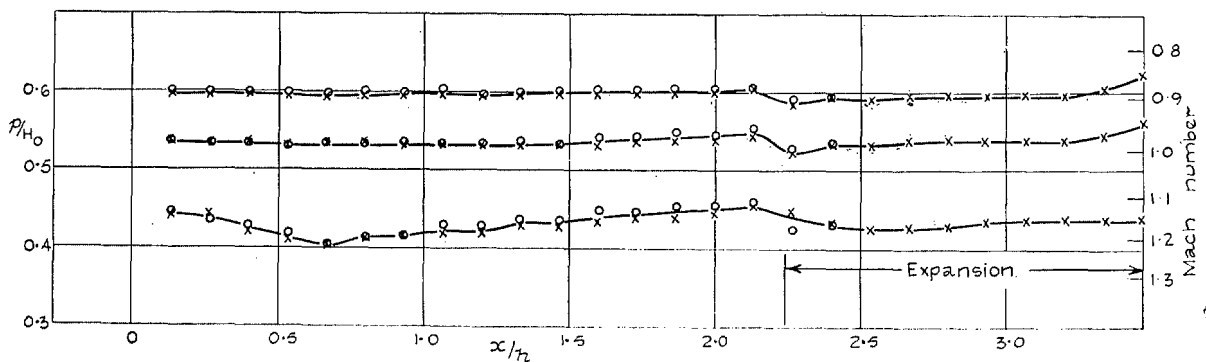
FIG. 13.   Pressure distributions along slotted wall D.   Area ratio = 0·111.

21
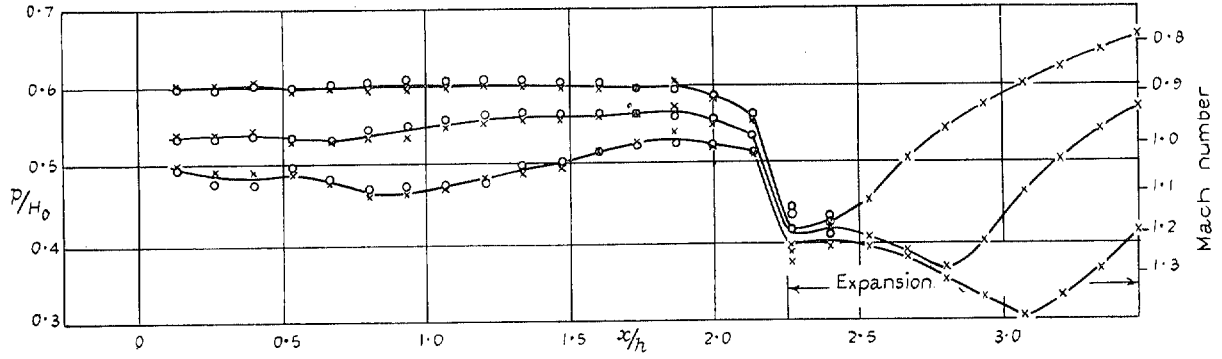
FIG. 14.   Pressure distribution along slotted wall E.   Area ratio = 0·040.
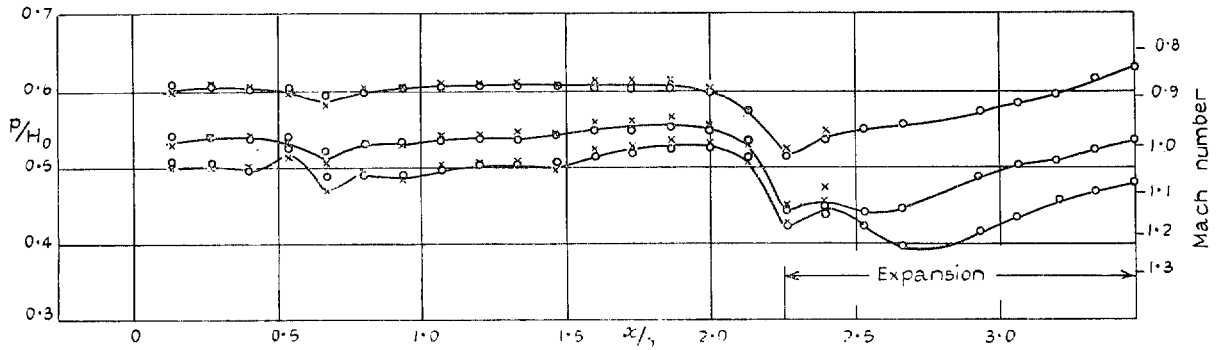
FIG. 15.   Pressure distribution along slotted wall F.   Area ratio = 0·040.
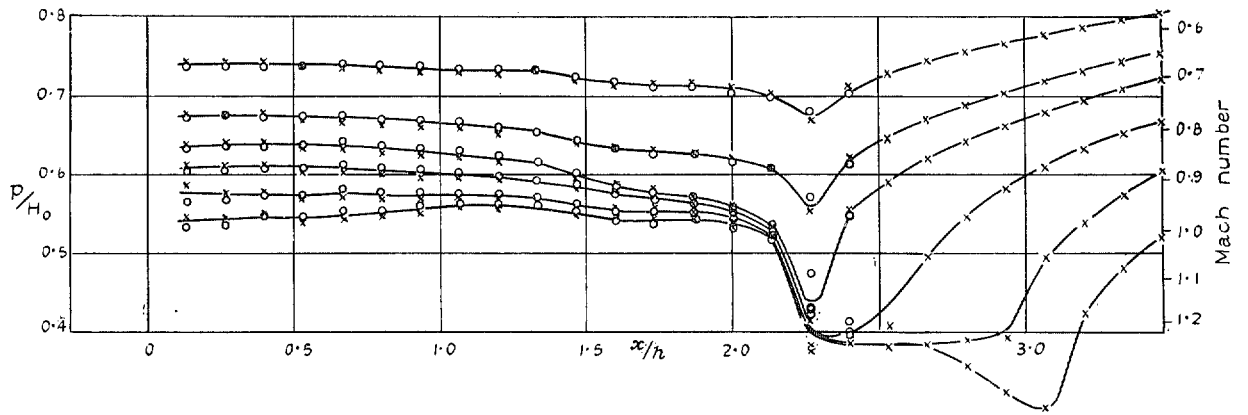
FIG. 16.   Pressure distribution along slotted wall G.   Area ratio = 0·020.
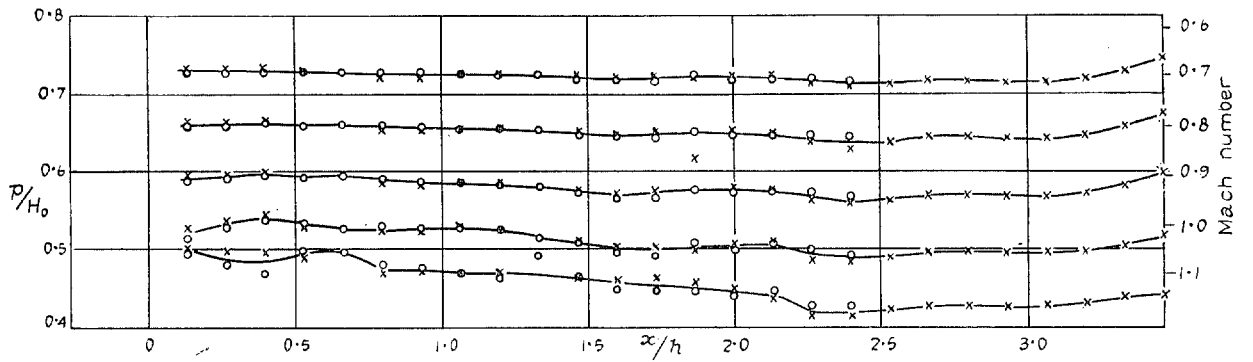
FIG. 17.   Pressure distribution along slotted wall H.   Area ratio = 0·040 with additional slots in expansion.

22
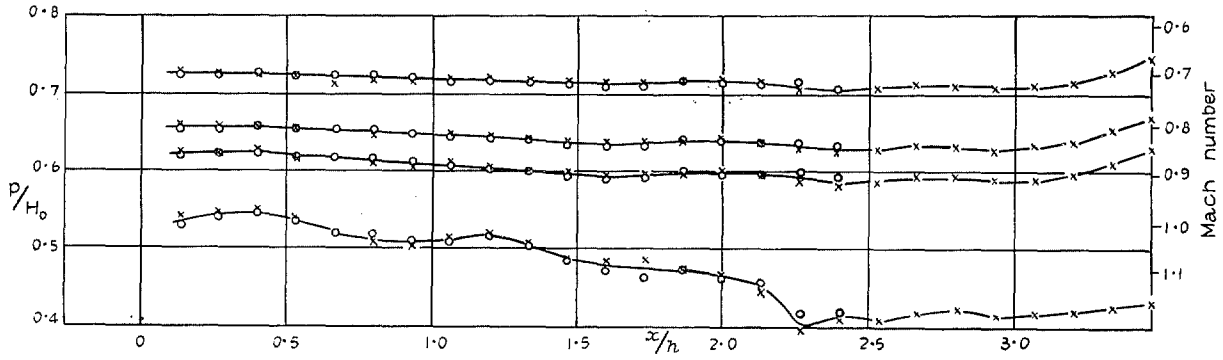
FIG. 18. Pressure distribution along slotted wall I. Area ratio = 0·020 with additional slots in expansion.
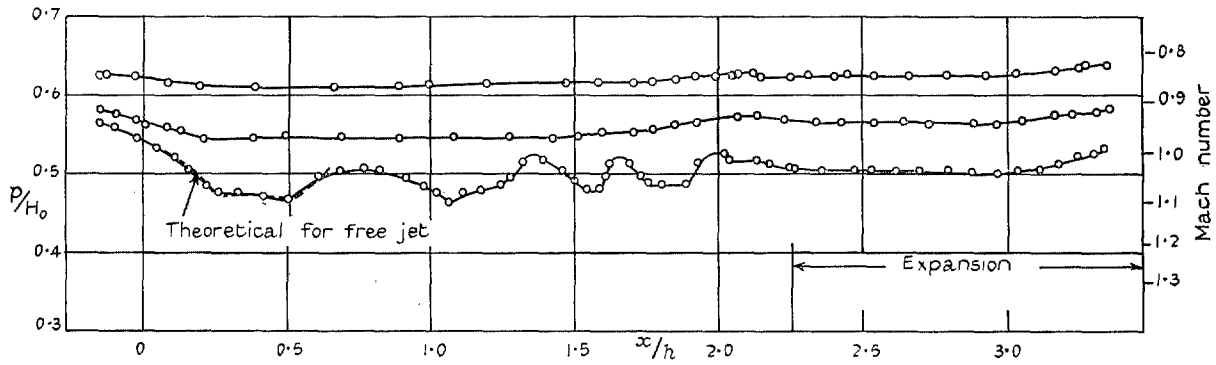
FIG. 19. Pressure distributions along axis with slotted wall A. Area ratio = 0·333.
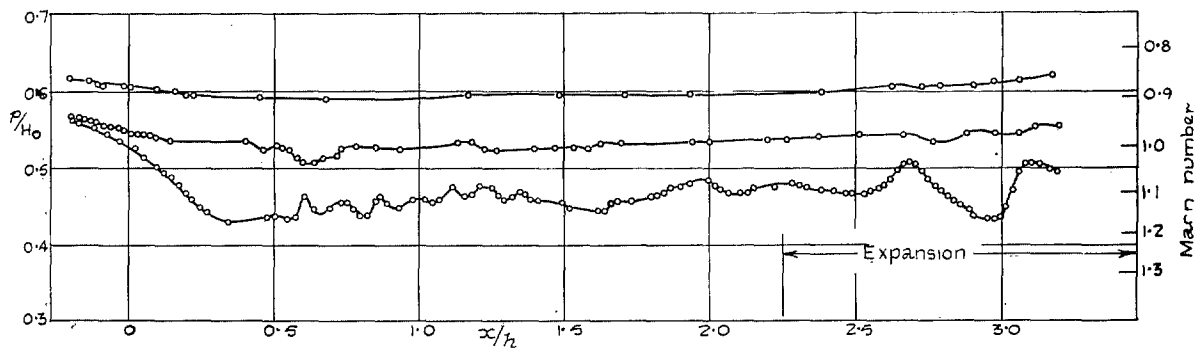
FIG. 20. Pressure distributions along axis with slotted wall B. Area ratio = 0·200.
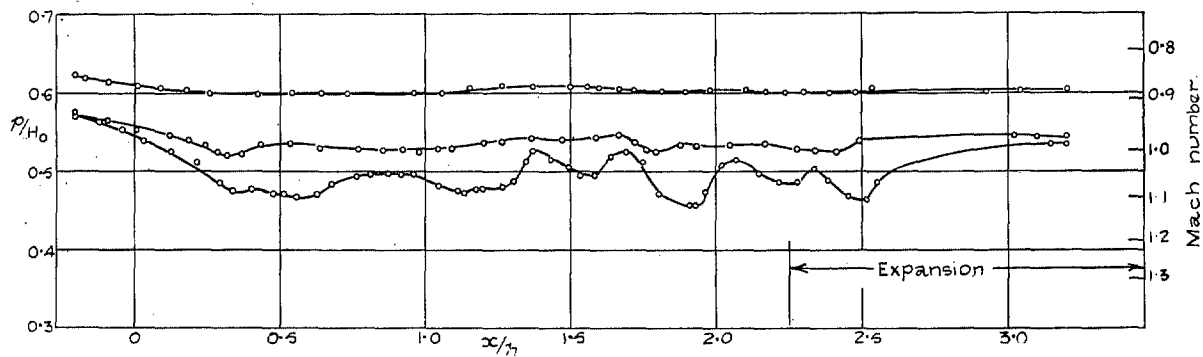
FIG. 21. Pressure distributions along axis with slotted wall C. Area ratio = 0·143.

23
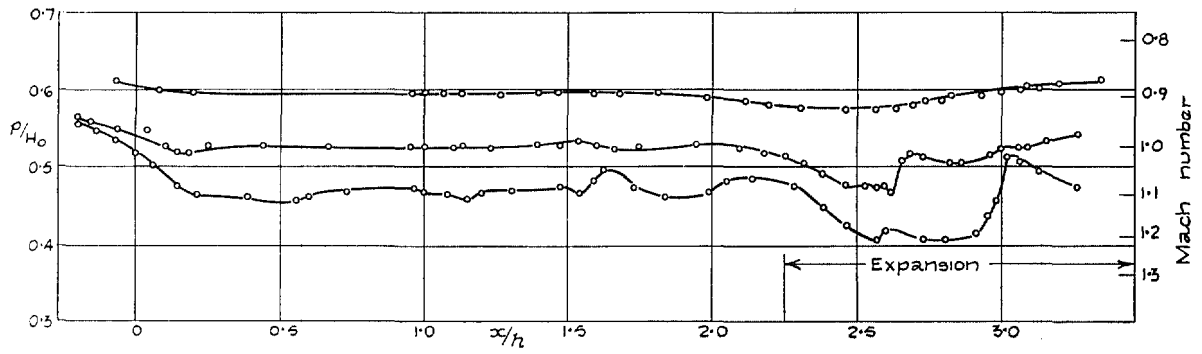
FIG. 22.   Pressure distributions along axis with slotted wall D.   Area ratio = 0·111.
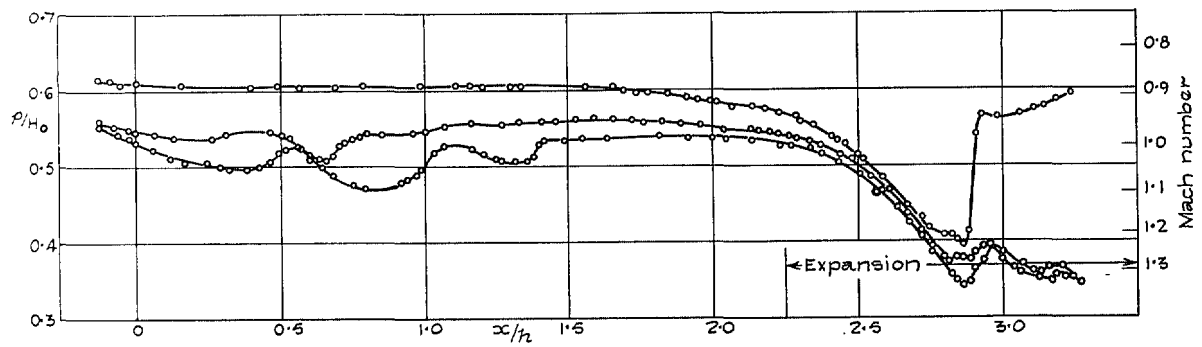
FIG. 23.   Pressure distributions along axis with slotted wall E.   Area ratio = 0·040.
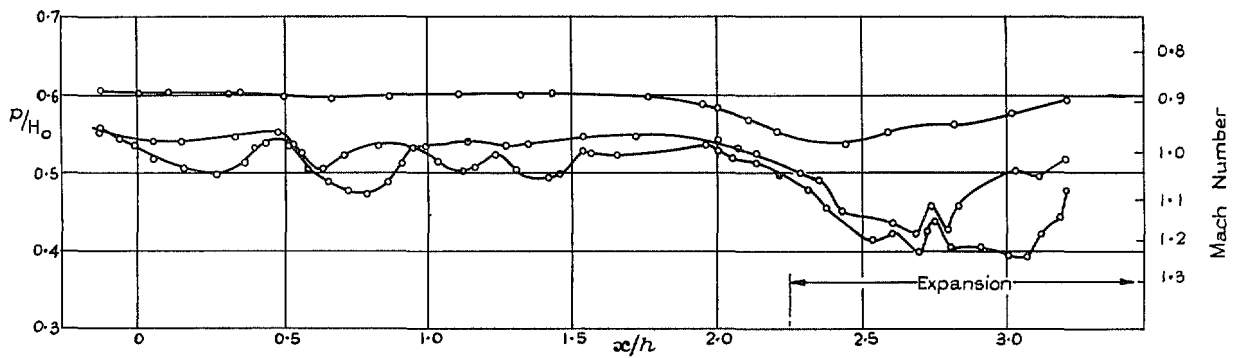
FIG. 24.   Pressure distributions along axis with slotted wall F.   Area ratio = 0·040.
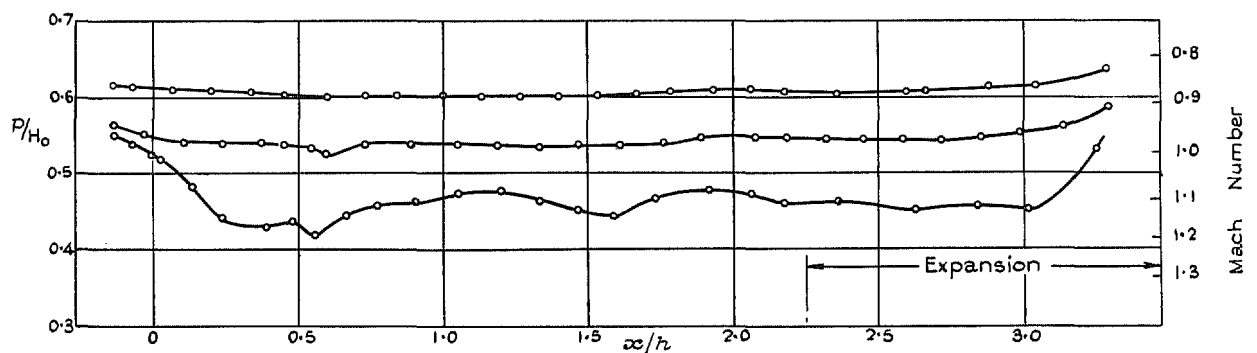
FIG. 25.   Pressure distributions along axis with perforated wall J.   Area ratio = 0·262.
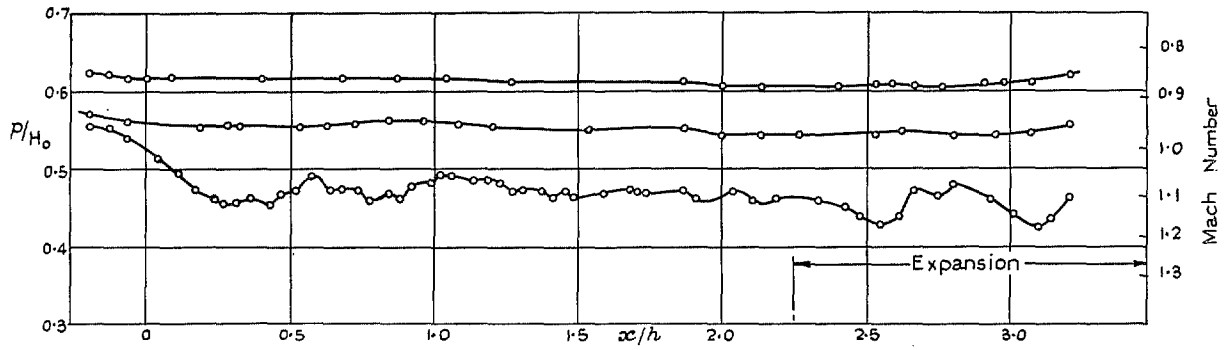
FIG. 26.   Pressure distributions along axis with perforated wall K.   Area ratio = 0·232.
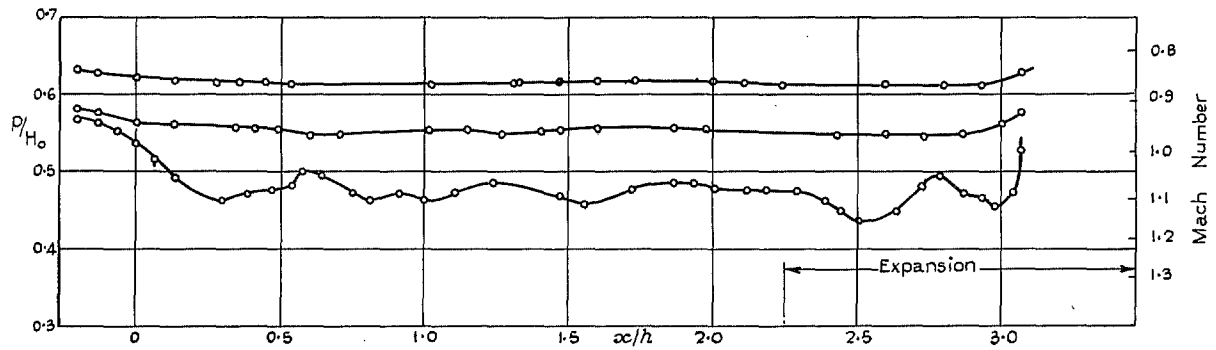
FIG. 27.   Pressure distributions along axis with perforated wall L.   Area ratio = 0·171.
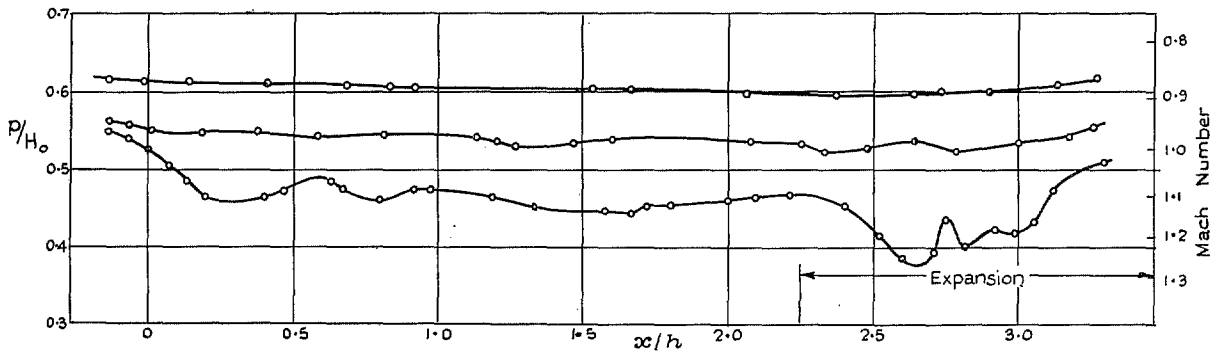
FIG. 28.   Pressure distributions along axis with perforated wall M.   Area ratio = 0·170.
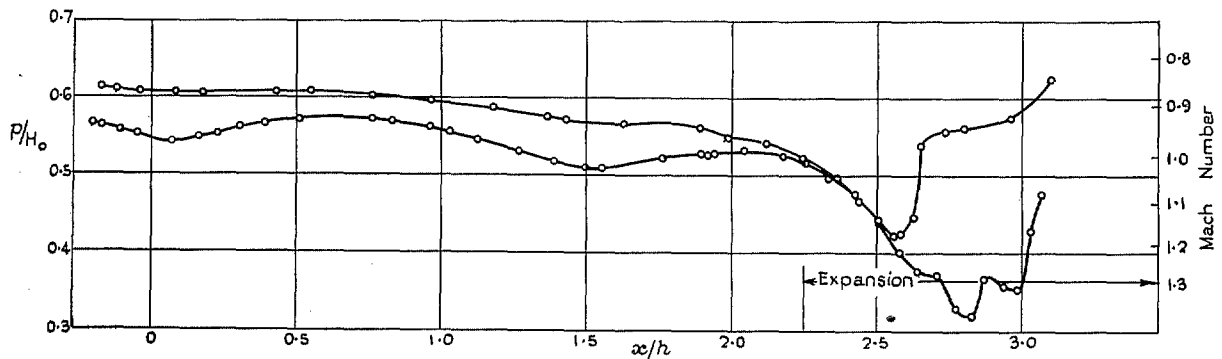
FIG. 29.   Pressure distributions along axis with perforated wall N.   Area ratio = 0·030.

25
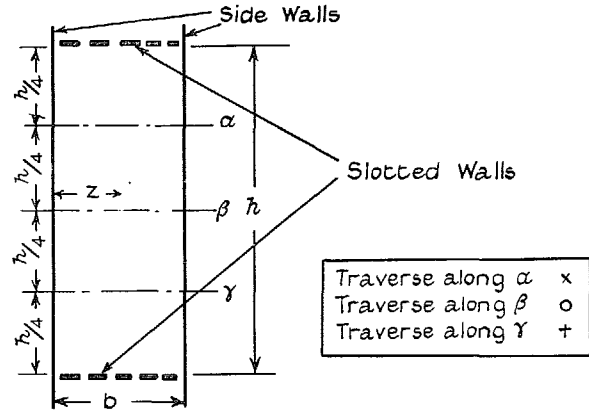
FIG. 30a.   Sketch showing positions of traverse lines.

FIG. 30d.   Wall C.   Area ratio $= 0\cdot143$.

FIG. 30b.   Wall A.   Area ratio $= 0\cdot333$.

FIG. 30e.   Wall D.   Area ratio $= 0\cdot111$.

FIG. 30c.   Wall B.   Area ratio $= 0\cdot200$.
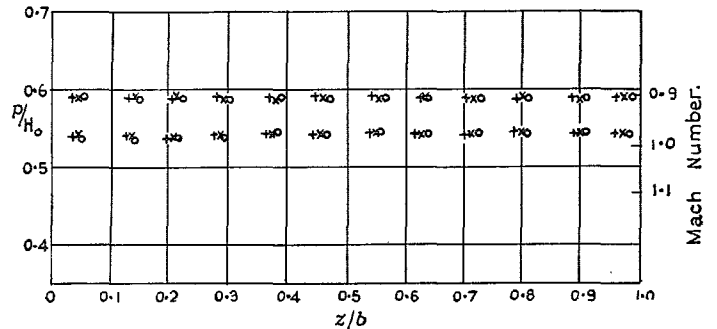
FIG. 30f.   Wall E.   Area ratio $= 0\cdot040$.

FIGS. 30b to 30f.   Pressure distributions across the empty slotted tunnel at $x/h = 1\cdot5$.

26
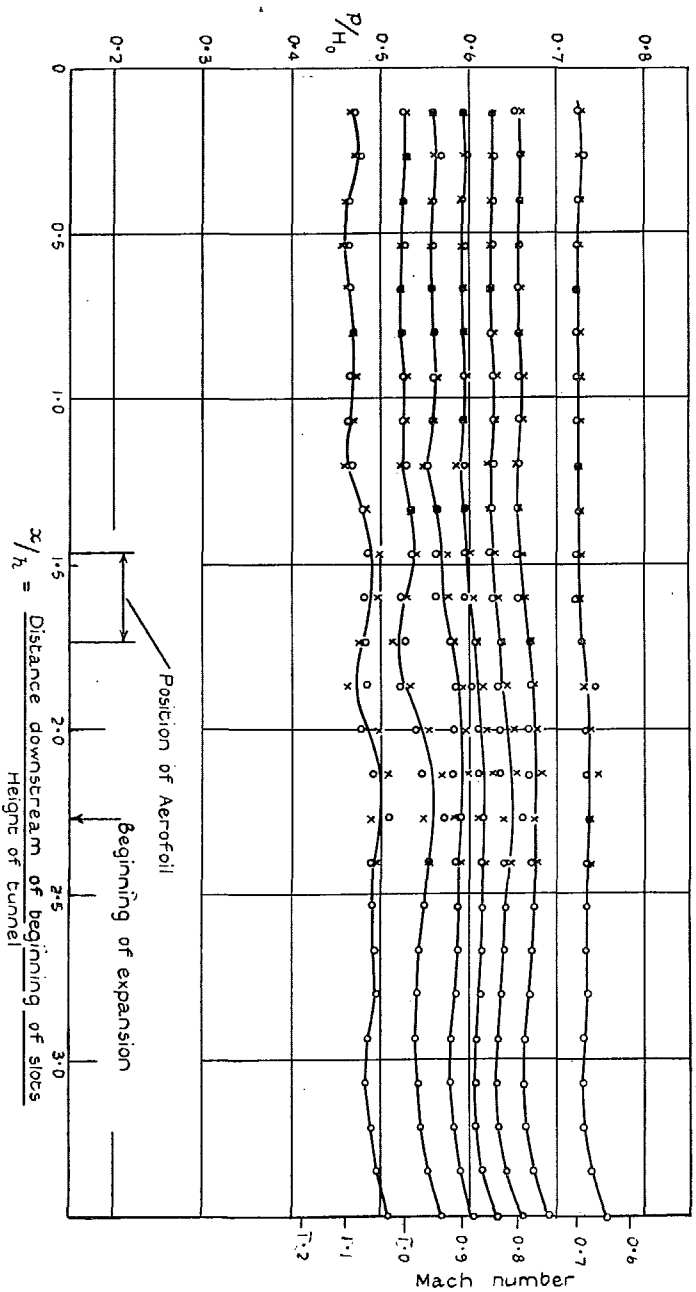
FIG. 32. Wall pressures with RAE 104 aerofoil at $\alpha = 0$ deg. Wall A. Area ratio $= 0.333$.

27

p/H_0

$x/h = \dfrac{\text{Distance downstream of beginning of slots}}{\text{Height of tunnel}}$

Mach number
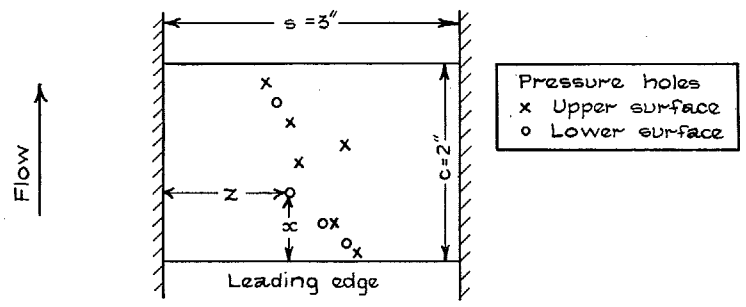
FIG. 31a. Model for the 9-in. × 3-in. Tunnel.

Pressure holes
x Upper surface
o Lower surface

Flow
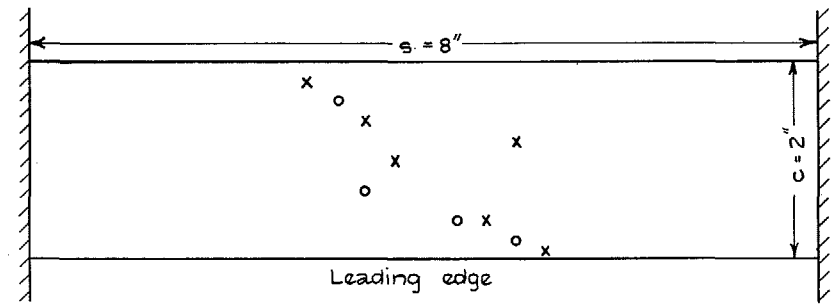
FIG. 31b. Model for the 20-in. × 8-in. Tunnel.

Positions of pressure holes.									
x/c	0.05	0.10	0.20	0.35	0.50	0.60	0.70	0.80	0.90
z/s for 20"×8" tunnel X	0.653		0.578		0.460	0.616	0.422		0.347
o		0.616	0.540	0.422				0.384	
z/s for 9"×3" tunnel X	0.662		0.582		0.458	0.622	0.418		0.338
o		0.622	0.542	0.418				0.378	
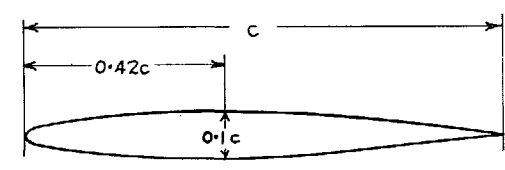
FIG. 31c. Section shape.

FIG. 31. Details of the RAE 104 aerofoils.
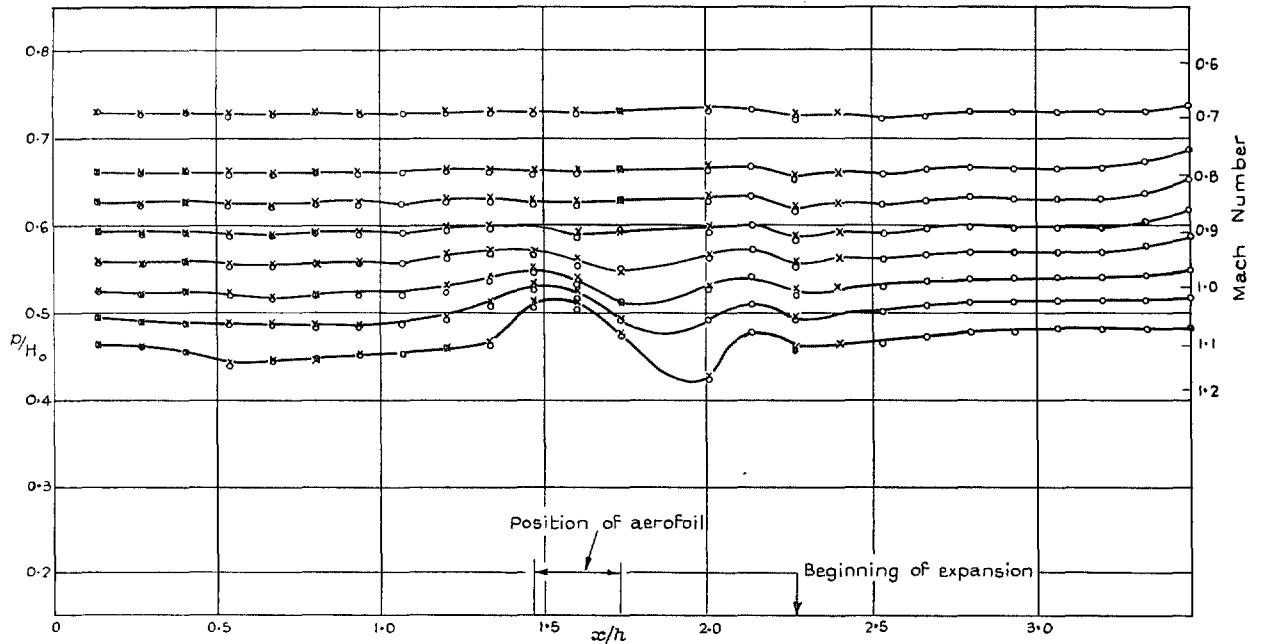
Fig. 33. Wall pressures with RAE 104 aerofoil at $\alpha = 0$ deg. Wall B. Area ratio $= 0 \cdot 200$.
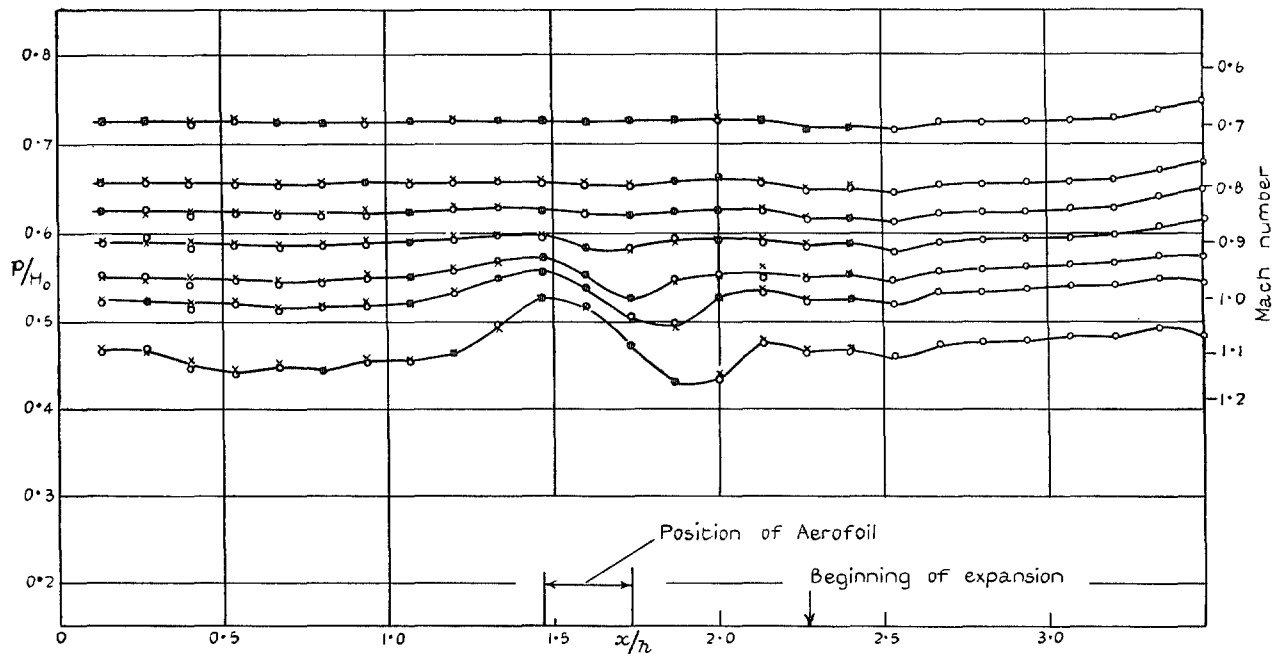
Fig. 34. Wall pressures with RAE 104 aerofoil at $\alpha = 0$ deg. Wall C. Area ratio $= 0 \cdot 143$.

28
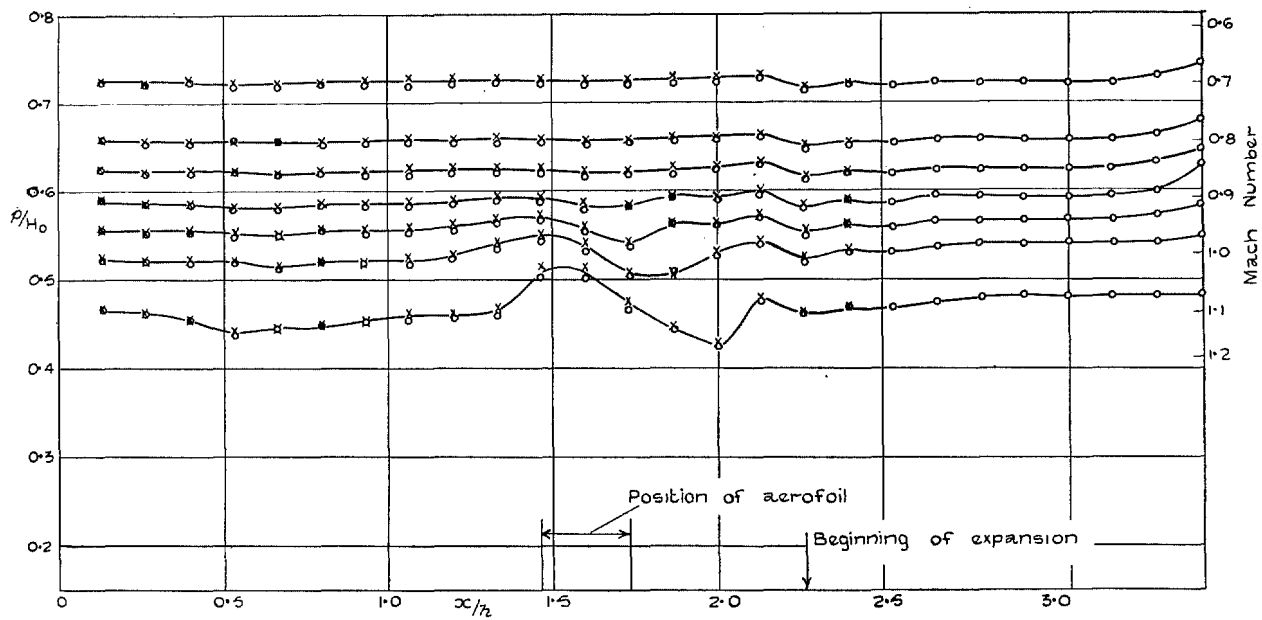
FIG. 35. Wall pressures with RAE 104 aerofoil at $\alpha = 0$ deg. Wall D. Area ratio $= 0 \cdot 111$.
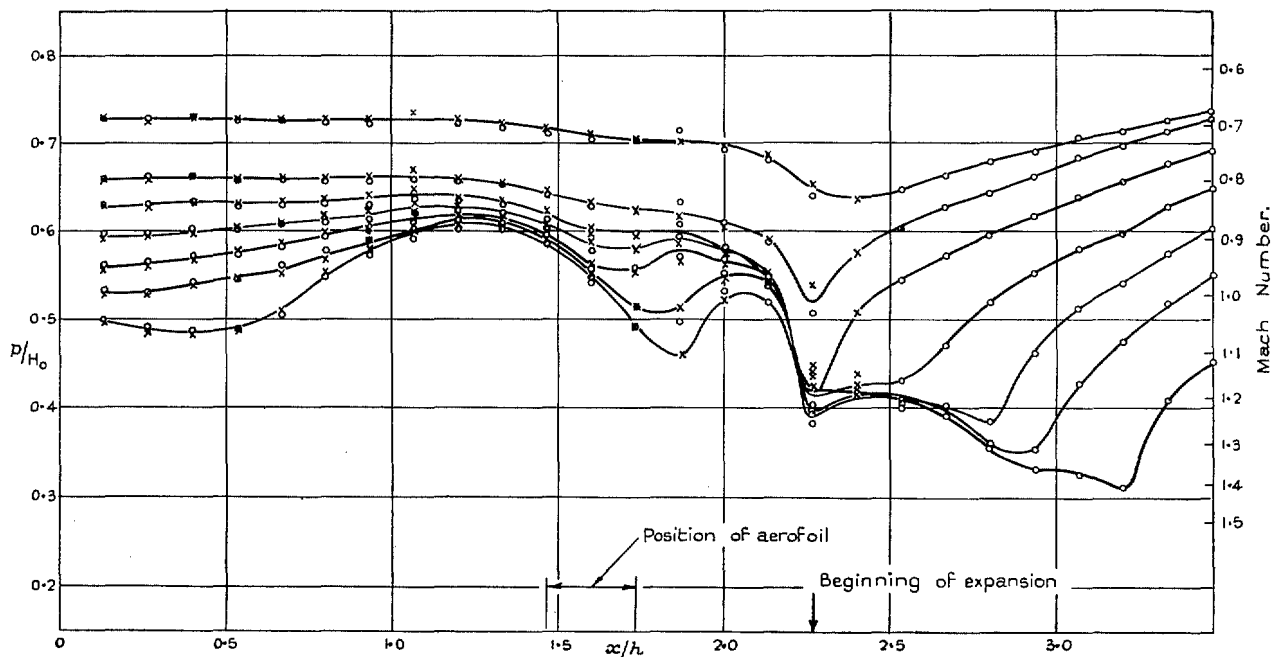
FIG. 36. Wall pressures with RAE 104 aerofoil at $\alpha = 0$ deg. Wall E. Area ratio $= 0 \cdot 040$.

29
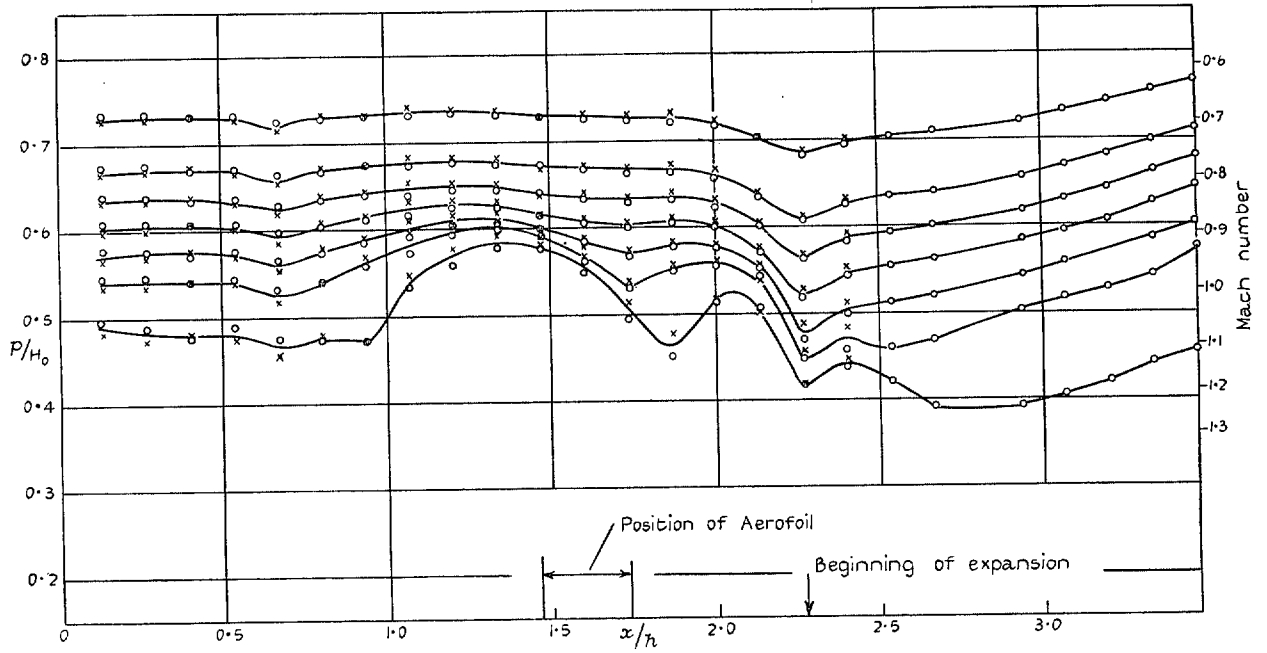
FIG. 37.   Wall pressures with RAE 104 aerofoil at $\alpha = 0$ deg.   Wall F.   Area ratio $= 0 \cdot 040$.
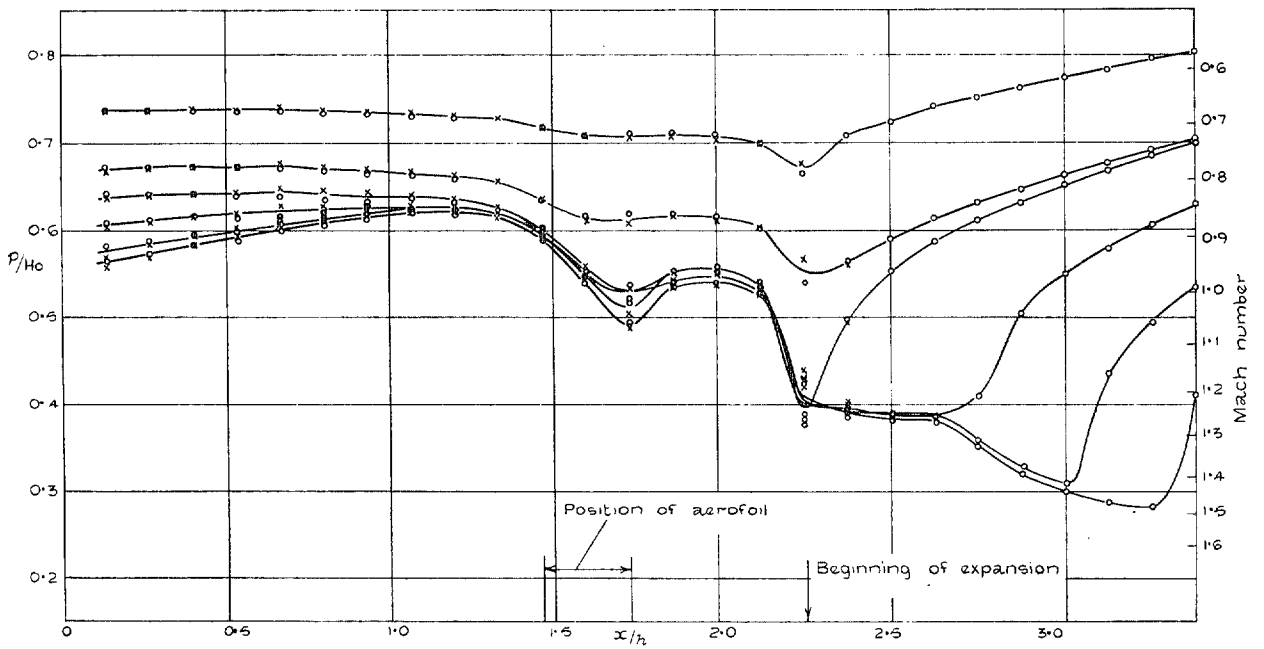
FIG. 38.   Wall pressures with RAE 104 aerofoil at $\alpha = 0$ deg.   Wall G.   Area ratio $= 0 \cdot 020$.

30
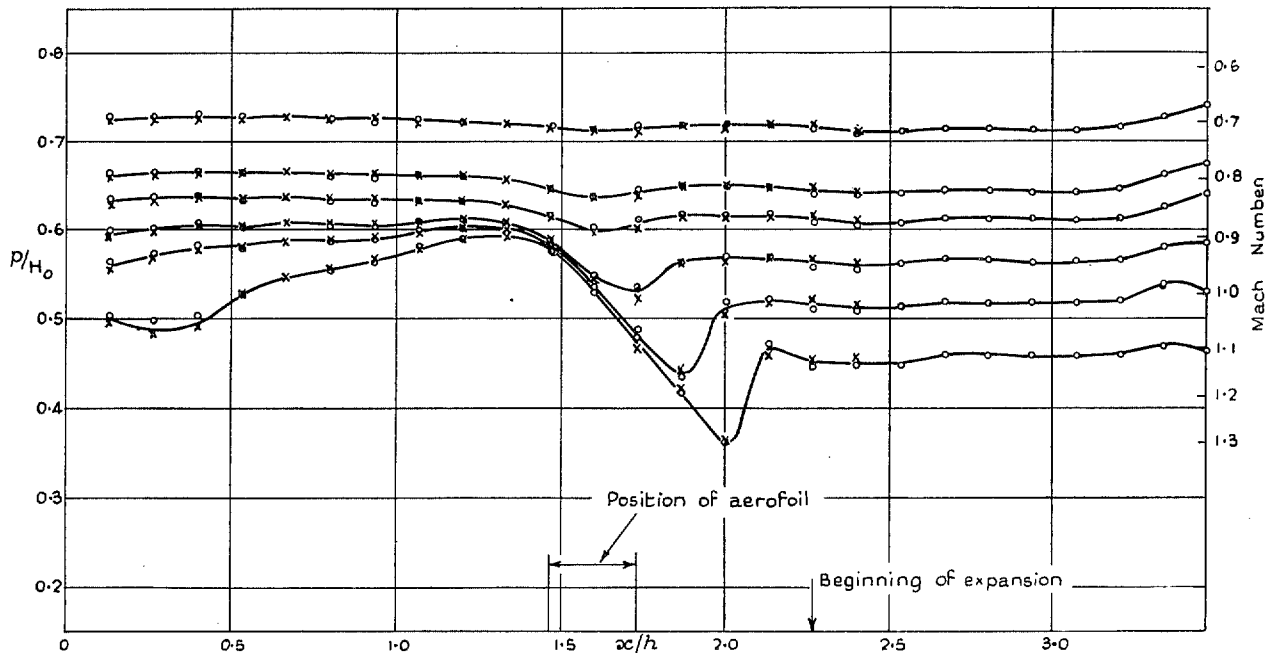
FIG. 39. Wall pressures with RAE 104 aerofoil at α = 0 deg. Wall H. Area ratio = 0·040.
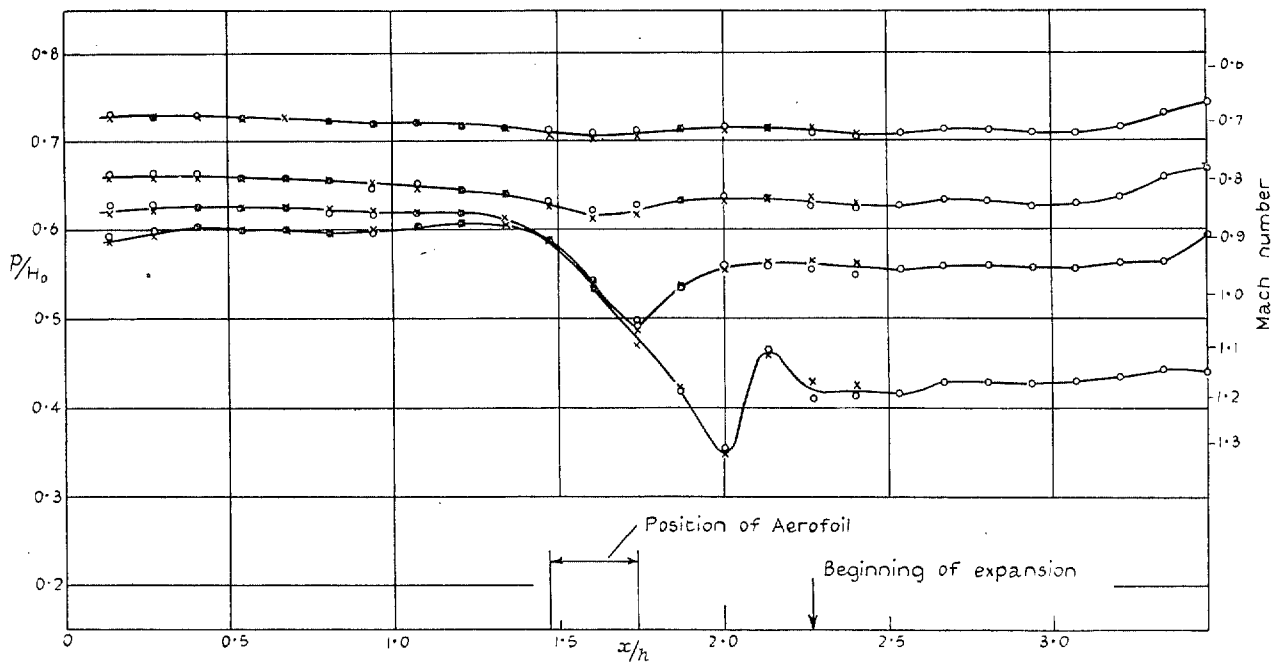
FIG. 40. Wall pressures with RAE 104 aerofoil at α = 0 deg. Wall I. Area ratio = 0·020.

31
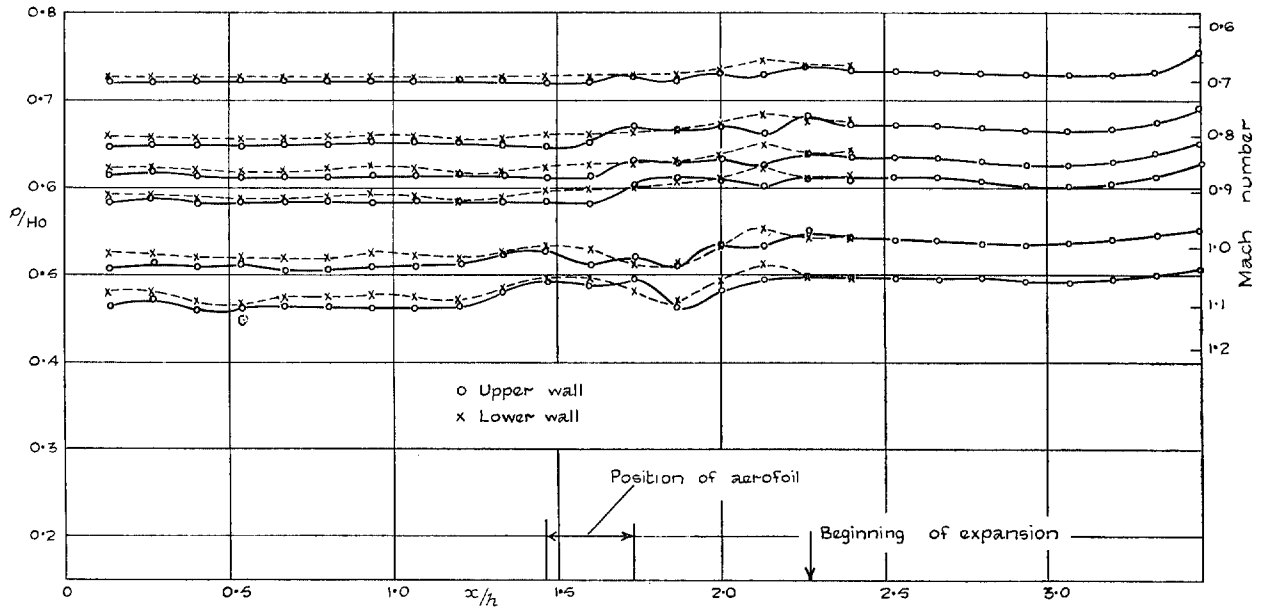
FIG. 41.   Wall pressures with RAE 104 aerofoil at α = + 2 deg.   Wall A.   Area ratio = 0·333.
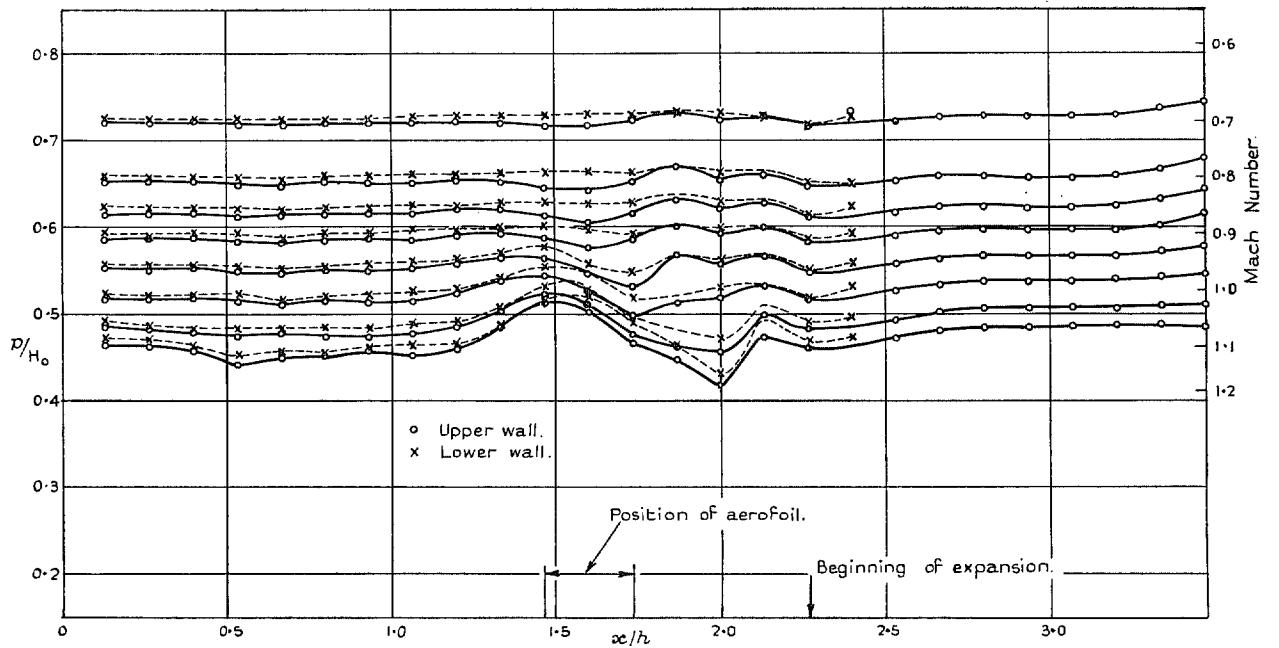
FIG. 42.   Wall pressures with RAE 104 aerofoil at α = + 2 deg.   Wall B.   Area ratio = 0·200.
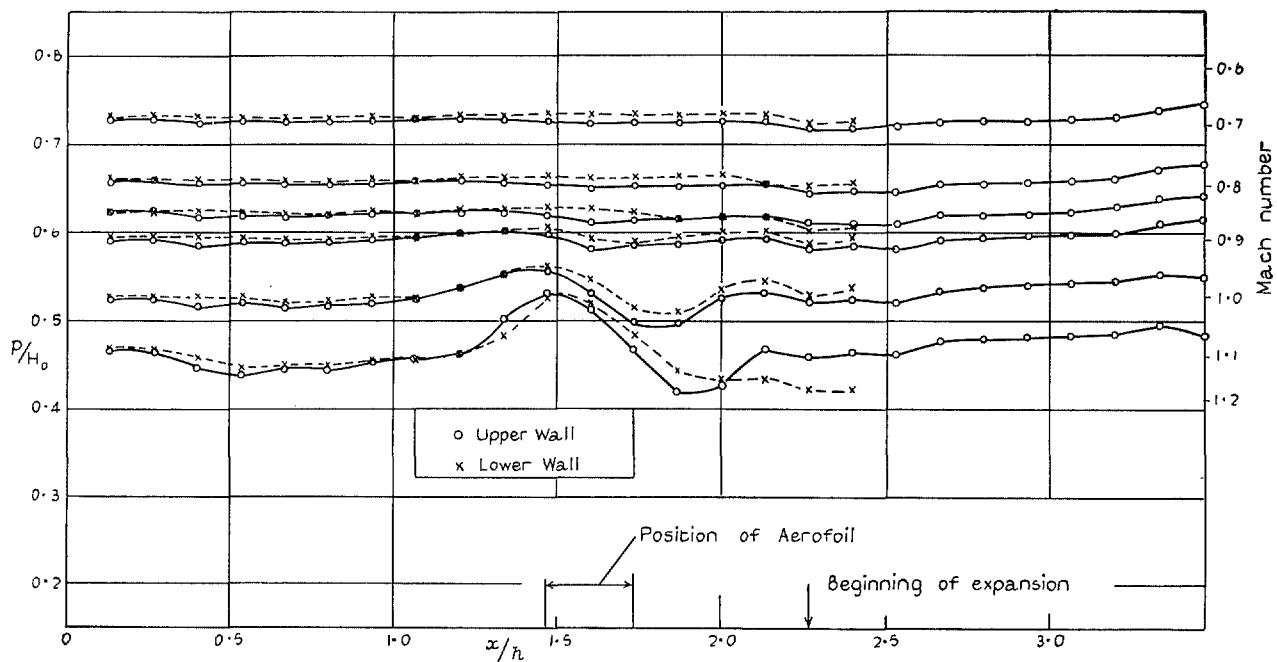
FIG. 43. Wall pressures with RAE 104 aerofoil at α = + 2 deg. Wall C. Area ratio = 0·143.
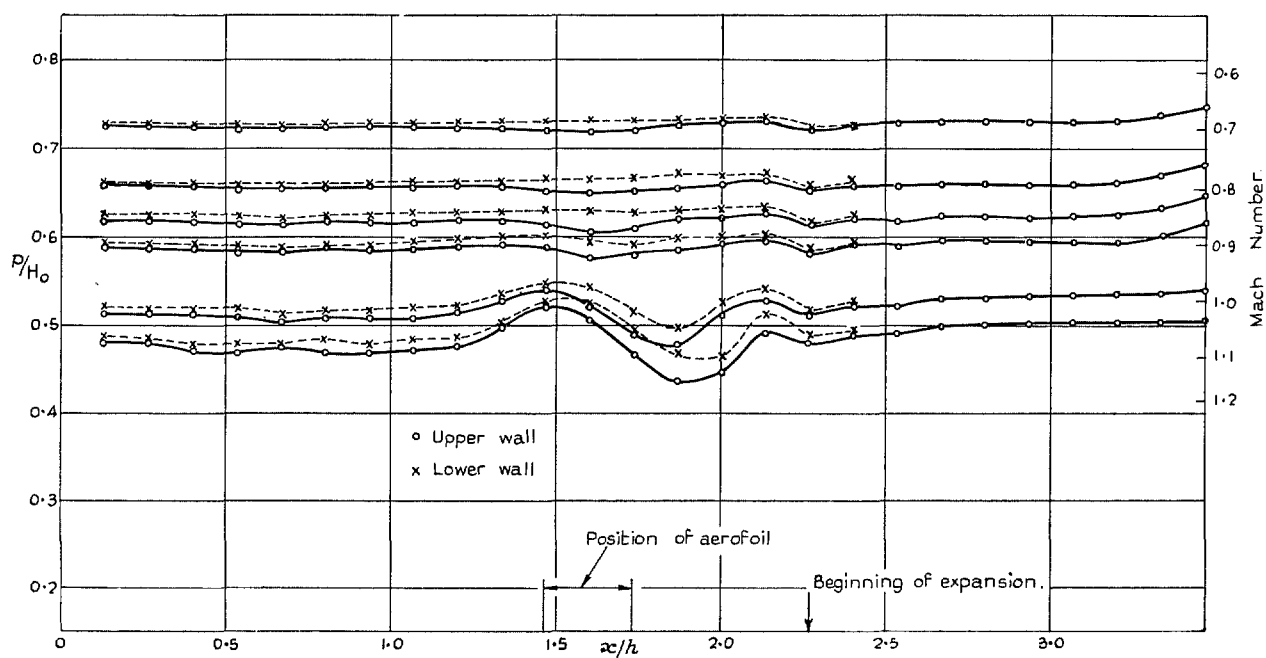
FIG. 44. Wall pressures with RAE 104 aerofoil at α = + 2 deg. Wall D. Area ratio = 0·111.

33
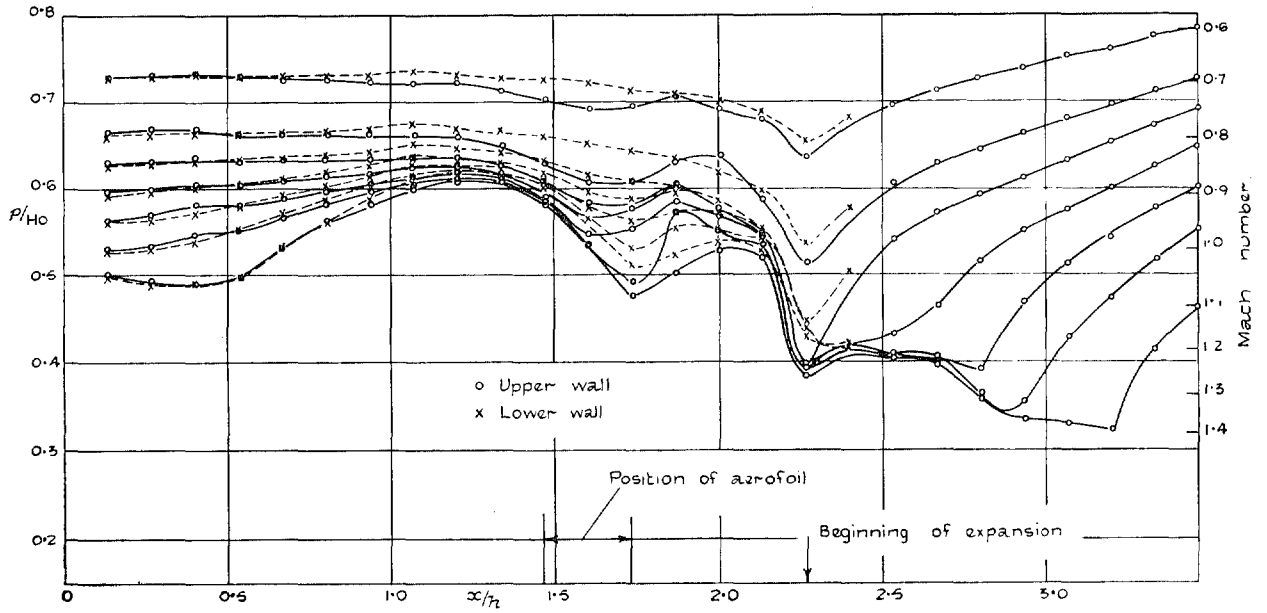
FIG. 45.   Wall pressures with RAE 104 aerofoil at α = + 2 deg.   Wall E.   Area ratio = 0·040.
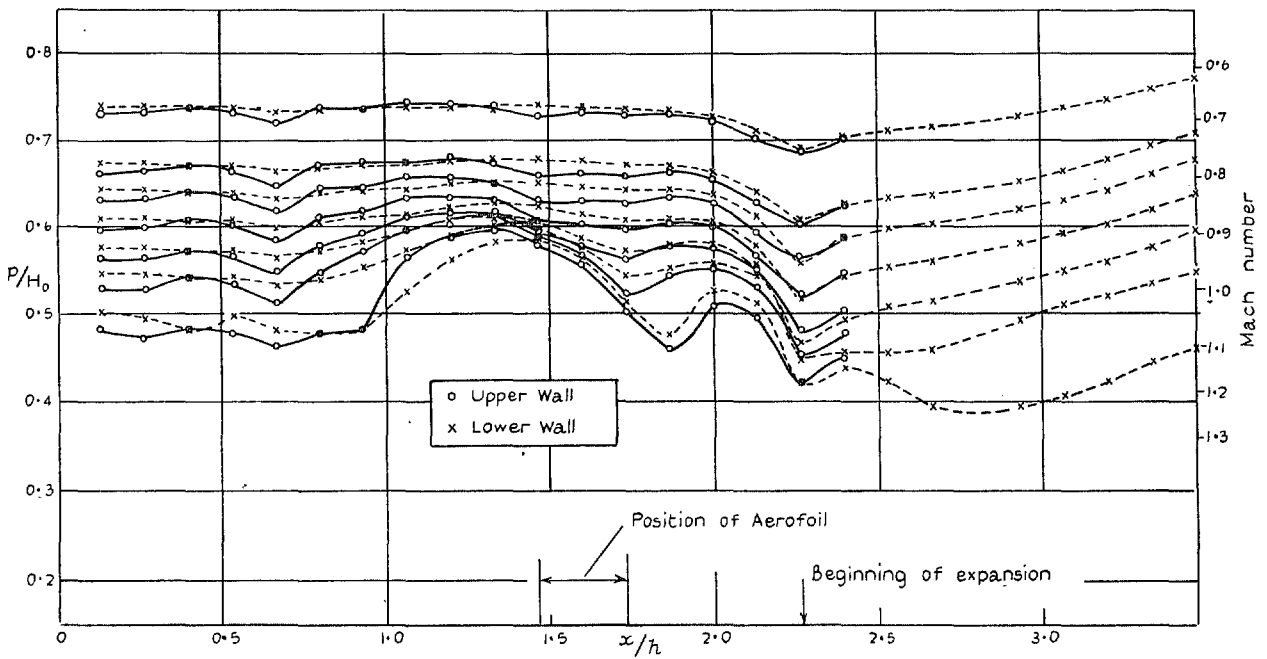
FIG. 46.   Wall pressures with RAE 104 aerofoil at α = + 2 deg.   Wall F.   Area ratio = 0·040.

34
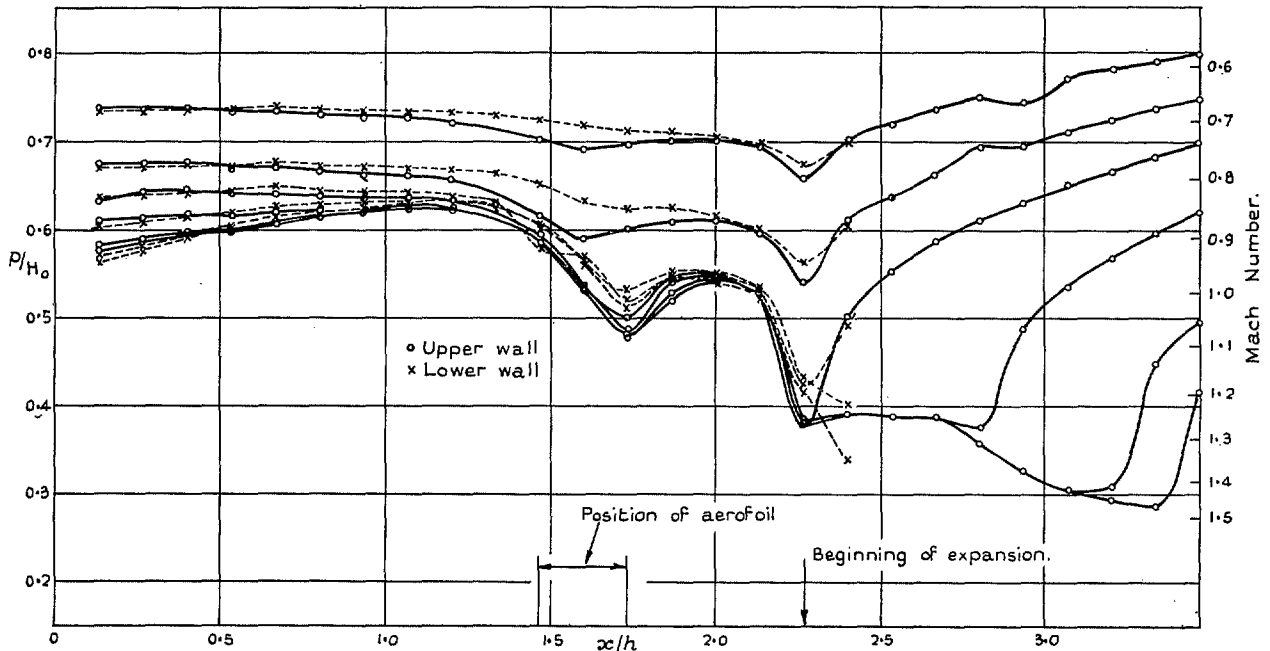
FIG. 47. Wall pressures with RAE 104 aerofoil at $\alpha = +2$ deg. Wall G. Area ratio $= 0 \cdot 020$.
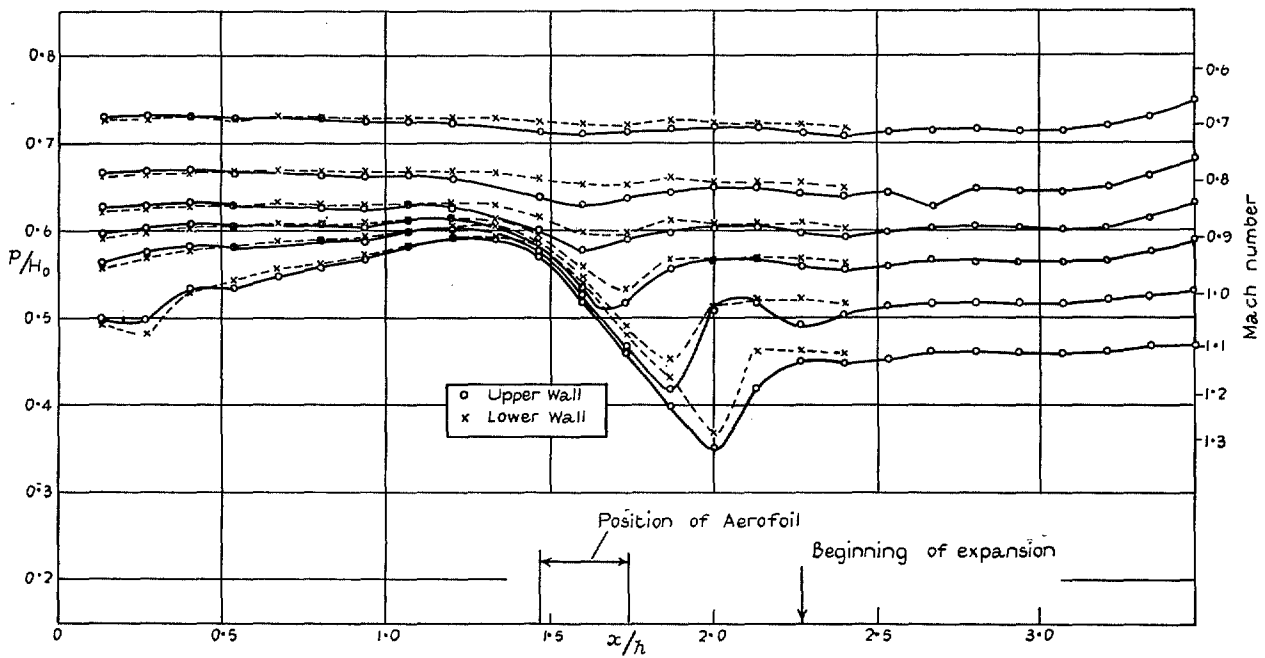
FIG. 48. Wall pressures with RAE 104 aerofoil at $\alpha = +2$ deg. Wall H. Area ratio $= 0 \cdot 040$.

35
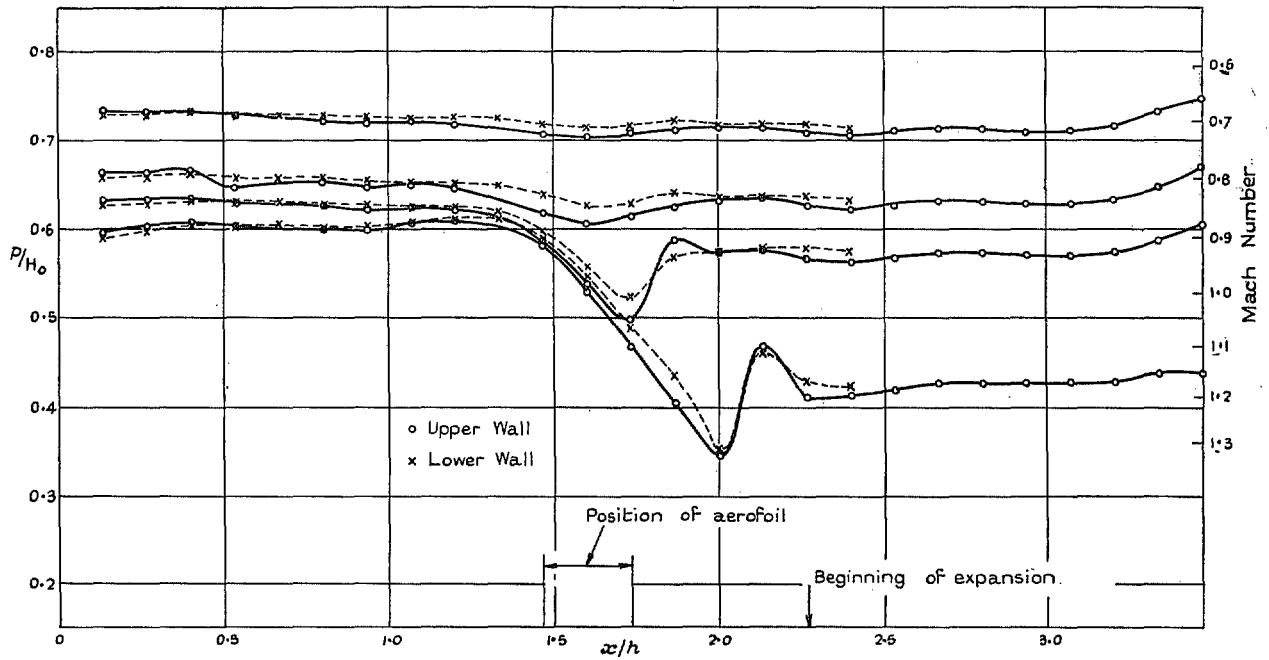
FIG. 49. Wall pressures with RAE 104 aerofoil at $\alpha = +2$ deg. Wall I. Area ratio $= 0 \cdot 020$.
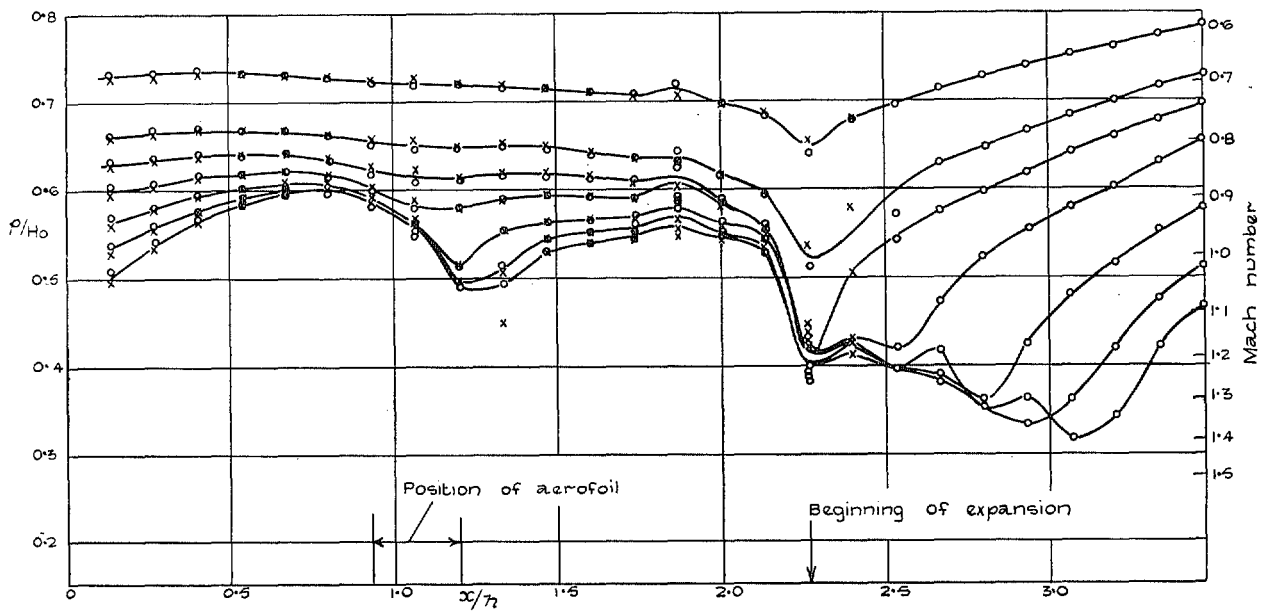
FIG. 50. Wall pressures with RAE 104 aerofoil at $\alpha = 0$ deg. Wall F. Area ratio $= 0 \cdot 040$.
Aerofoil in upstream position.

36
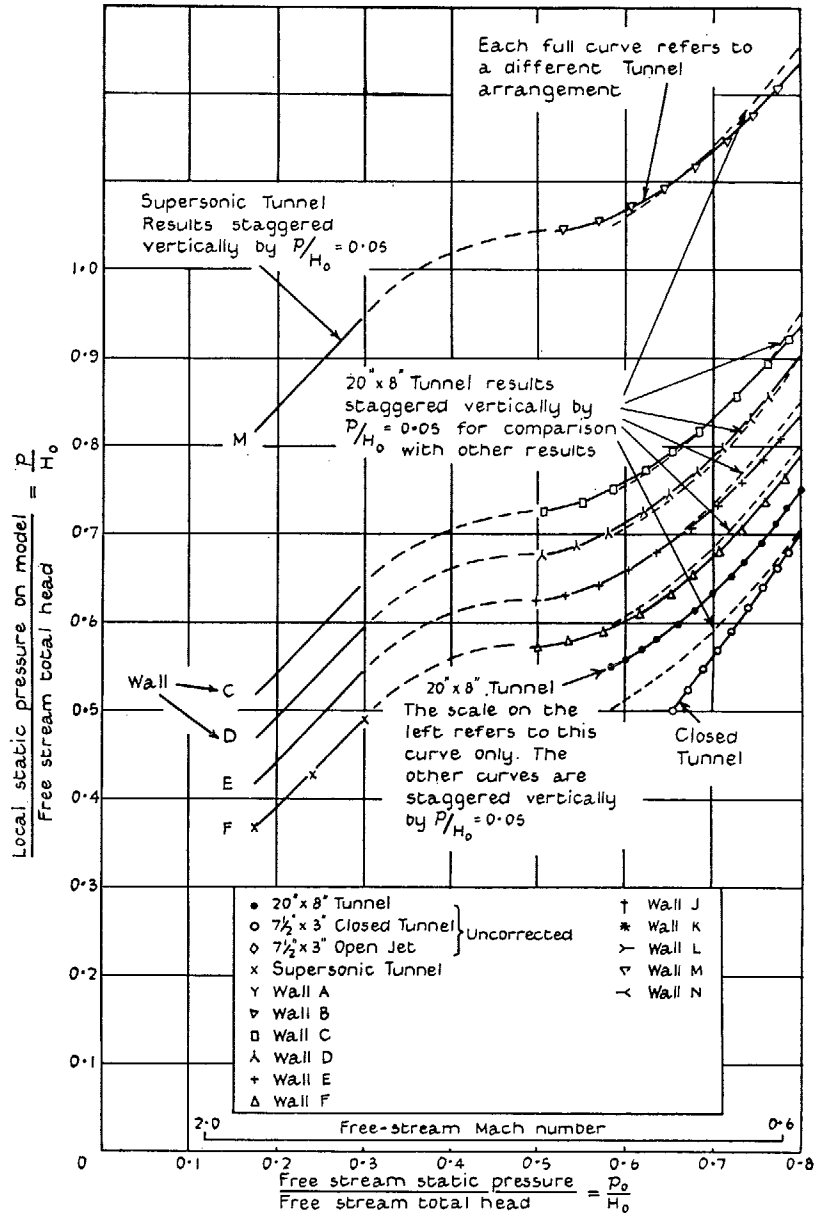
FIG. 51. Sketch illustrating the method of plotting in Figs. 52 to 60. Each curve applies to a particular point on the chord and, for tests at incidence, to either the upper or lower surface of the aerofoil.
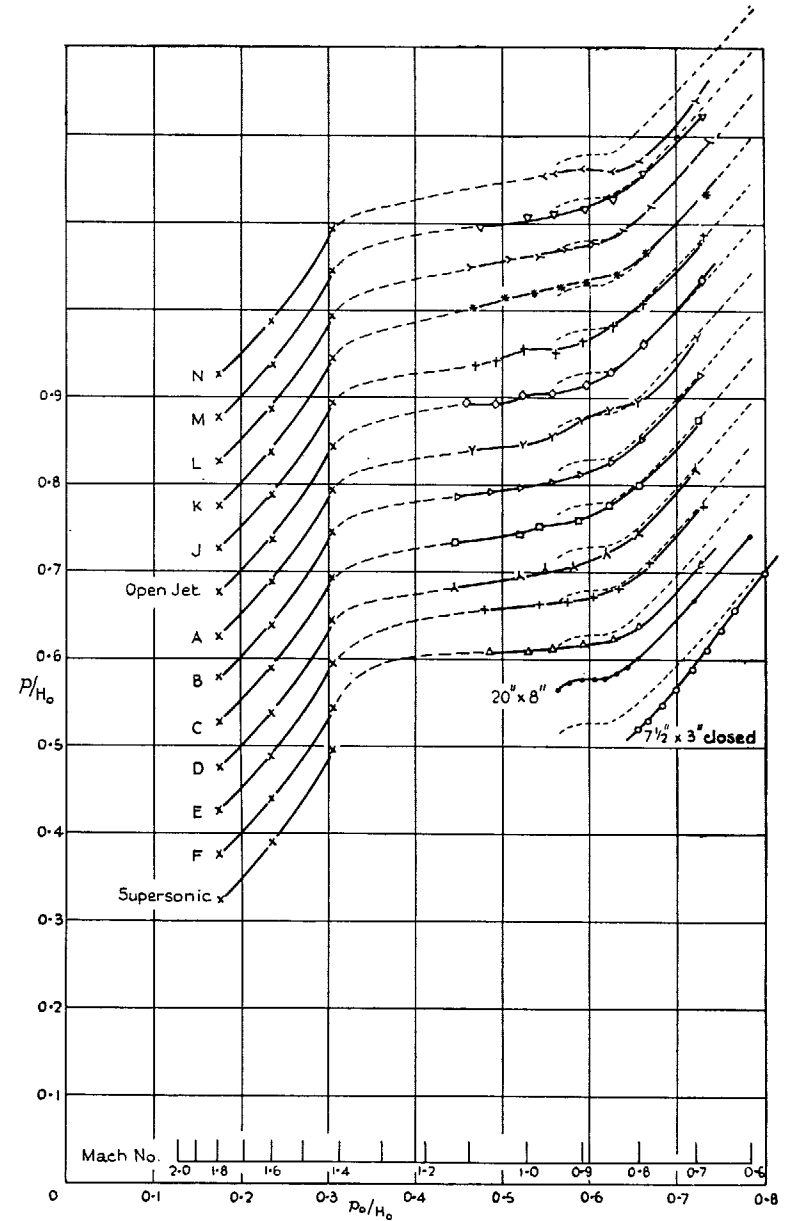
FIG. 52. Pressures at 0·05 chord on RAE 104 aerofoil at $\alpha = 0$ deg.
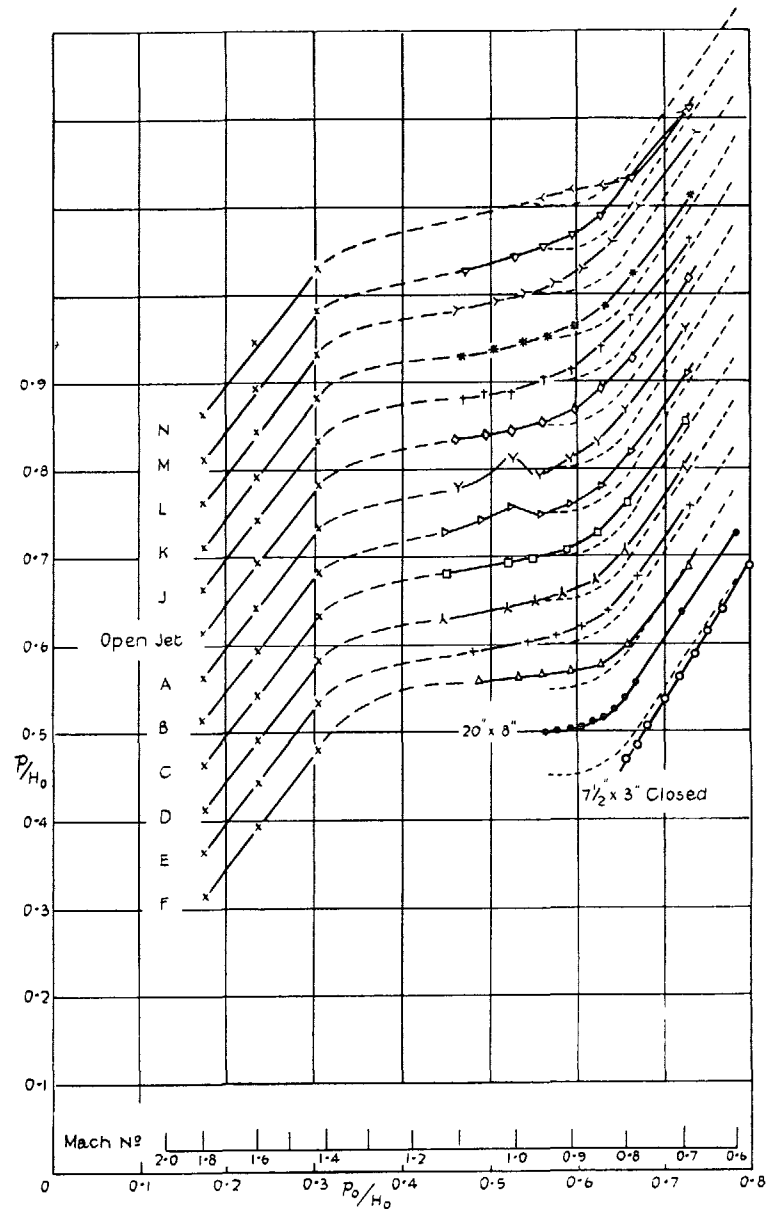
FIG. 53. Pressures at $0 \cdot 1$ chord on RAE 104 aerofoil at $\alpha = 0$ deg.
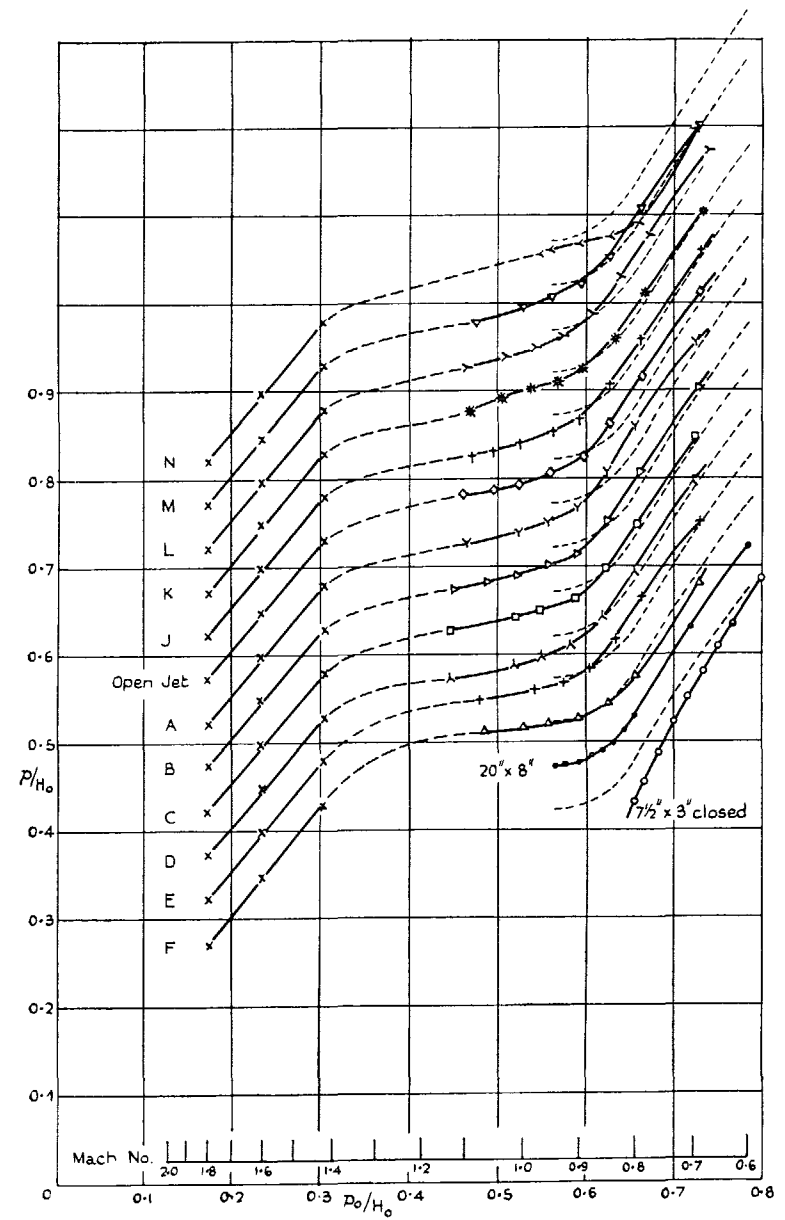
FIG. 54. Pressures at $0 \cdot 2$ chord on RAE 104 aerofoil at $\alpha = 0$ deg.
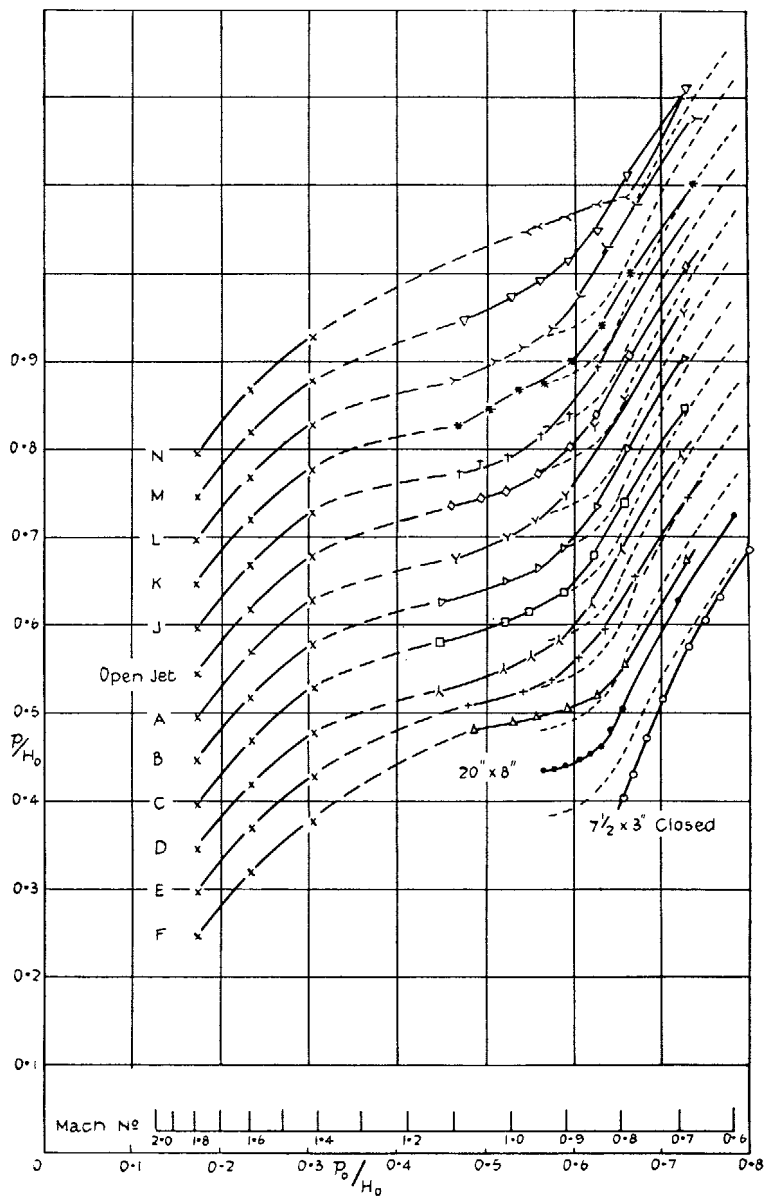
FIG. 55. Pressures at 0·35 chord on RAE 104 aerofoil at α = 0 deg.
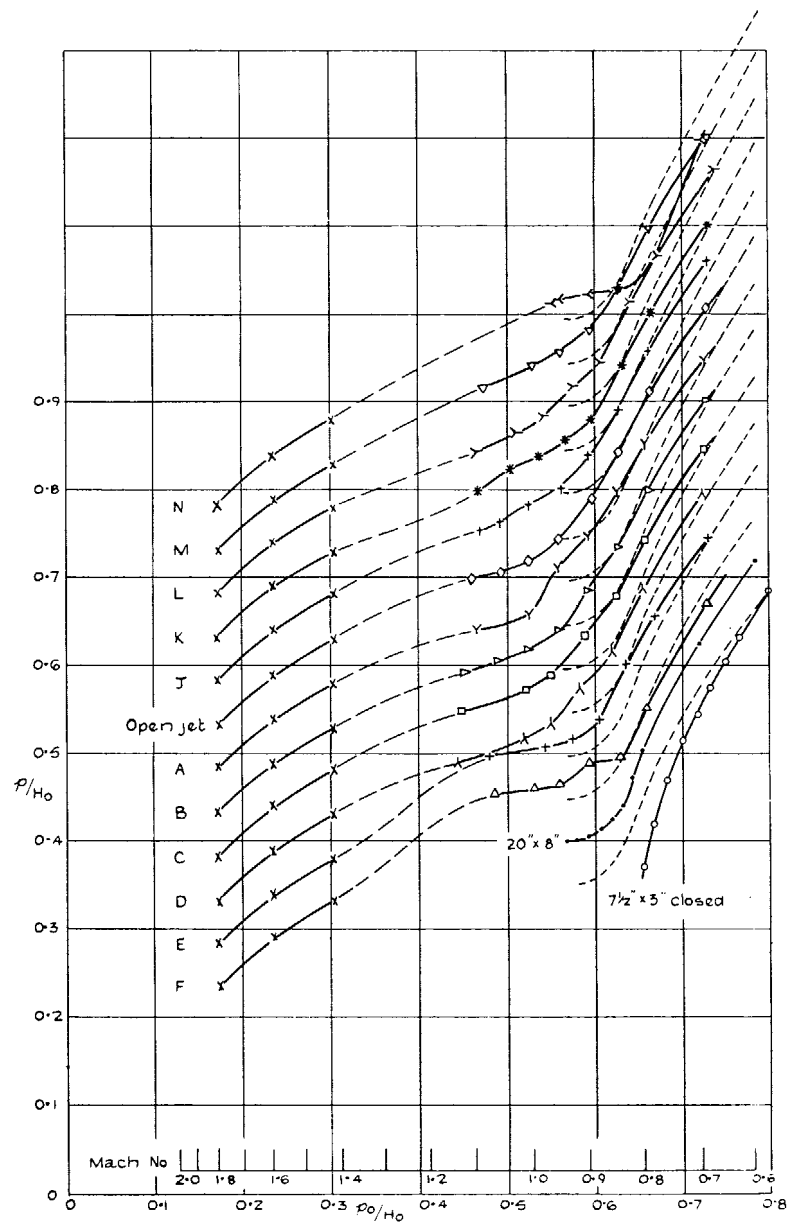
FIG. 56. Pressures at 0·5 chord on RAE 104 aerofoil at α = 0 deg.
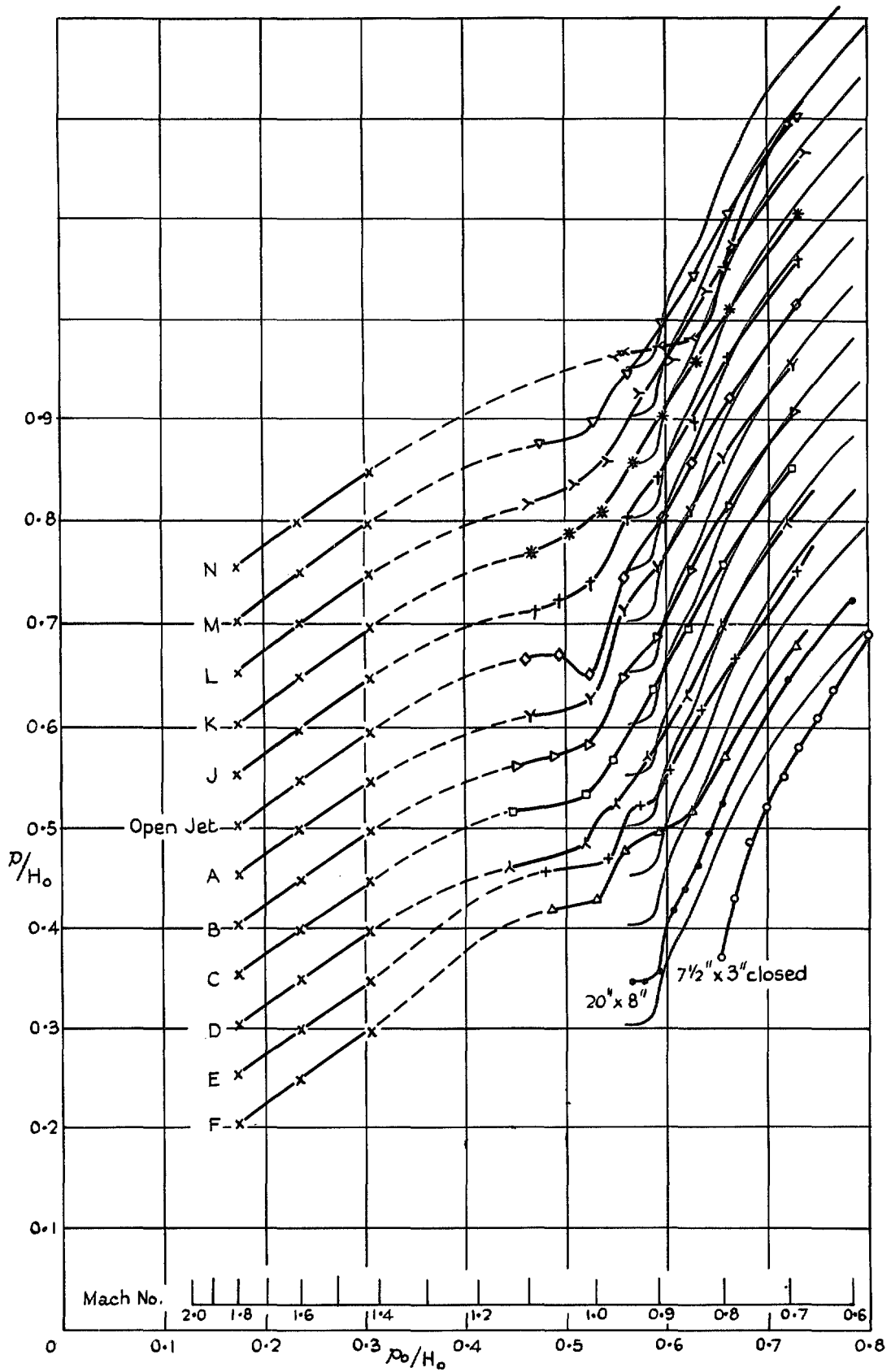
FIG. 57.   Pressures at 0·6 chord for α = 0 deg.
Results for the 20-in. × 8-in. Tunnel shown in red.

40
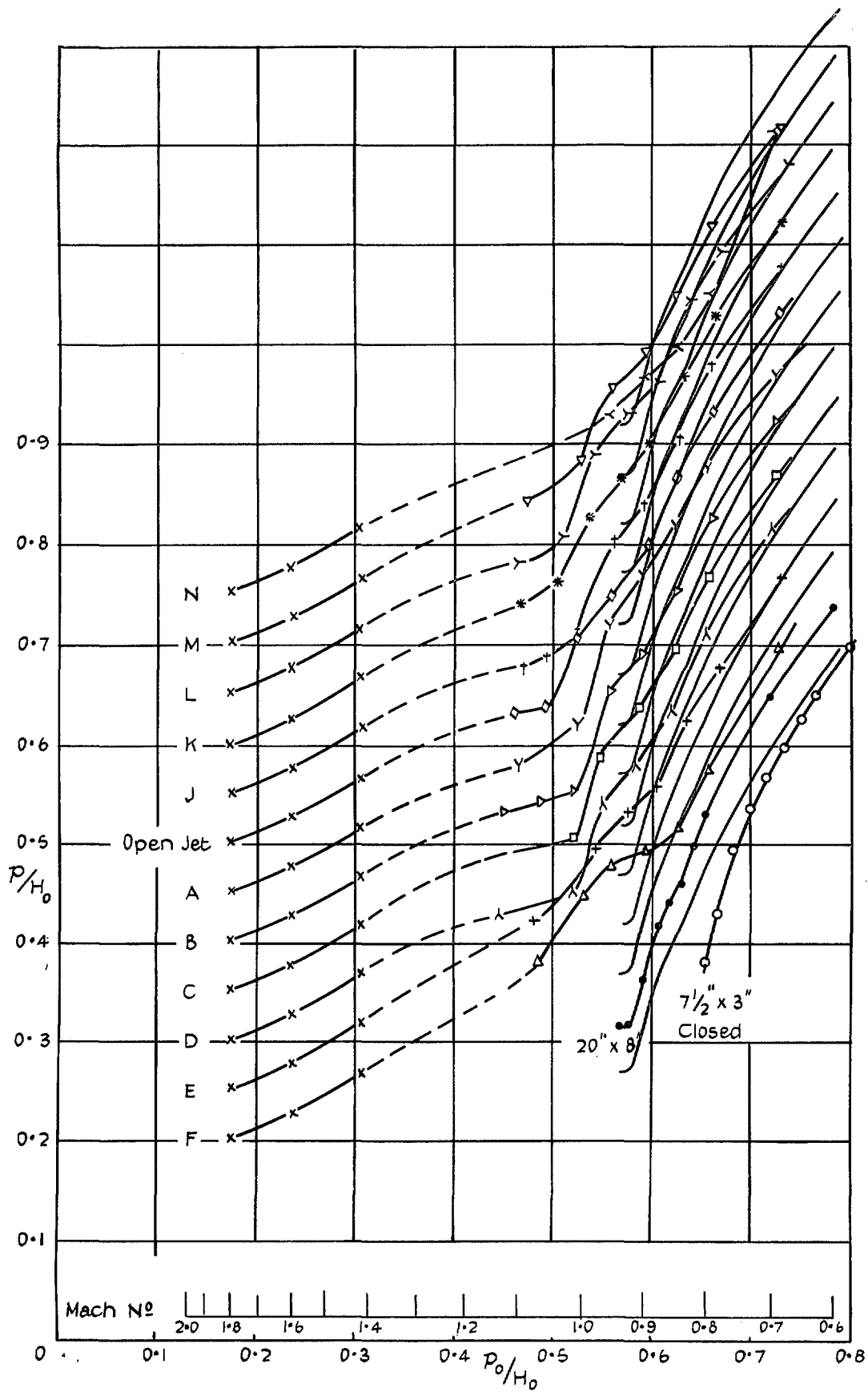
Fig. 58. Pressures at $0 \cdot 7$ chord for $\alpha = 0$ deg.
Results for the 20-in. $\times$ 8-in. Tunnel shown in red.

41
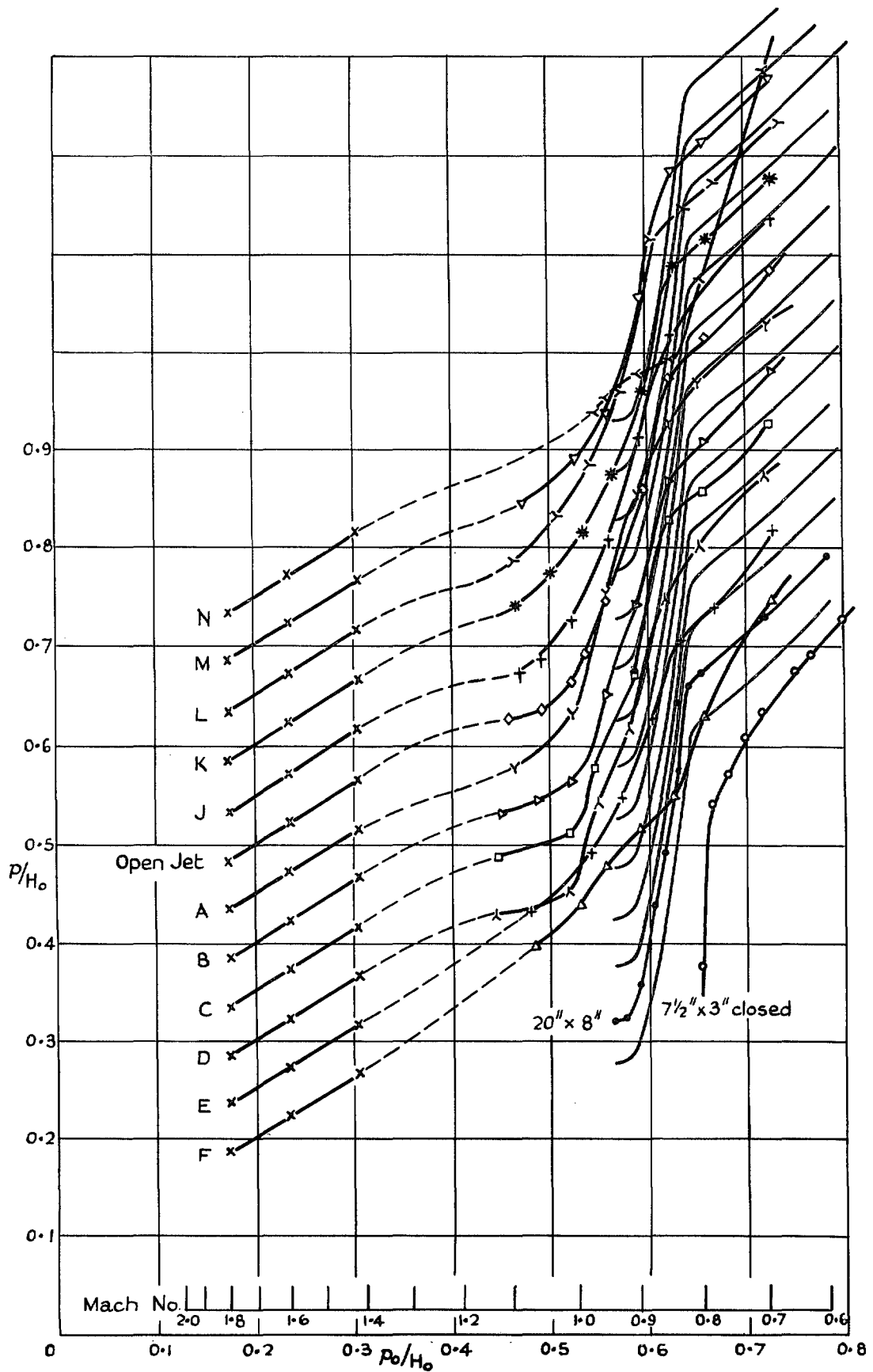
Fig. 59. Pressures at $0 \cdot 8$ chord for $\alpha = 0$ deg.
Results for the 20-in. $\times$ 8-in. Tunnel shown in red.

42
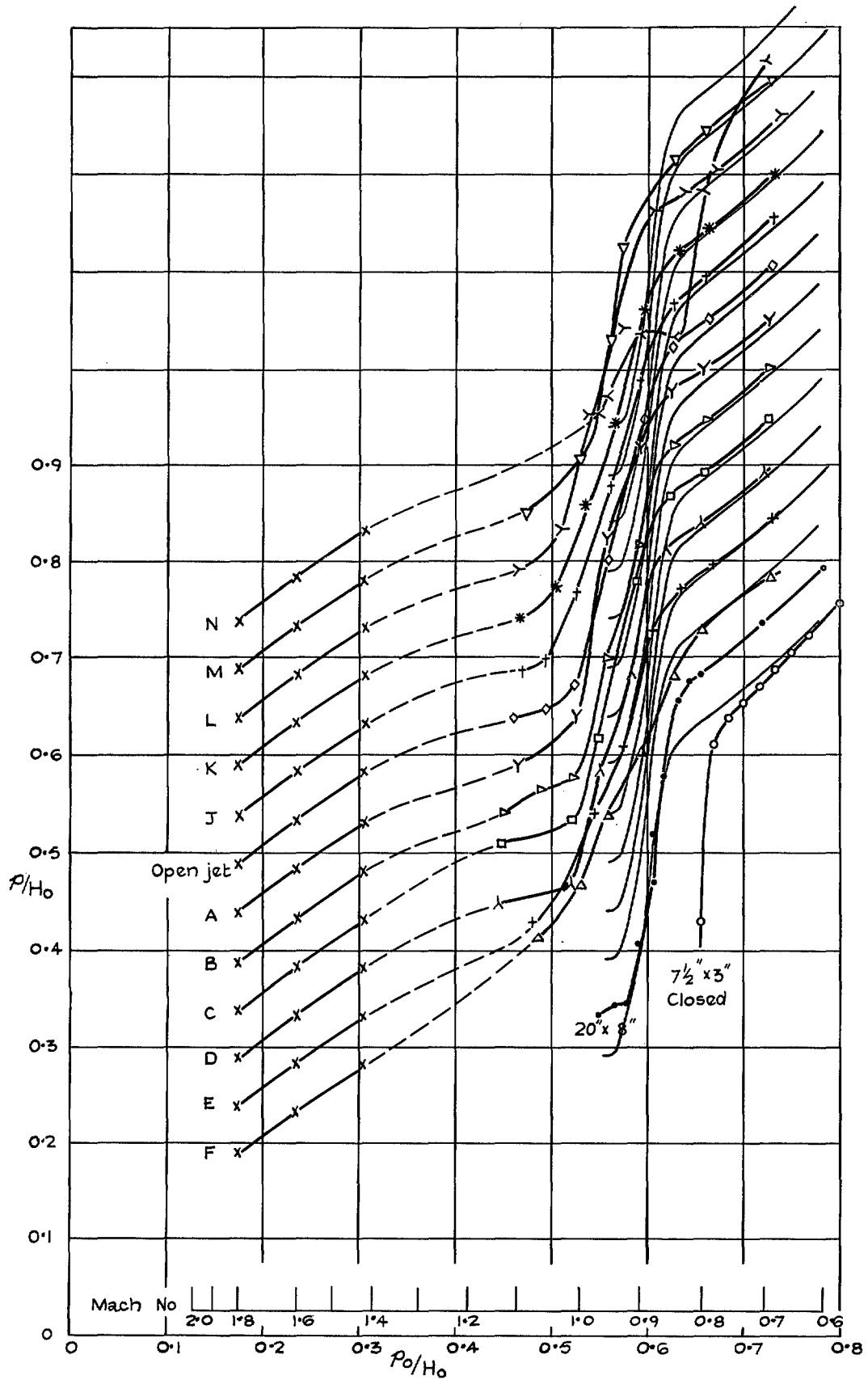
FIG. 60.   Pressures at 0·9 chord for α = 0 deg.
Results for the 20-in. × 8-in. Tunnel shown in red.

43

M= 0·700
$\frac{p_o}{H_o}$=0·721

M=0·800
$\frac{p_o}{H_o}$=0·656

M=0·840
$\frac{p_o}{H_o}$=0·630

M=0·860
$\frac{p_o}{H_o}$=0·617

M=0·880
$\frac{p_o}{H_o}$=0·604

M=0·900
$\frac{p_o}{H_o}$=0·591

M=0·920
$\frac{p_o}{H_o}$=0·579

M=0·940
$\frac{p_o}{H_o}$=0·566
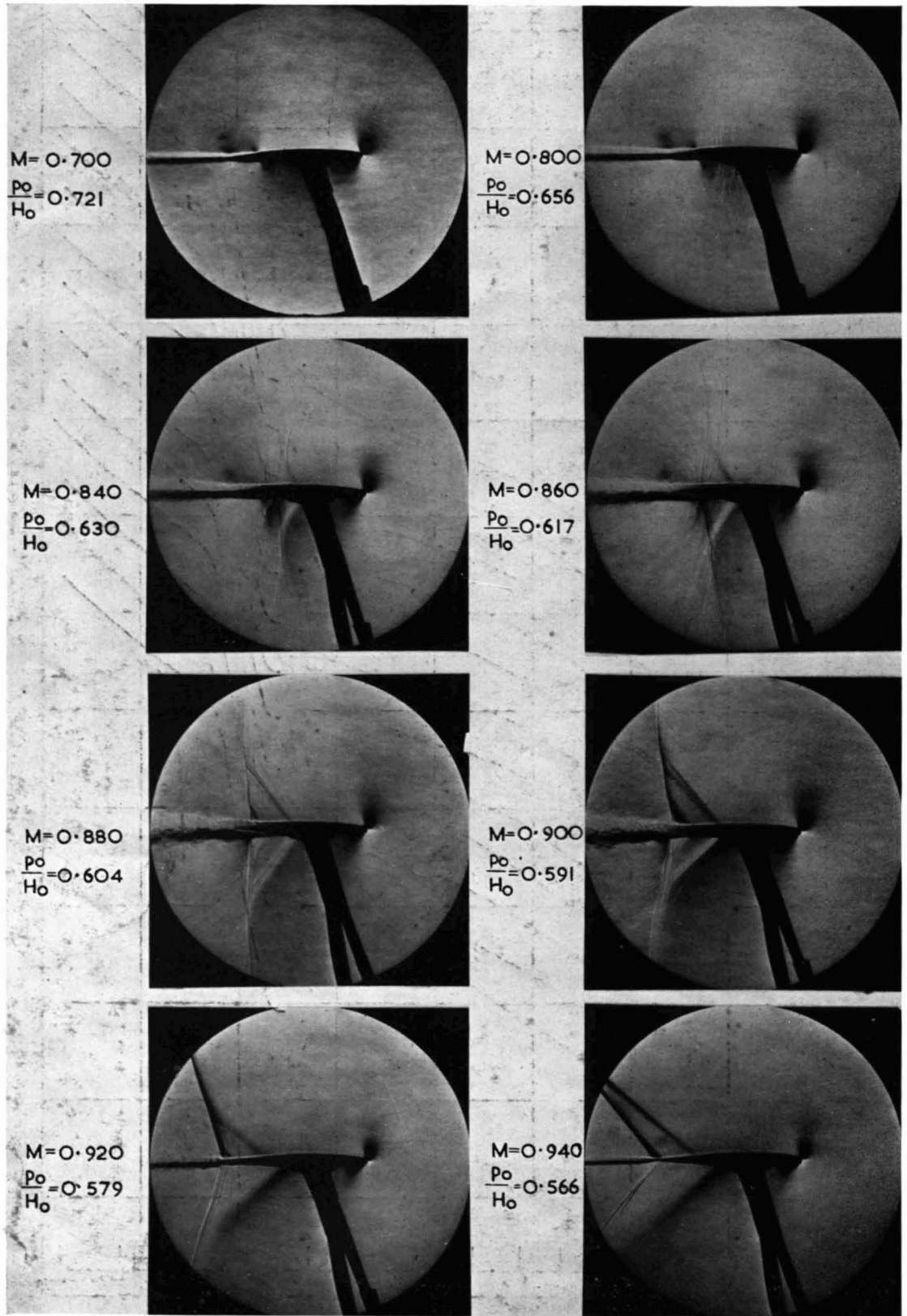
Fig. 61.   Photographs of the flow round the RAE 104 aerofoil at $\alpha = 0$ deg.   20-in. $\times$ 8-in. Tunnel.

M= 0·681
$\frac{Po}{Ho}$=0·733

M= 0·706
$\frac{Po}{Ho}$=0·717

M= 0·731
$\frac{Po}{Ho}$=0·701

M= 0·759
$\frac{Po}{Ho}$=0·683

M= 0·789
$\frac{Po}{Ho}$=0·667

M= 0·802
$\frac{Po}{Ho}$=0·655

M= 0·802
$\frac{Po}{Ho}$=0·655

M= 0·802
$\frac{Po}{Ho}$=0·655
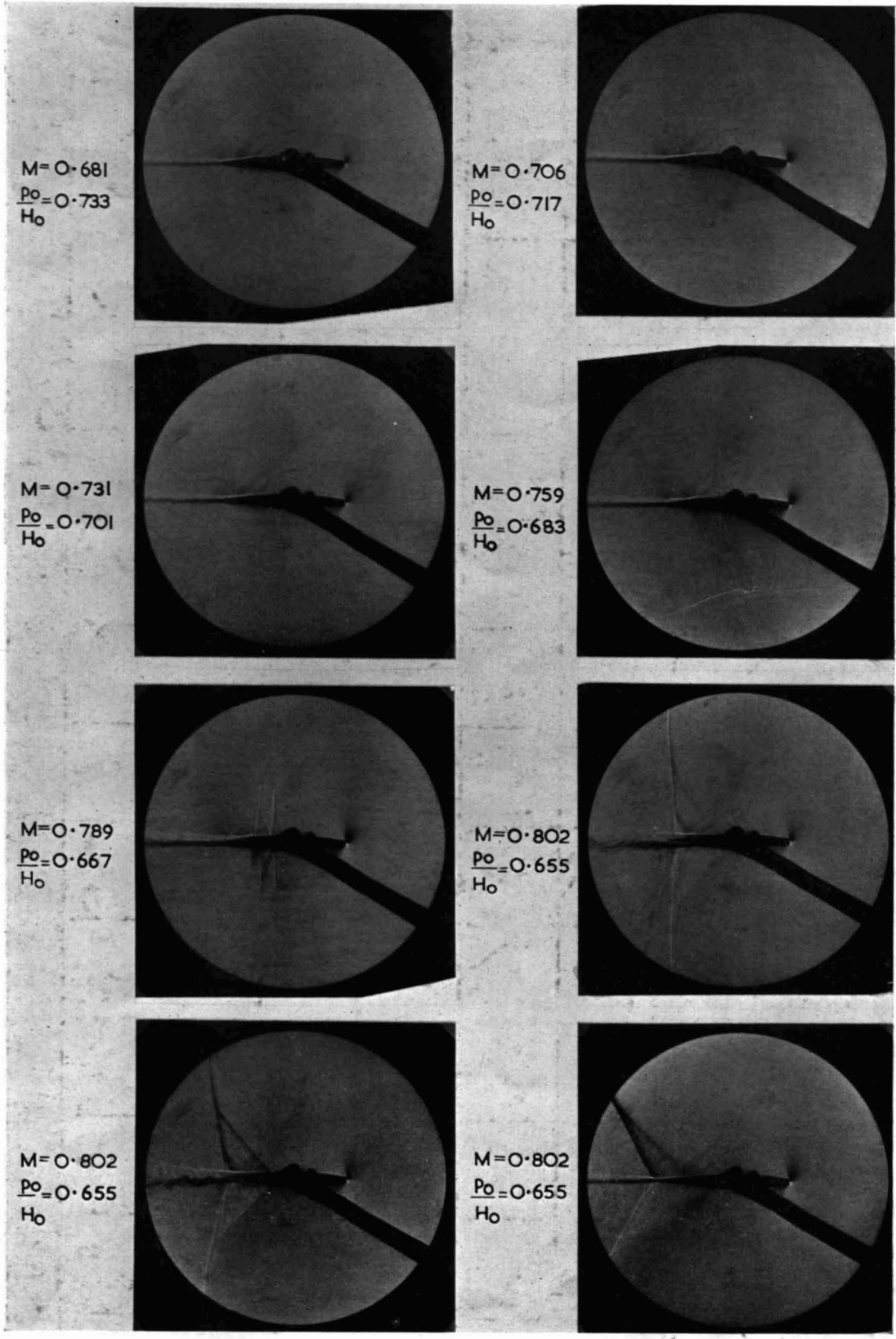
FIG. 62.   Photographs of the flow round the RAE 104 aerofoil at $\alpha = 0$ deg. $7\frac{1}{2}$-in. $\times$ 3-in. Closed Tunnel.

45
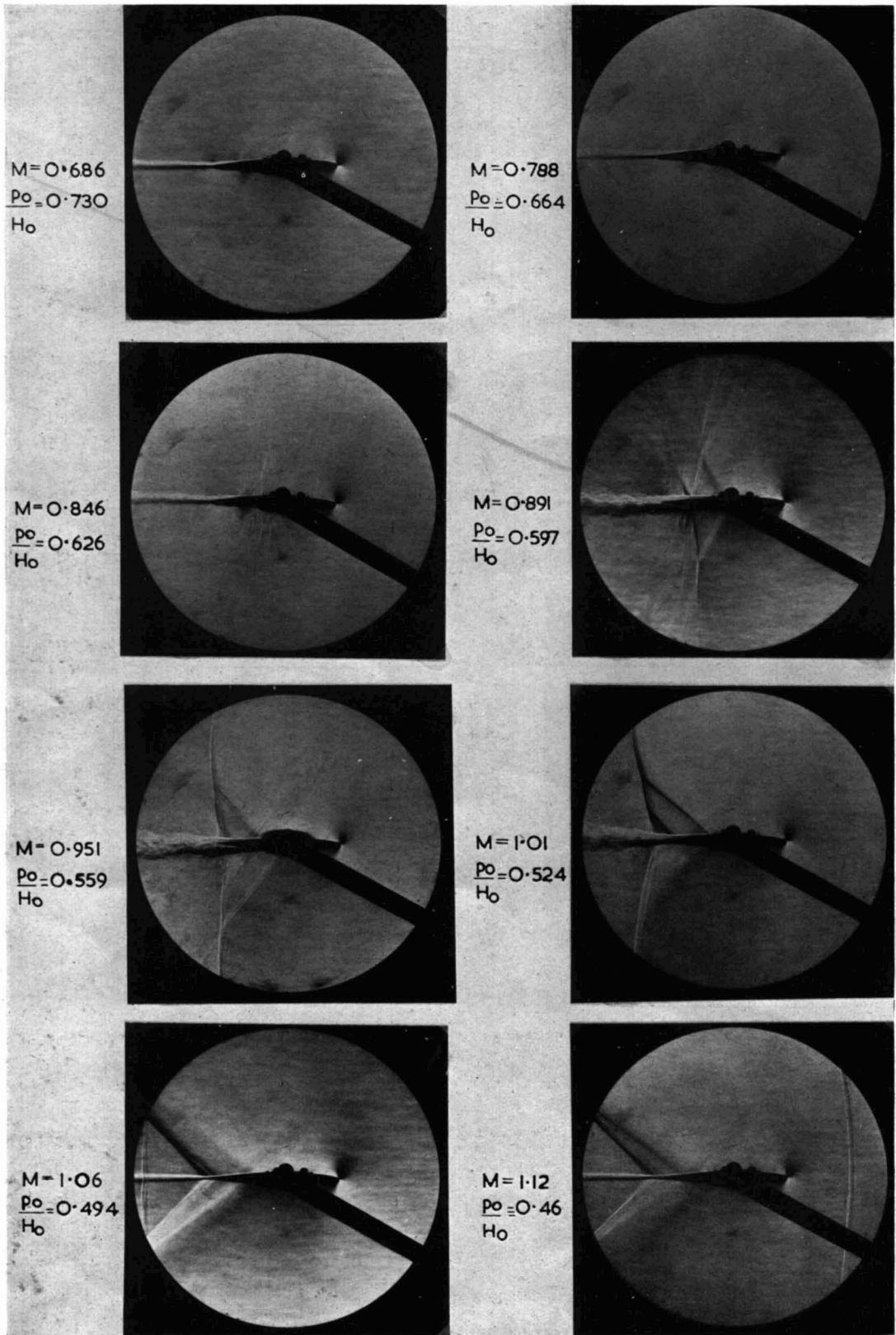
FIG. 63.   Photographs of the flow round the RAE 104 aerofoil at $\alpha = 0$ deg. $7\frac{1}{2}$-in. $\times$ 3-in. Open Jet.

46
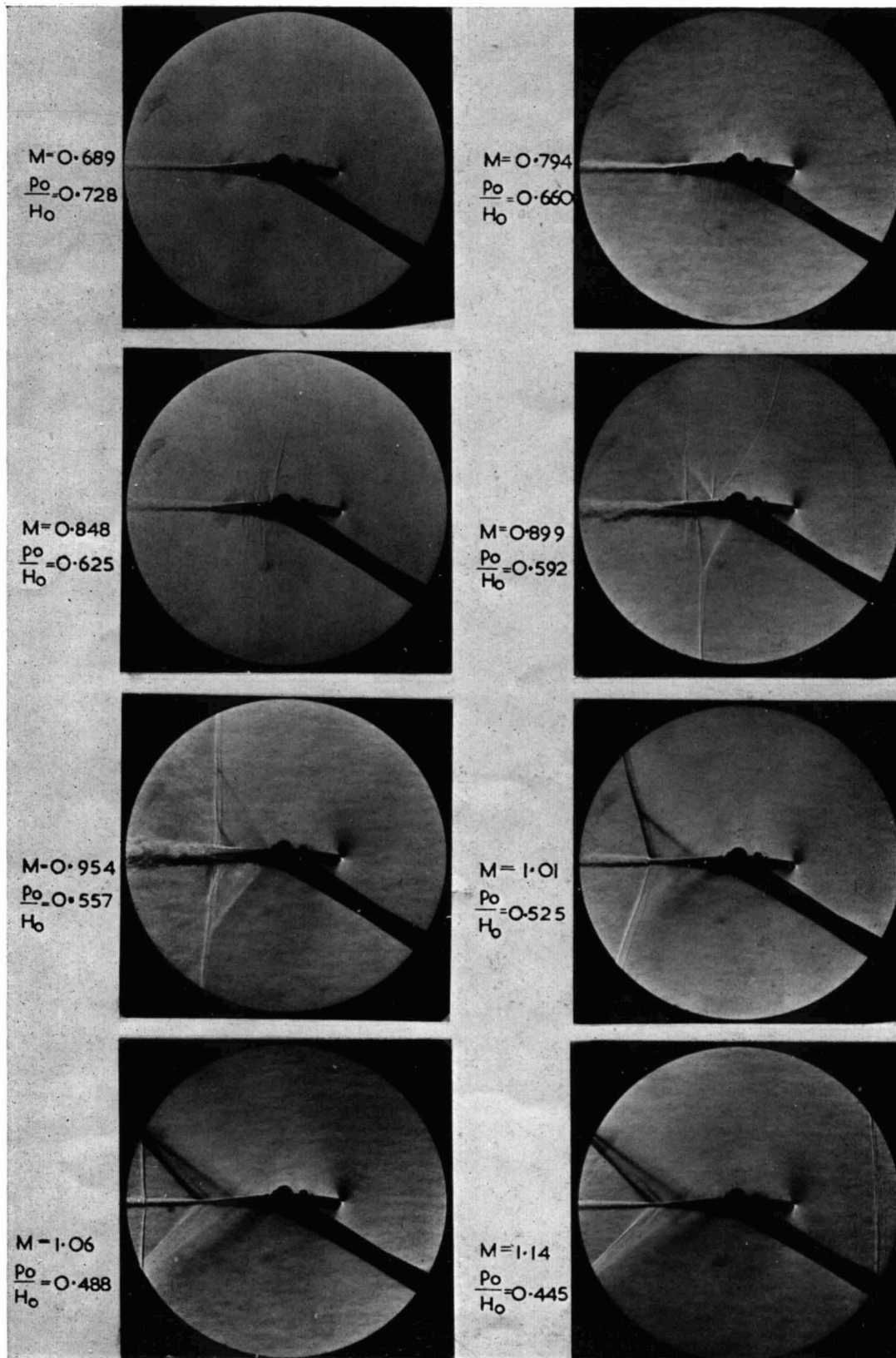
FIG. 64.   Photographs of the flow round the RAE 104 aerofoil at $\alpha = 0$ deg.   Wall B.
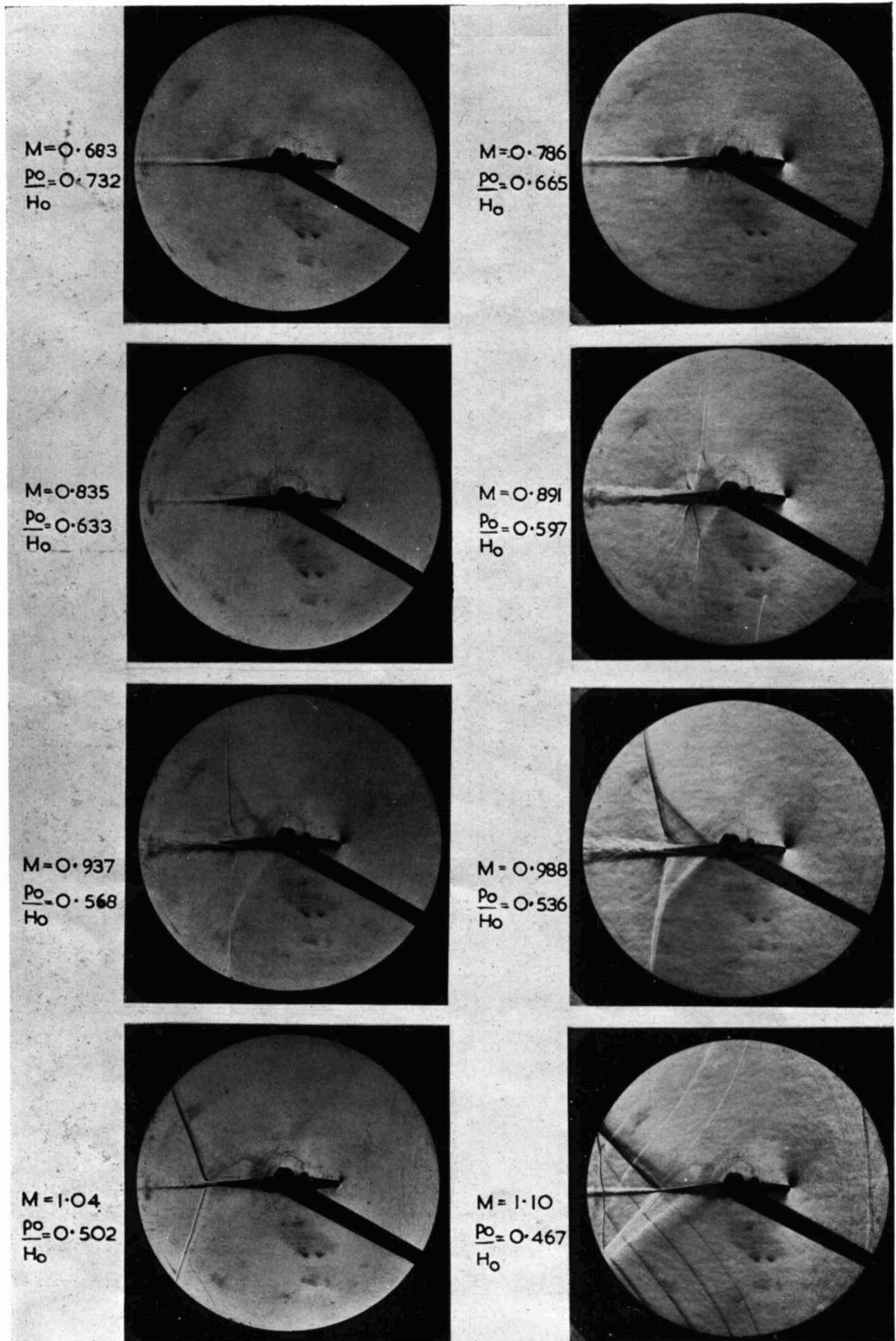
FIG. 65.   Photographs of the flow round the RAE 104 aerofoil at $\alpha = 0$ deg.   Wall K.

48
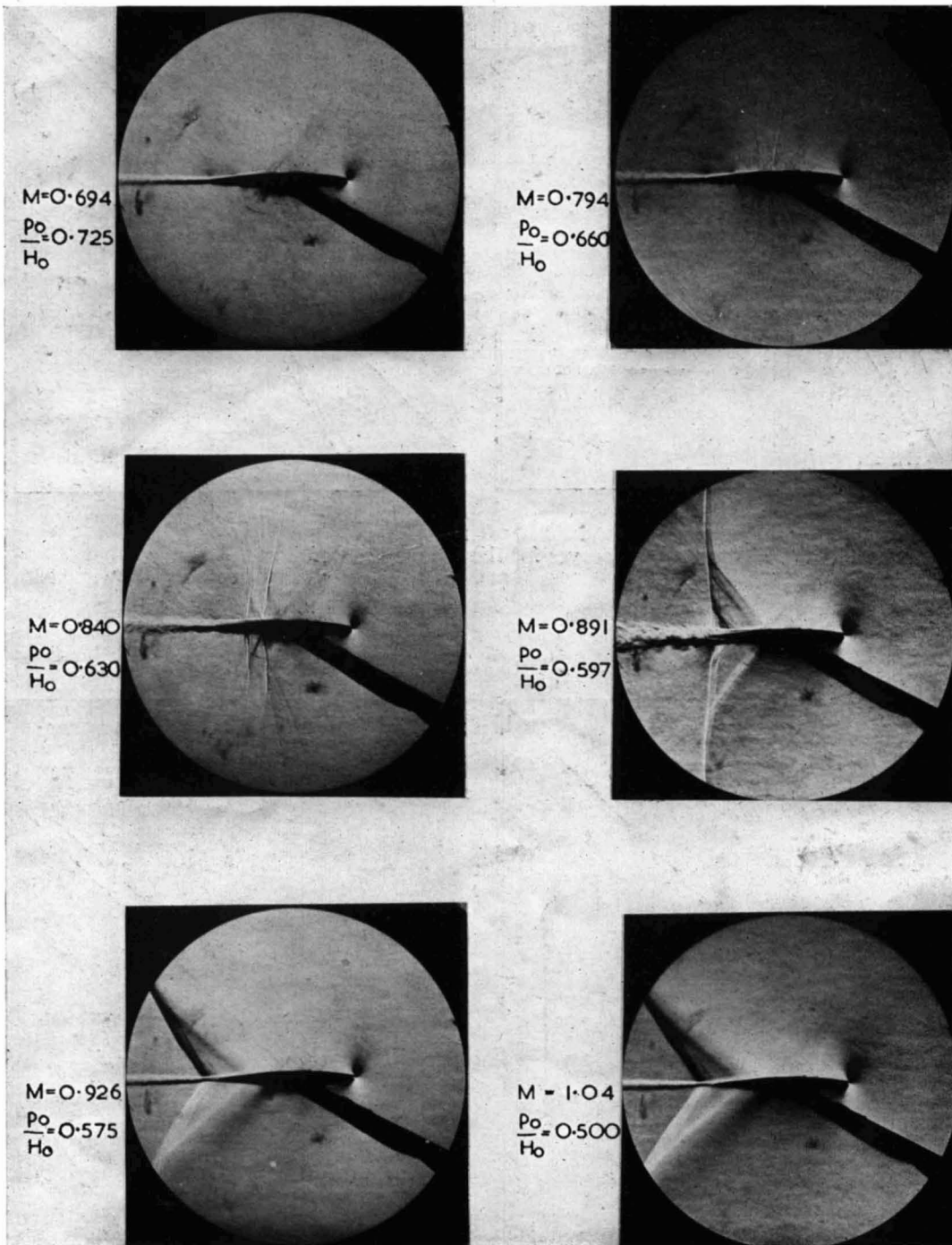
FIG. 66. Photographs of the flow round the RAE 104 aerofoil at $\alpha = 0$ deg. Wall H.

49
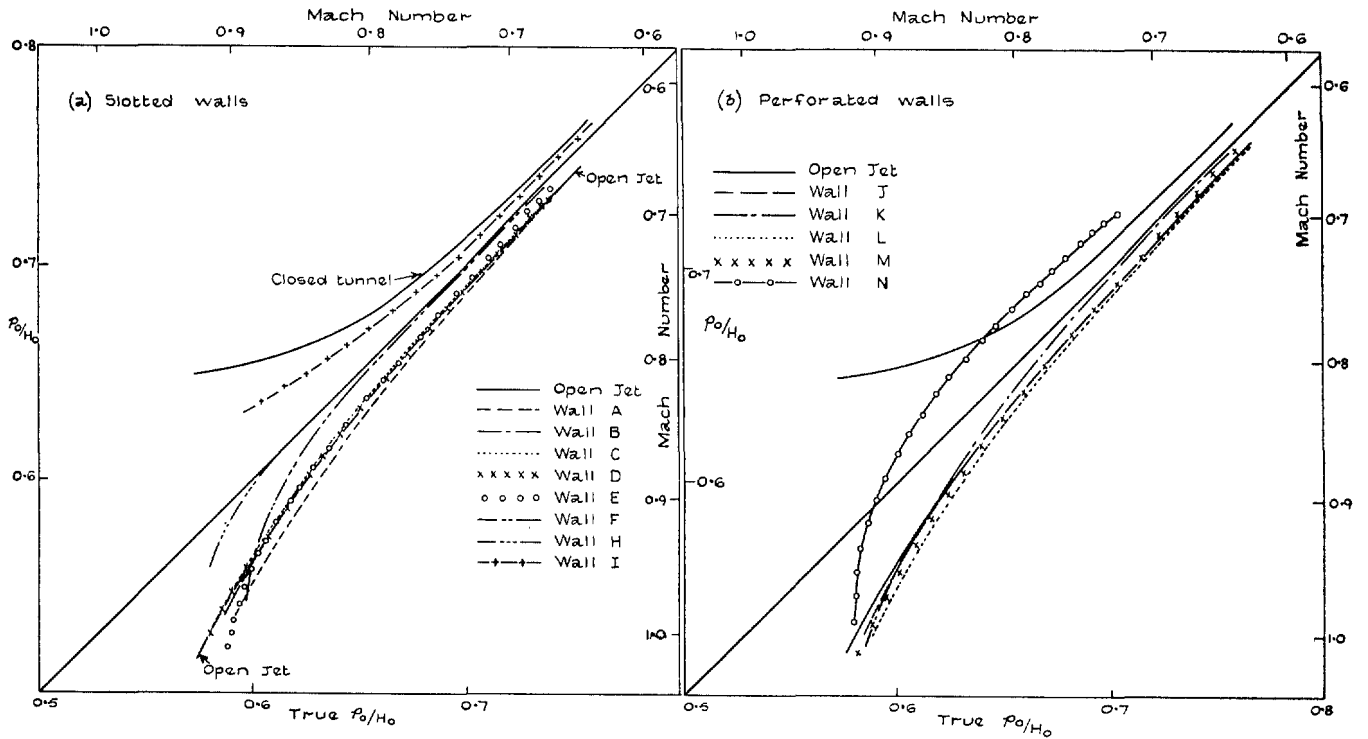
FIG. 67. Mean blockage curves for the RAE 104 aerofoil at $\alpha = 0$ deg.
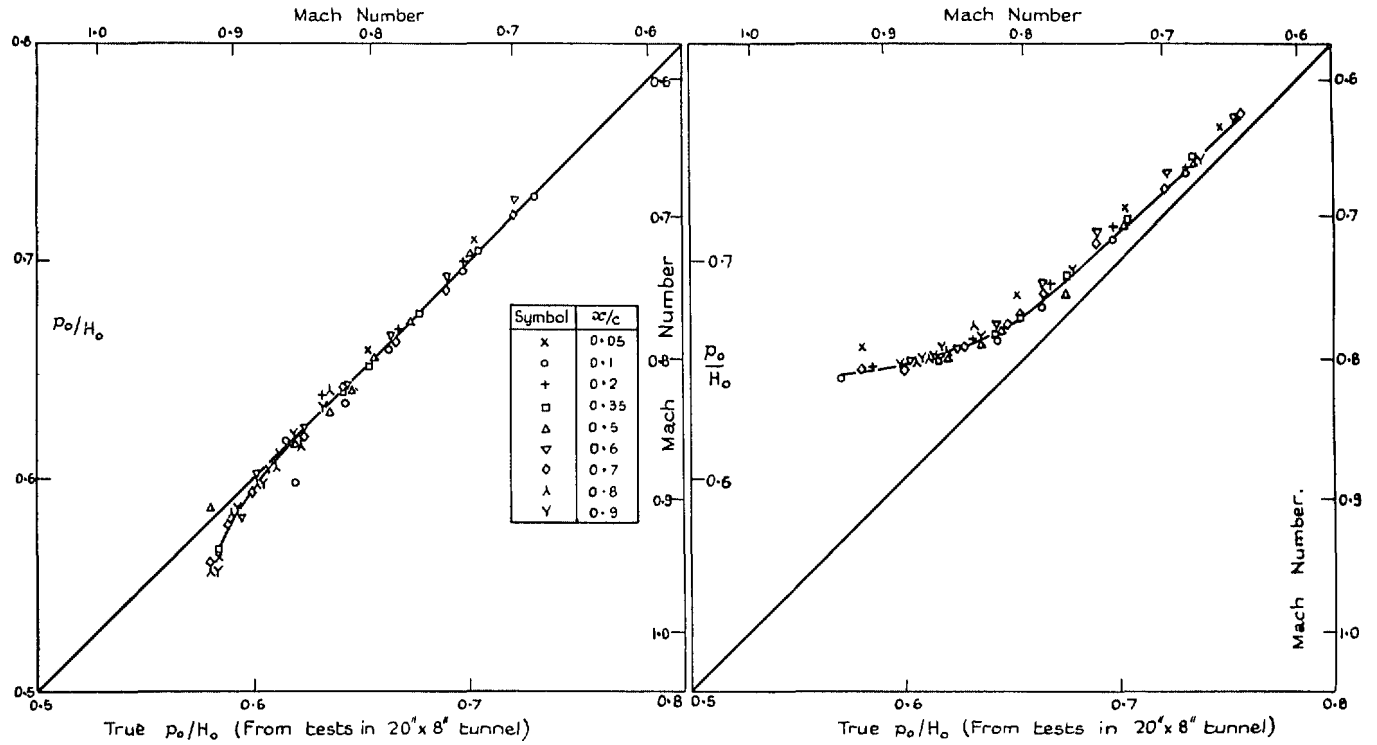
FIG. 68a. Blockage curve for wall H.

FIG. 68b. Blockage curve for the $7\frac{1}{2}$-in. $\times$ 3-in. Closed Tunnel.

FIG. 68.

50
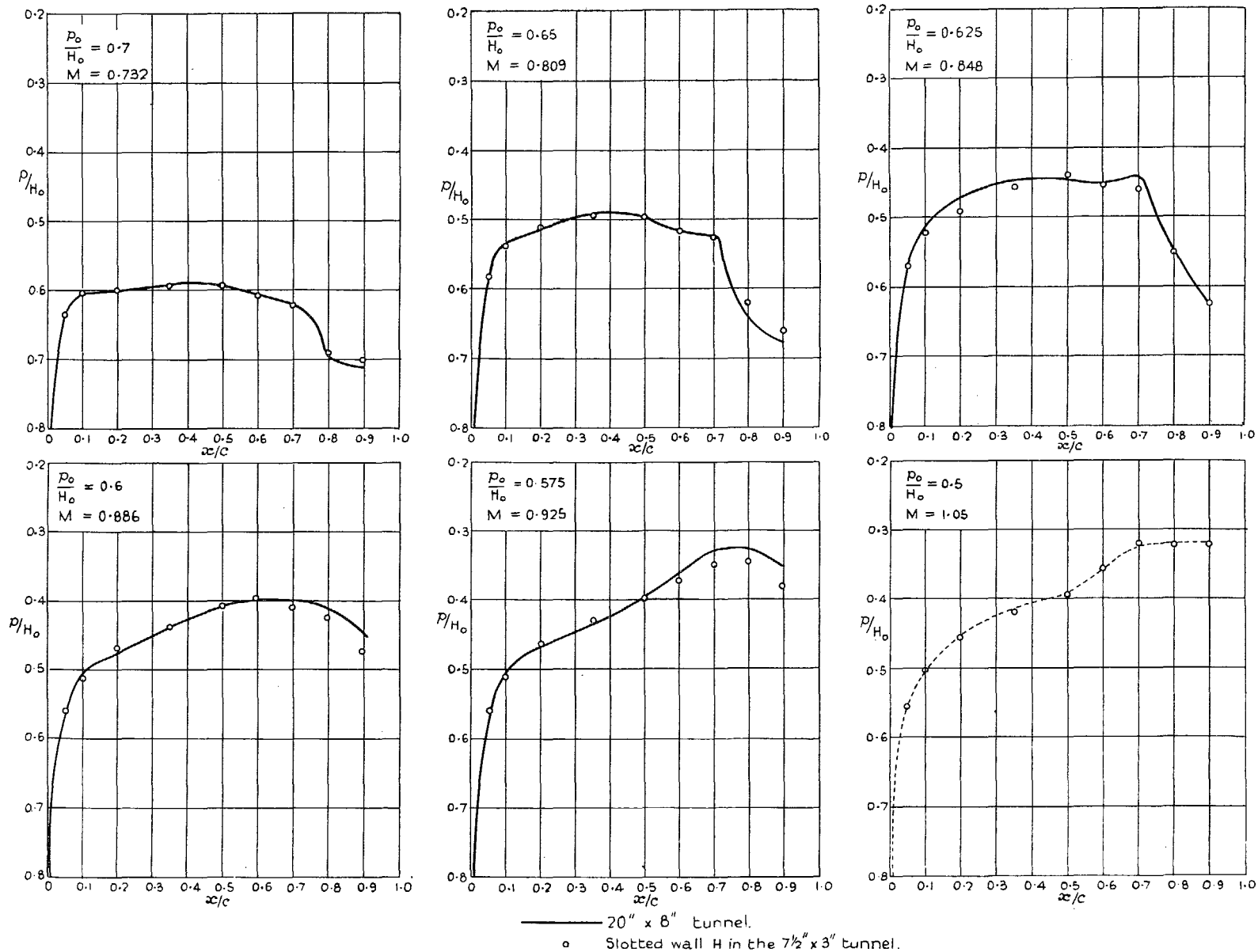
FIG. 69.   Pressure distributions at $\alpha = 0$ deg on the RAE 104 aerofoil in the 20-in. $\times$ 8-in. and $7\frac{1}{2}$-in. $\times$ 3-in. (wall H) Tunnel.
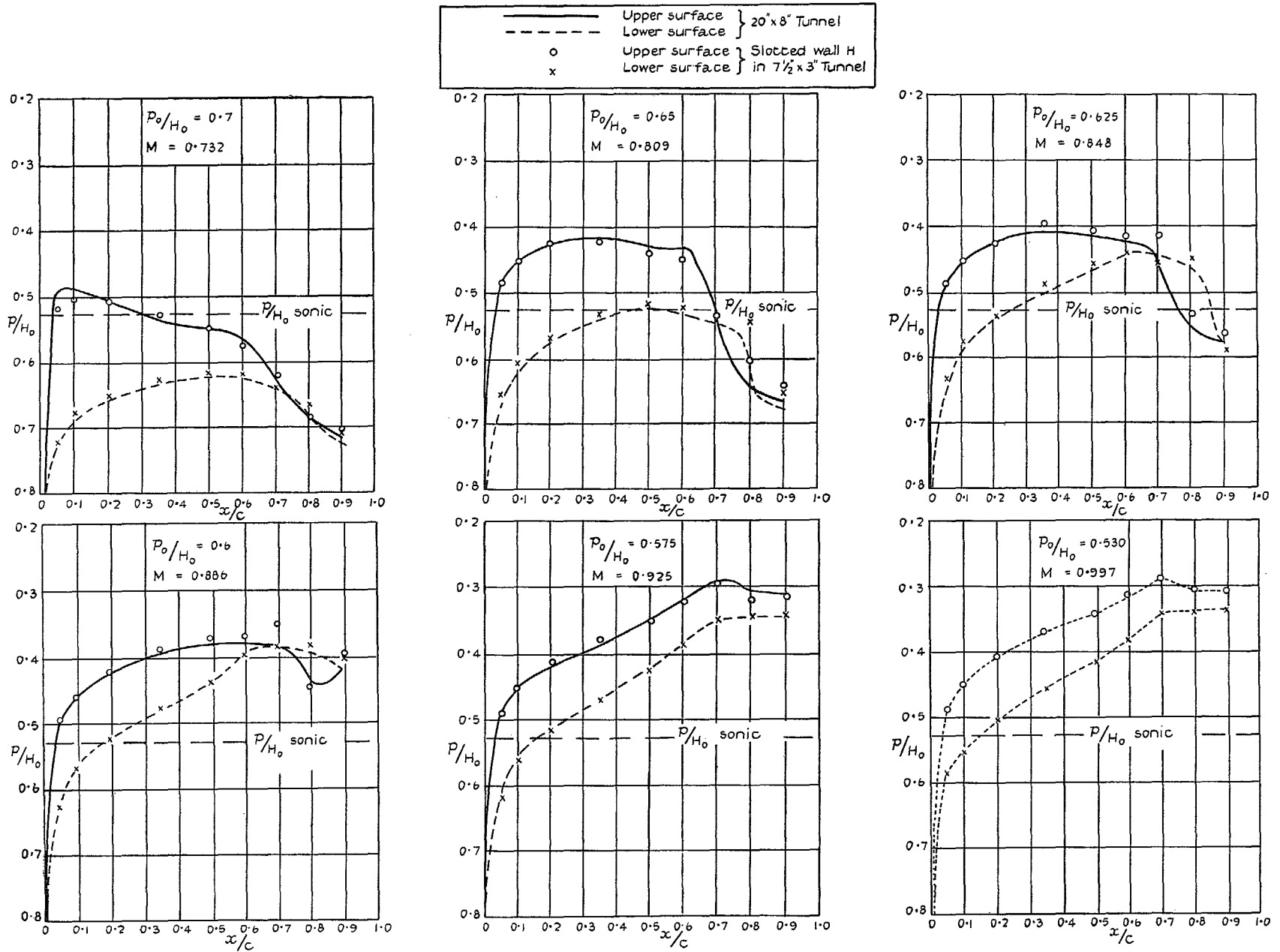
FIG. 70.   Pressure distributions at $\alpha = 2$ deg on the RAE 104 aerofoil in the 20-in. $\times$ 8-in. and $7\frac{1}{2}$-in. $\times$ 3-in. (wall H) Tunnels.
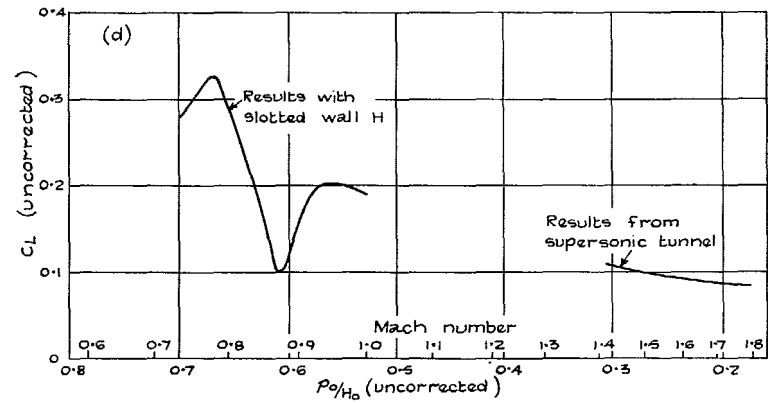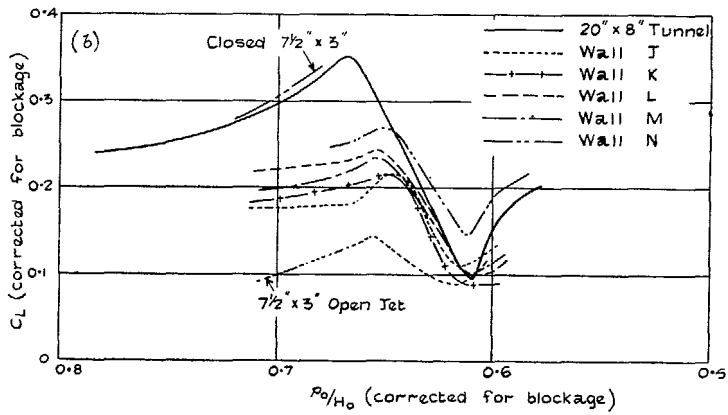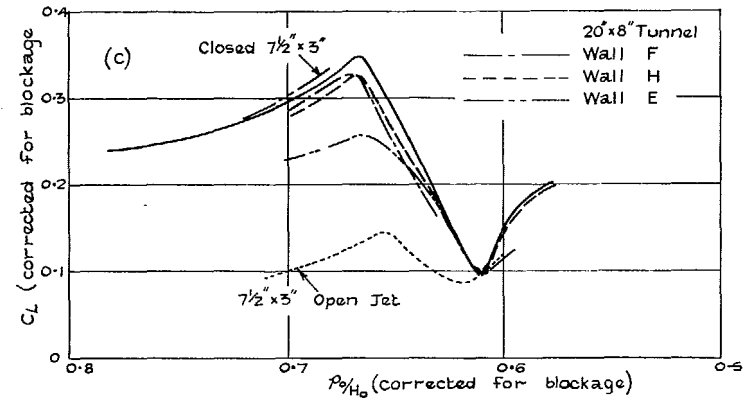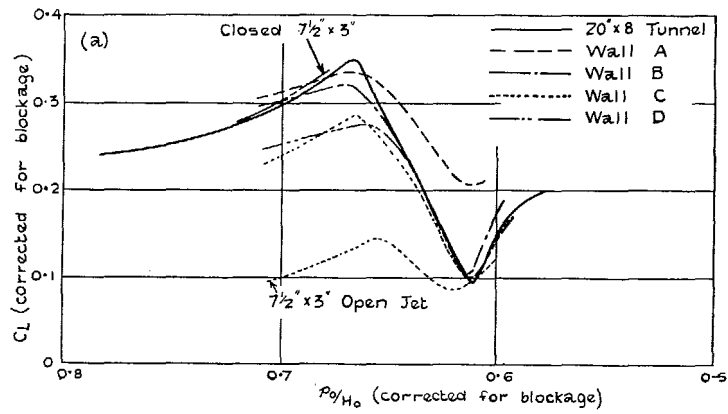
FIG. 71. Lift curves for the RAE 104 aerofoil at $\alpha = 2$ deg.

FIG. 72.   Corrections in the closed and open jets.

(a)

$M_{local} = 1$

x———x 20″x8″ Tunnel $\quad P_0/H_0 = 0.605$, M = 0.879
+—·—+ 7½″x3″ Closed Tunnel $\quad P_0/H_0 = 0.655$, M = 0.802 (Just choked)
o————o 7½″x3″ Open Tunnel $\quad P_0/H_0 = 0.570$, M = 0.934

P/H_0

Distance from leading edge x/c

(b)

$M_{local} = 1$

x———x 20″x8″ Tunnel $\quad P_0/H_0 = 0.585$, M = 0.910
+—·—+ 7½″x3″ Closed Tunnel $\quad P_0/H_0 = 0.655$, M = 0.802 (Fully choked)
o————o 7½″x3″ Open Tunnel $\quad P_0/H_0 = 0.540$, M = 0.981

P/H_0

Distance from leading edge x/c

FIG. 73. Pressure distributions on the RAE 104 aerofoil at $\alpha = 0$ deg.

(a)

+——— Upper surface
———— Lower surface } 20″x8″ tunnel $\frac{P_0}{H_0} = 0.603$ M = 0.882.

----x--- Upper surface
--o--- Lower surface } 7½″x3″ closed tunnel $\frac{P_0}{H_0} = 0.658$ M = 0.797
(just choked)

P/H_0

Distance from leading edge x/c

(b)

+——— Upper surface
———— Lower surface } 20″x8″ tunnel $\frac{P_0}{H_0} = 0.598$ M = 0.890

---x--- Upper surface
--o--- Lower surface } 7½″x3″ tunnel $\frac{P_0}{H_0} = 0.658$ M = 0.797
(Fully choked).

P/H_0

Distance from leading edge x/c.

FIG. 74. Pressure distributions on the RAE 104 Aerofoil at $\alpha = 2$ deg.

FIG. 75. Photographs of the flow round 6 per cent double wedge at $\alpha = 0$ deg.   Wall C.
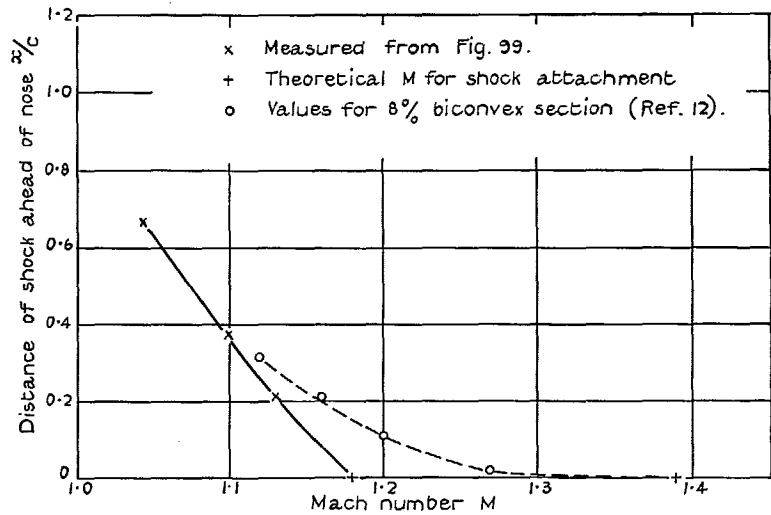
FIG. 76. Position of detached bow wave for 6 per cent double wedge at $\alpha = 0$ deg with walls C.
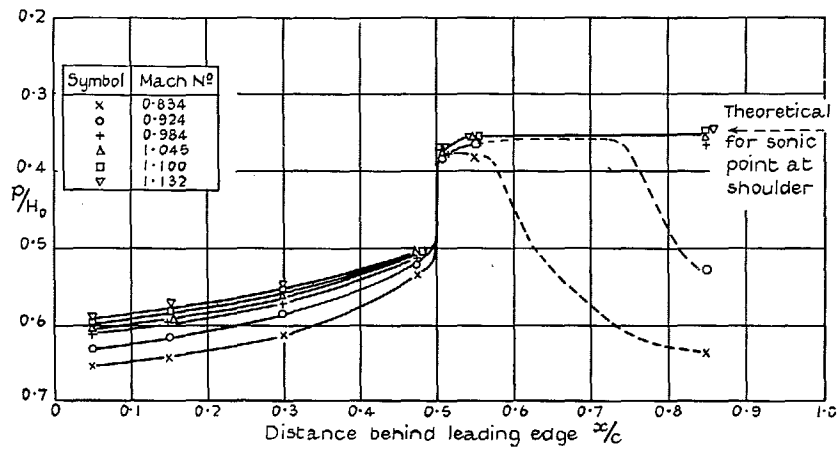
FIG. 77. Pressures on 6 per cent double wedge at $\alpha = 0$ deg with walls C.
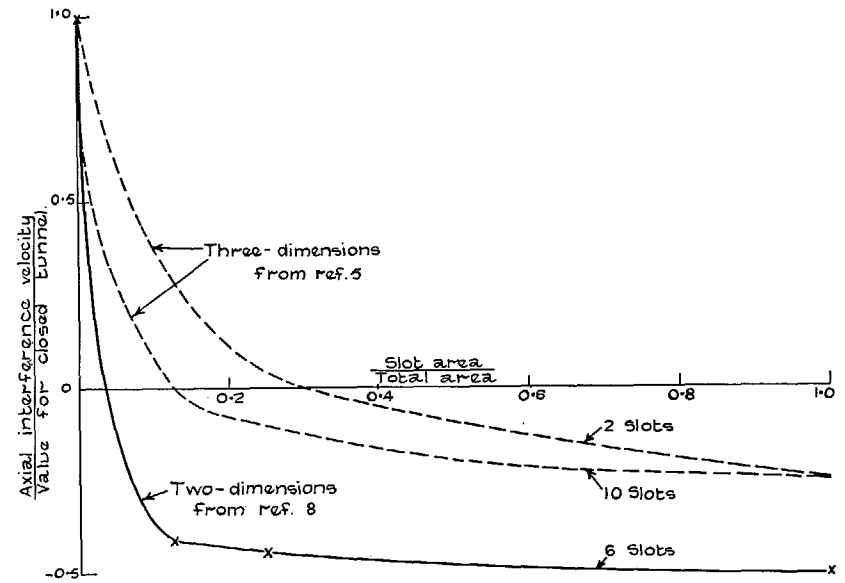
FIG. 78. Calculated interference velocities.
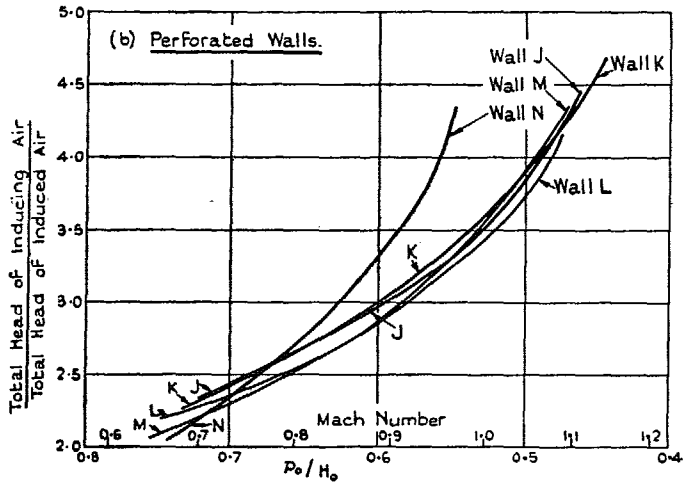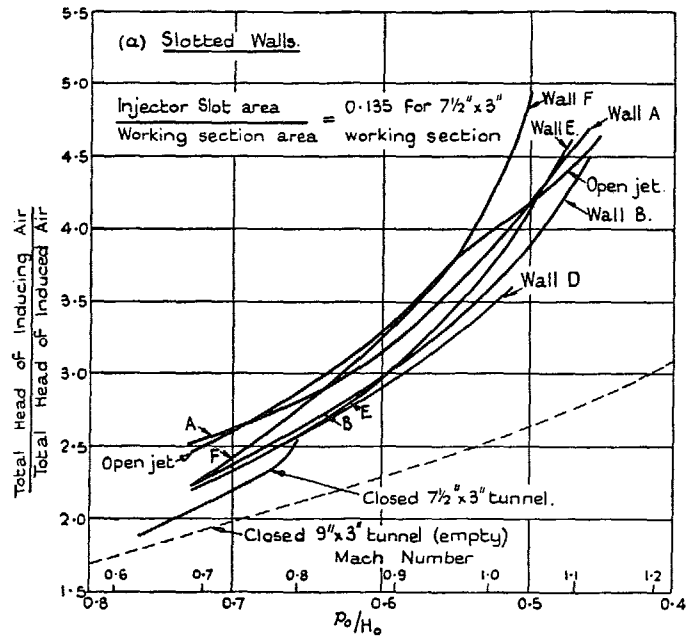
FIG. 79. Power requirements with RAE 104 Aerofoil at $\alpha = 0$ deg.
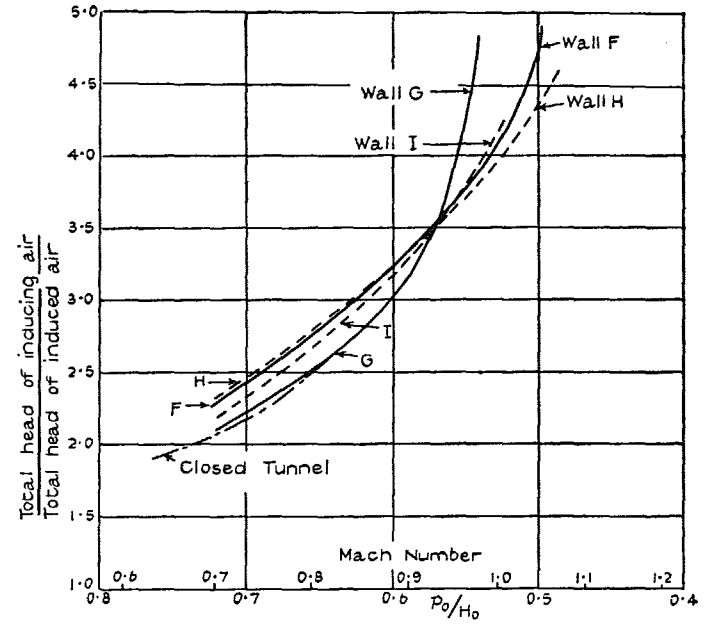
FIG. 80. Effect on power requirements of additional slots in the expansion. RAE 104 aerofoil at $\alpha = 0$ deg.
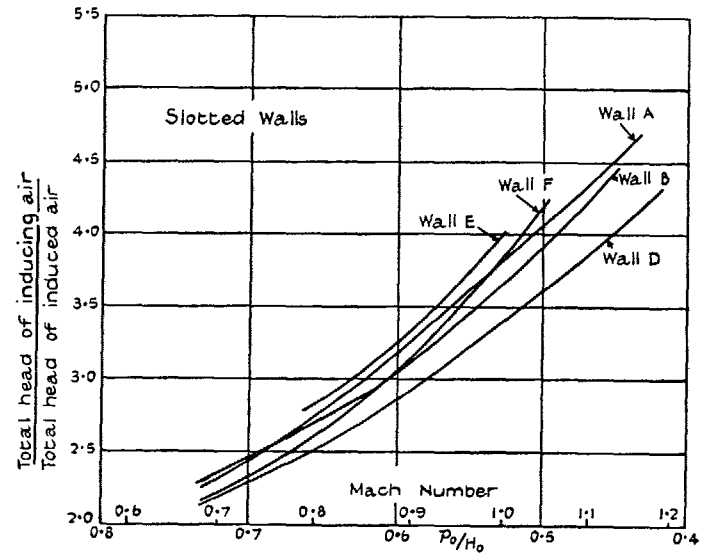
FIG. 81. Power requirements with the empty tunnel.
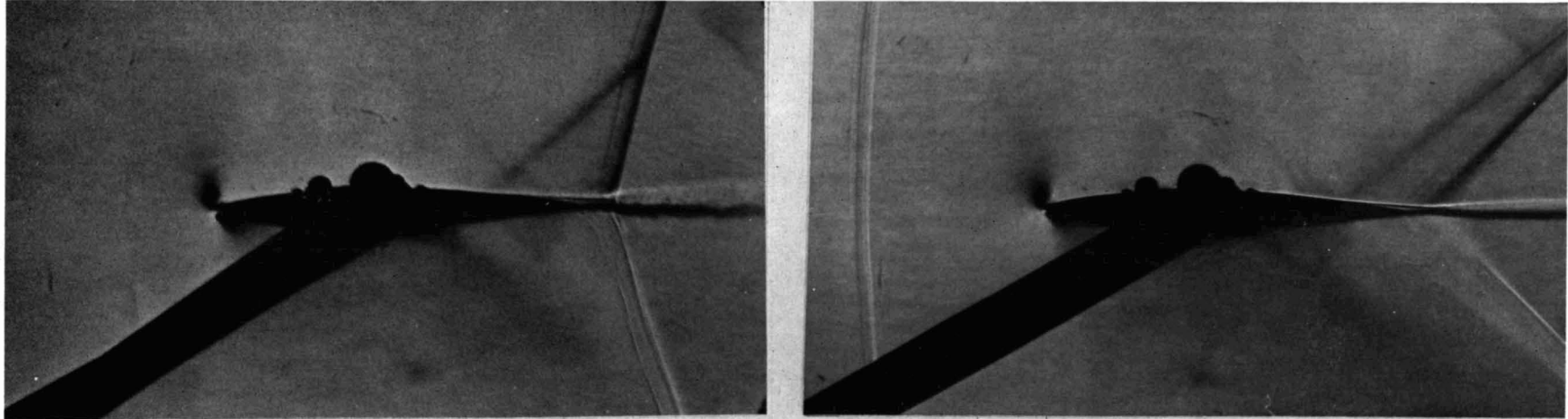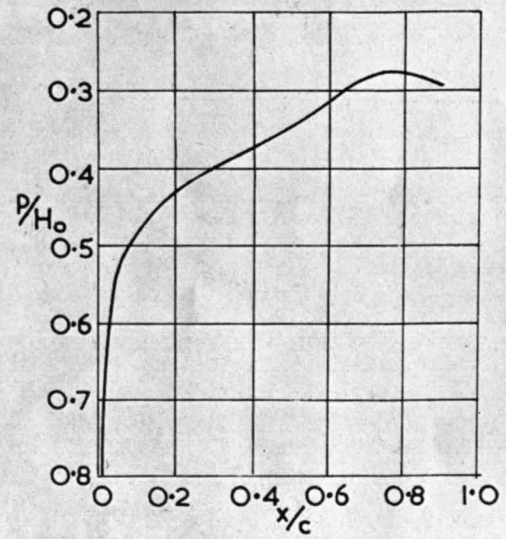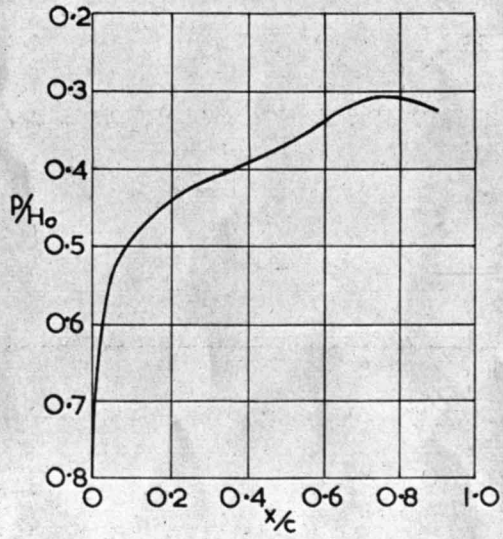
FIG. 82.   Flow round the RAE 104 aerofoil ($\alpha = 0$ deg) at free-stream Mach numbers just below and just above unity.

Publications of the
Aeronautical Research Council

ANNUAL TECHNICAL REPORTS OF THE AERONAUTICAL RESEARCH COUNCIL (BOUND VOLUMES)

1938 Vol. I Aerodynamics General, Performance, Airscrews. 50s. (51s. 2d.)
  Vol. II Stability and Control, Flutter, Structures, Seaplanes, Wind Tunnels, Materials. 30s. (31s. 2d.)

1939 Vol. I. Aerodynamics General, Performance, Airscrews, Engines. 50s. (51s. 2d.)
  Vol. II. Stability and Control, Flutter and Vibration, Instruments, Structures, Seaplanes, etc. 63s (64s 2d.)

1940 Aero and Hydrodynamics, Aerofoils, Airscrews, Engines, Flutter, Icing, Stability and Control, Structures, and a miscellaneous section. 50s. (51s. 2d.)

1941 Aero and Hydrodynamics, Aerofoils, Airscrews, Engines, Flutter, Stability and Control, Structures 63s (64s. 2d.)

1942 Vol I. Aero and Hydrodynamics, Aerofoils, Airscrews, Engines. 75s. (76s. 3d.)
  Vol. II. Noise, Parachutes, Stability and Control, Structures, Vibration, Wind Tunnels. 47s. 6d (48s 8d.)

1943 Vol. I. Aerodynamics, Aerofoils, Airscrews. 80s. (81s. 4d.)
  Vol. II Engines, Flutter, Materials, Parachutes, Performance, Stability and Control, Structures. 90s. (91s 6d.)

1944 Vol. I. Aero and Hydrodynamics, Aerofoils, Aircraft, Airscrews, Controls. 84s. (85s. 8d.)
  Vol II. Flutter and Vibration, Materials, Miscellaneous, Navigation, Parachutes, Performance, Plates and Panels. Stability, Structures, Test Equipment, Wind Tunnels. 84s (85s. 8d.)

Annual Reports of the Aeronautical Research Council—

1933–34	1s. 6d. (1s. 8d.)	1937	2s. (2s. 2d.)
1934–35	1s. 6d. (1s. 8d.)	1938	1s. 6d. (1s. 8d.)
April 1, 1935 to Dec. 31, 1936	4s. (4s. 4d.)	1939–48	3s. (3s. 2d.)

Index to all Reports and Memoranda published in the Annual Technical Reports, and separately—

April, 1950   -   -   -   R. & M. No. 2600   2s. 6d. (2s. 7½d.)

Author Index to all Reports and Memoranda of the Aeronautical Research Council—

1909–January, 1954.   R. & M. No. 2570   15s. (15s. 4d.)

Indexes to the Technical Reports of the Aeronautical Research Council—

December 1, 1936 — June 30, 1939	R. & M. No. 1850	1s. 3d. (1s. 4½d.)
July 1, 1939 — June 30, 1945	R. & M. No. 1950	1s. (1s. 1½d.)
July 1, 1945 — June 30, 1946	R. & M. No. 2050	1s. (1s. 1½d.)
July 1, 1946 — December 31, 1946	R. & M. No. 2150	1s. 3d. (1s. 4½d.)
January 1, 1947 — June 30, 1947	R. & M. No. 2250	1s. 3d. (1s. 4½d.)

Published Reports and Memoranda of the Aeronautical Research Council—

Between Nos. 2251–2349	R. & M. No. 2350	1s. 9d. (1s. 10½d.)
Between Nos. 2351–2449	R. & M. No. 2450	2s. (2s. 1½d.)
Between Nos. 2451–2549	R. & M. No. 2550	2s. 6d. (2s. 7½d.)
Between Nos. 2551–2649	R. & M. No. 2650	2s. 6d. (2s. 7½d.)

Prices in brackets include postage

HER MAJESTY'S STATIONERY OFFICE